2017

Understanding Megakaryopoiesis And Thrombopoiesis Using Human Stem Cells Models

Xiu Li Sim
University of Pennsylvania, simxiuli@gmail.com

Understanding Megakaryopoiesis And Thrombopoiesis Using Human Stem Cells Models

Abstract

Human stem cell models (CD34+ hematopoietic progenitors, embryonic stem cells and induced pluripotent stem cells (iPSCs)) are powerful tools for the study of megakaryopoiesis and thrombopoiesis, particularly in situations where mouse models are unavailable or do not accurately recapitulate human physiology or development. In the first part of this thesis, we identified and characterized novel megakaryocyte (MK) maturation stages in MK cultures derived from human stem cells. An immature, low granular (LG) MK pool (defined by side scatter on flow cytometry) gives rise to a mature high granular (HG) pool, which then becomes damaged by apoptosis and GPIbα (CD42b) shedding. We define an undamaged HG/CD42b+ MK subpopulation, which endocytoses fluorescently-labeled coagulation factor V (FV) from the medium into alpha-granules and releases functional FV+CD42b+ platelet-like particles in vitro and when infused into immunodeficient mice. Importantly, these FV+ platelets have the same size distribution as infused human donor platelets and are preferentially incorporated into clots after laser injury. Using drugs to protect HG MKs from apoptosis and CD42b shedding, we also demonstrate that apoptosis precedes CD42b shedding and that apoptosis inhibition enriches the FV+ HG/CD42b+ MKs, leading to increased platelet yield in vivo, but not in vitro. These studies identify a transition between distinct MK populations in vitro, including one that is primed for platelet release. Technologies to optimize and select these platelet-ready MKs may be important to efficiently generate functional platelets from in vitro-grown MKs. In the second part of this thesis, we used patient-specific iPSCs to model Thrombocytopenia Absent Radius (TAR) syndrome, a rare congenital disorder characterized by low platelet counts and bilateral absence of the radius. We generated several iPSC lines from patients and controls and confirmed that the patient lines had decreased expression of RBM8A, the candidate disease gene for TAR syndrome. We differentiated patient and control iPSCs to hematopoietic progenitor cells (HPCs) and MKs and showed that HPCs derived from TAR iPSCs exhibited decreased MK colony-forming potential but differentiated normally into MKs in liquid culture. When we restored RBM8A expression in TAR iPSCs using a doxycycline inducible system, we saw no effect on megakaryopoiesis. We then knocked out RBM8A in TAR iPSCs and found that a complete deficiency in RBM8A expression was lethal for iPSCs, HPCs, MKs and erythrocytes. These studies suggest that we were unable to determine a specific role for RBM8A in primitive (embryonic) megakaryopoiesis and perhaps future studies to direct iPSCs towards the definitive (adult) MK lineage may better elucidate RBM8A's role in TAR syndrome.

Degree Type

Dissertation

Degree Name

Doctor of Philosophy (PhD)

Graduate Group

Cell & Molecular Biology

First Advisor

Paul Gadue

Keywords

Factor V, Megakaryocytes, Platelets, Stem Cells, Transfusion

UNDERSTANDING MEGAKARYOPOIESIS AND THROMBOPOIESIS USING HUMAN STEM CELLS MODELS

Xiu Li Sim

A DISSERTATION

In

Cell and Molecular Biology

Presented to the Faculties of the University of Pennsylvania

in

Partial Fulfillment of the Requirements for the

Degree of Doctor of Philosophy

2017

Supervisor of Dissertation:

Paul Gadue, Associate Professor of Pathology and Laboratory Medicine

Graduate Group Chair Person:

Daniel S. Kessler, Professor of Cell and Developmental Biology

Dissertation Committee

Mortimer Poncz, Professor of Pediatrics

Wei Tong, Associate Professor of Pediatrics

Nancy A. Speck, Professor of Cell and Developmental Biology

Peter S. Klein, Professor of Medicine

UNDERSTANDING MEGAKARYOPOIESIS AND THROMBOPOIESIS USING HUMAN STEM CELLS MODELS

ACKNOWLEDGMENT

This work would not have been possible without the help and support of my official advisor, Paul and my unofficial but equally important advisor, Debbie. I would like to thank them for the scientific discussions, and more importantly, the tremendous amount of moral support they have given me over the years. I am also grateful to my thesis committee chair, Morty, who only noticed my existence in the last 2 years of my PhD, but was instrumental in pushing me to finish this work. I am very fortunate to be surrounded by fantastic colleagues, who became my friends and occupy a special place in my heart. Thank you all for the drama and gossip that spiced up the otherwise monotonous daily grind. Last but not least, I would like to thank my family, in particular, my parents and my mother-in-law, who took care of us in numerous ways, my daughter, Emily, who brought so much joy and laughter to our family and of course, my husband, Lu, whose love and encouragement gave me the courage and confidence to reach the finish line.

ABSTRACT

UNDERSTANDING MEGAKARYOPOIESIS AND THROMBOPOIESIS USING HUMAN STEM CELLS MODELS

Xiu Li Sim

Paul Gadue

Human stem cell models ($CD34^+$ hematopoietic progenitors, embryonic stem cells and induced pluripotent stem cells (iPSCs)) are powerful tools for the study of megakaryopoiesis and thrombopoiesis, particularly in situations where mouse models are unavailable or do not accurately recapitulate human physiology or development. In the first part of this thesis, we identified and characterized novel megakaryocyte (MK) maturation stages in MK cultures derived from human stem cells. An immature, low granular (LG) MK pool (defined by side scatter on flow cytometry) gives rise to a mature high granular (HG) pool, which then becomes damaged by apoptosis and GPIbα (CD42b) shedding. We define an undamaged HG/$CD42b^+$ MK subpopulation, which endocytoses fluorescently-labeled coagulation factor V (FV) from the medium into alpha-granules and releases functional FV^+CD42b^+ platelet-like particles in vitro and when infused into immunodeficient mice. Importantly, these FV^+ platelets have the same size distribution as infused human donor platelets and are preferentially incorporated into clots after laser injury. Using drugs to protect HG MKs from apoptosis and CD42b shedding, we also demonstrate that apoptosis precedes CD42b shedding and that apoptosis inhibition enriches the FV^+ HG/$CD42b^+$ MKs, leading to increased platelet yield in vivo, but not in vitro. These studies identify a transition between distinct MK populations in vitro, including one that is primed for platelet release. Technologies to optimize and select these platelet-ready MKs may be important to efficiently generate functional platelets from in vitro-grown MKs. In the second part of this thesis, we used

patient-specific iPSCs to model Thrombocytopenia Absent Radius (TAR) syndrome, a rare congenital disorder characterized by low platelet counts and bilateral absence of the radius. We generated several iPSC lines from patients and controls and confirmed that the patient lines had decreased expression of *RBM8A*, the candidate disease gene for TAR syndrome. We differentiated patient and control iPSCs to hematopoietic progenitor cells (HPCs) and MKs and showed that HPCs derived from TAR iPSCs exhibited decreased MK colony-forming potential but differentiated normally into MKs in liquid culture. When we restored *RBM8A* expression in TAR iPSCs using a doxycycline inducible system, we saw no effect on megakaryopoiesis. We then knocked out *RBM8A* in TAR iPSCs and found that a complete deficiency in *RBM8A* expression was lethal for iPSCs, HPCs, MKs and erythrocytes. These studies suggest that we were unable to determine a specific role for *RBM8A* in primitive (embryonic) megakaryopoiesis and perhaps future studies to direct iPSCs towards the definitive (adult) MK lineage may better elucidate *RBM8A*'s role in TAR syndrome.

TABLE OF CONTENTS

LIST OF TABLES

CHAPTER 2

LIST OF ILLUSTRATIONS

CHAPTER 1

CHAPTER 2

CHAPTER 3

CHAPTER 4

LIST OF ABBREVIATIONS

AAVS1	Adeno-associated virus integration site 1
ADAM17	Disintegrin and metalloproteinase domain-containing protein 17
AGM	Aorta-gonad-mesonephros
bFGF	Basic fibroblast growth factor
CAG	CMV early enhancer/chicken beta actin
CAS9	CRISPR-associated protein 9
cDNA	Complementary DNA
CFU	Colony-forming unit
CMP	Common myeloid progenitor
COL18A	Endostatin
CRISPR	Clustered regularly interspaced short palindromic repeats
CTL	Control
DNA	Deoxyribonucleic acid
EJC	Exon junction complex
ESC	Embryonic stem cell
FACS	Fluorescence activated cell sorting
FSC-A	Forward scatter
FV	Factor V
GFP	Green fluorescent protein
gRNA	Guide RNA
GMP	Granulocyte-macrophage progenitor
HG	High granular
HPC	Hematopoietic progenitor cell
HSC	Hematopoietic stem cell
IMS	Invaginated membrane system
iPSC	Induced pluripotent stem cell
Kb	Kilobases
LG	Low granular
MK	Megakaryocyte
MEF	Mouse embryonic fibroblast
MEP	Megakaryocyte-erythrocyte progenitor
mRNA	Messenger RNA
NEO	Neomycin
NOD/SCID	Non-obese diabetic/severe combined immunodeficiency
NSG	NOD/SCID interleukin receptor 2 gamma
PAR1	Protease-activated receptor 1
PF4	Platelet factor 4
PGK	Phosphoglycerate Kinase
PLP	Platelet-like particle
PURO	Puromycin
PS	Phosphatidylserine
RBM8A	RNA binding motif protein 8A
RNA	Ribonucleic acids
rTTA	Reverse tetracycline transcriptional activator
SNP	Single nucleotide polymorphism
SSC-A	Side scatter
TAR	Thrombocytopenia absent radius
TPO	Thrombopoietin
TRE	Tetracycline response element

TUNEL	Terminal deoxynucleotidyl transferase dUTP nick end labeling
UTR	Untranslated region
VEGF	Vascular endothelial growth factor
VWF	Von willebrand factor
WT	Wild type
ZFN	Zinc finger nuclease

CHAPTER 1

Introduction and Overview

1.1 Characteristics and Functions of Megakaryocytes (MKs) and Platelets

Megakaryocytes (MKs) are rare, large, polyploid blood cells present in the bone marrow[1] at a low frequency of 1 in 10,000 nucleated cells.[2] The main function of a MK is to produce platelets, although secondary roles in regulating the hematopoietic stem cell (HSC) niche and function in the bone marrow have also been described.[3,4] Platelets are anucleate cell fragments that are primarily important for hemostasis, but also have roles in modulating angiogenesis, inflammatory responses, lymphatic development, wound healing and repair.[5–10]

1.2 Megakaryopoiesis and Thrombopoiesis

HSCs give rise to MKs in a process termed megakaryopoiesis while MKs release platelets in a process termed thrombopoiesis.

1.2.1 Hierarchical Model of Hematopoiesis

In the classical model of hematopoiesis, self-renewing, multi-potent HSCs give rise to all the blood lineages, including the MK lineage, through a series of increasingly committed progenitors. In this model, the HSC goes through a multi-potent progenitor stage followed by a common myeloid progenitor (CMP) stage before differentiating into bi-potent granulocyte-macrophage progenitors (GMPs) and megakaryocyte-erythrocyte progenitors (MEPs)[11–14] (Figure 1.1). MEPs, as its name suggests, give rise to MKs and erythrocytes. However, recent studies suggested that there may be more straightforward pathways going from HSCs to MKs, with the identification of MK/platelet-biased HSCs, which directly give rise to MK progenitors (Figure 1.1).[15–18] The evidence for these

differentiation pathways came from studies of the mouse hematopoietic system and whether the same hematopoietic hierarchy holds true for humans remains to be tested.

1.2.2 Primitive and Definitive Megakaryopoiesis

The understanding of megakaryopoiesis is further complicated by the separation of hematopoiesis into two distinct waves during development. The first wave of hematopoiesis, termed primitive hematopoiesis, occurs in the yolk sac of the developing embryo.[19,20] Primitive hematopoiesis generates predominantly embryonic red blood cells, macrophages, MKs and platelets.[21,22] The second wave of hematopoiesis, termed definitive hematopoiesis, starts in the yolk sac, but migrates to the aorta-gonad-mesonephros (AGM) region and then the fetal liver, before finally settling in the bone marrow.[19] HSCs arise during the definitive hematopoietic phase in the AGM and give rise to the full range of blood lineages.

Studies have suggested that primitive and definitive megakaryopoiesis may be regulated differently,[23,24] resulting in functional changes with ontogeny. Embryonic and fetal MKs are known to be more proliferative than adult MKs and produce platelets quickly without reaching high ploidy.[22,25–27] In contrast, adult MKs have increased ploidy as compared to embryonic and fetal MKs and are more efficient in releasing platelets.[25] Transcriptome profiling of primitive yolk sac MKs, definitive fetal liver MKs and adult MKs revealed that more than 1/3 of the genes that were continuously upregulated with MK ontogeny included cytoskeleton proteins and proteins involved in polyploidization, proplatelet formation and platelet functions, a probable explanation for why definitive adult MKs have higher ploidy and are likely more efficient platelet producers than primitive embryonic MKs.[24] Further studies are necessary to better understand exactly how megakaryopoiesis changes with ontogeny and how different are the resulting MKs and

platelets in terms of function and characteristics. These differences are important especially since MKs derived from human embryonic stem cells (ESCs) and human induced pluripotent stem cell (iPSCs) are more similar to embryonic/fetal MKs than adult MKs,[24,28,29] raising implications for the generation of stem cell-derived MKs and platelets for transfusions.

1.2.3 Changes Accompanying MK Maturation

Megakaryopoiesis is driven mainly by thrombopoietin (TPO)[30–32] and is characterized by the upregulation of MK-specific cell surface markers (CD41, CD42a, CD42b, c-mpl)[33] and the expression of transcription factors associated with MK development (e.g. *GATA1, FLI1, RUNX1, NFE2* etc).[34] The resulting MKs undergo a complex maturation process, which involves 1) endomitosis to become a large polyploid cell,[35] 2) the formation of an invaginated membrane system (IMS),[36] 3) the formation of platelet-specific granules[37,38] (alpha granules, dense granules, lysosomes) and 4) the synthesis and endocytosis of granular content (RNA, platelet-specific proteins) to be distributed into platelets.[39–44] (Figure 1.2).

The role of high ploidy in MK function is not completely understood. Polyploidization is thought to help increase cell size and cytoplasmic volume to increase the number of platelets released from a single MK. Indeed, although MKs of lower ploidy (e.g. embryonic/fetal MKs, cord blood-derived MKs) are fully capable of releasing platelets, they are known to generate fewer platelets than MKs of high ploidy.[22,25–27] Polyploidy may also influence terminal MK through functional gene amplification[45] and coordinating expression of genes involved in DNA replication, platelet release and function.[46]

The IMS massively increases the membrane surface within the MK, serving as a membrane reservoir for platelet formation.[36,47] The IMS also has a role in extending proplatelets through its interaction with actin filaments, which drive the proplatelet formation process.[47,48]

Platelets derive most of their RNA and many proteins from the MKs.[49,50] These proteins and RNA are pre-packaged in granules[37,38] before being distributed into platelets. Most of these RNA and proteins are synthesized by the MKs,[39,40] but some proteins, such as fibrinogen, immunoglobulins and coagulation factor V, are endocytosed by mature MKs from their environment and packaged for distribution into platelets.[42,43,51] Platelets themselves, also endocytose certain proteins from their environment, such as fibrinogen and angiogenesis regulators like vascular endothelial growth factor (VEGF) and basic fibroblast growth factor (bFGF).[43,52,53]

1.2.4 Sites and Process of Thrombopoiesis

One model of thrombopoiesis involves mature MKs migrating from the osteoblastic niche, down a stromal cell-derived factor (SDF-1) gradient to the vascular niche,[54,55] where they extend proplatelets into the bone marrow sinusoids (Figure 1.2).[56,57] These proplatelets then fragment to release platelets into the bloodstream. Evidence for the proplatelet model of thrombopoiesis comes from the observations of proplatelet structures in in vitro mouse and human MK cultures[58,59] as well as live imaging and electron micrographs of MKs in the murine bone marrow, showing MKs extending proplatelet-like protrusions into microvessels.[56,57,60,61] The directionality of proplatelet extension is guided by a transendothelial sphingosine 1-phosphate (S1P) gradient and the subsequent shedding of proplatelets into the circulation is prompted by high S1P concentrations in the blood.[57] The observed proplatelet fragments that are shed are

considerably larger than platelets,[56] but as they continue to mature and morph in the bloodstream with the help of vascular shear forces, they become smaller preplatelet intermediates and then finally, platelets.[62] Recently, a new platelet release mechanism involving the rupturing of MKs through a interleukin-1a (IL-1a)-dependent pathway has been suggested (Figure 1.2).[63] This mechanism results in the rapid release of large numbers of platelets, which may account for rapid thrombopoiesis in times of acute platelet needs.

Apart from the bone marrow sinusoids, another primary site of platelet release is in the lung capillary bed, the first capillary bed encountered by any cell leaving the bone marrow. When MKs were isolated from blood entering and leaving the human lung by elutriation and manually counted on Wright-Giemsa-stained cytopsin slides, Levine et. al. detected 10 times more intact MKs in the vessels entering the lung capillary bed as compared to the vessels leaving the lung capillary bed.[64] Moreover, 98% of the MKs leaving the lung had little or no cytoplasm remaining.[64] These results, together with other independent observations of circulating MKs and platelets release in the lung, suggest that intact MKs leave the bone marrow, get trapped in the pulmonary capillaries and release platelets at this site.[64–67] Evidence of higher platelet counts in the post-pulmonary vessels compared to the pre-pulmonary vessels[68] also support this theory. More recently, MKs were shown to release proplatelets and preplatelets in the lung by live imaging using intravital microscopy and it was estimated that the lung produces about half of the platelets in mice,[69] suggesting that both the lung capillary bed and the bone marrow sinusoids are important sites of terminal platelet production.

1.2.5 Defects in megakaryopoiesis and thrombopoiesis

Defects in megakaryopoiesis and/or thrombopoiesis can lead to thrombocytopenia or thrombocytosis, conditions where platelet counts are abnormally low or high, respectively. Understanding the underlying etiology of these abnormal conditions will often lead to the identification of proteins regulating important aspects of megakaryopoiesis and thrombopoiesis and a better understanding of the biology of these processes. Therefore, these studies have important clinical implications for the treatment of these conditions as well as the generation of in vitro platelets for transfusion.

1.3 Thrombocytopenia Absent Radius (TAR) syndrome

TAR syndrome is a rare congenital disorder characterized primarily by thrombocytopenia and bilateral absence of the radius.[70] TAR patients may also present varying degrees of other clinical features, including skeletal malformations in the upper and lower limbs, cardiac abnormalities, cow's milk allergy and several other unusual features.[70] The etiology of TAR syndrome has not been elucidated but studies have shown that TAR patients have severely reduced number of mature MKs, suggesting that they may have defects in MK development and/or maturation.[71–73]

Interestingly, platelet counts in TAR patients gradually improve with age and may approach near normal range in adulthood,[70,74] suggesting that the defects in megakaryopoiesis or thrombopoiesis may be specific to infancy.

1.3.1 The Genetic Basis of TAR Syndrome

Most TAR patients have a deletion of one copy of the *RBM8A* gene and a single nucleotide polymorphism (SNP) in the 5' untranslated region (UTR) or first intron of the

intact copy[75] (Figure 1.3). The deletion of the *RBM8A* gene is most commonly due to a microdeletion on chromosome 1q21.1,[75,76] but can also be a result of null mutations.[75] The microdeletion in TAR patients varies in size, but a minimum deletion of 200 kilobases (kb) has been described to cause TAR syndrome. The minimal deleted region encompasses 11 genes, including *RBM8A*,[76] all of which have no known roles in megakaryopoiesis or thrombopoiesis. The strongest evidence for the involvement of *RBM8A* in TAR syndrome is the identification of 2 TAR patients, who have one null *RBM8A* allele and the 5' UTR SNP in the intact *RBM8A* allele.[75] The 5' UTR SNP (G/A) and the first intronic SNP (G/C) are present in the normal population with frequencies of 3.05% and 0.42% respectively and do not result in any abnormal phenotype when present in isolation.[75] Additionally, family members of TAR patients, who are carriers of the 1q21.1 microdeletion present a normal phenotype,[75,76] suggesting that haploinsufficiency of the genes in the microdeletion is not sufficient to cause TAR syndrome or any obvious hematologic/bone phenotype.

Therefore, compound inheritance of a null *RBM8A* allele together with one of two low-frequency SNPs in the non-coding region (5' UTR/first intron) of the *RBM8A* gene is necessary to result in TAR syndrome.[75] Although the exact role of the SNP is unclear, it has been hypothesized that the deletion and the SNP together result in sub-optimal expression of *RBM8A*,[75] which may negatively impact megakaryopoiesis and/or thrombopoiesis.

1.3.2 Y14 and the Exon Junction Complex

The *RBM8A* gene encodes the Y14 protein, which is one of the proteins that make up the exon junction complex (EJC).[77–79] The EJCs mark and bind to the exon junctions of spliced mRNAs and accompany the export of spliced mRNAs from the nucleus to the

cytoplasm, where they are being translated.[80] The presence of the EJC on spliced mRNAs enhances the translation of the mRNAs.[81] In particular, the EJC has a central role in mRNA surveillance and nonsense-mediated decay of mRNAs with premature stop codons.[82–84] Given that the EJC is involved in these important general cellular functions, it is unsurprising that it is ubiquitously expressed[85] and is present in all hematopoietic cells,[75] thus it is unclear how a deficiency in Y14 or EJC function can lead to specific defects in megakaryopoiesis or thrombopoiesis. Albers et. al.[75] suggested several possible hypotheses for the disease mechanism of TAR syndrome. Either there is a MK-specific deficiency in *RBM8A*/Y14 due to a MK-specific regulation of *RBM8A*/Y14 expression that is dependent on the non-coding SNP or that global deficiency of *RBM8A*/Y14 specifically regulate physiological mRNA abundance in a tissue-specific manner. However, all these hypotheses are speculative at this point.

1.3.3 Animal Models of Y14 Deficiency

Y14 is highly conserved between species.[75] In Drosophila, knockdown of Y14's ortholog (tsu) caused major defects in abdomen formation.[86] In the zebra fish, knockdown of Y14 led to extreme malformations and death at 2 days post-fertilization.[75] Together, these data suggest that *RBM8A*/Y14 plays an important role in embryogenesis, but does not give us any information on how it can specifically impact megakaryopoiesis or thrombopoiesis. As the genetic cause of TAR syndrome was only uncovered recently in 2012,[75] there have not been any published reports on a mouse model of TAR syndrome.

1.4 The Use of Human Stem Cell Models to Understand the Biology of Megakaryopoiesis and Thrombopoiesis

Since MKs represent 0.01% of all the nucleated cells in the bone marrow,[2] it is a challenge to study megakaryopoiesis or thrombopoiesis using primary human bone

marrow MKs. An alternative system to study human-specific MK biology is to use MKs differentiated from human stem cells.

Since the identification of TPO as the main cytokine driving megakaryopoiesis,[30–32] many laboratories have been successful in differentiating a variety of human stem cells into MKs and platelets.[59,87–94] These human stem cell sources include ESCs, iPSCs, cord blood and adult $CD34^+$ hematopoietic progenitors.

ESCs and iPSCs are particularly attractive stem cell sources as they are self-renewable, proliferative and amenable to genetic manipulation. With these stem cell models, we are able to obtain large numbers of MKs with high purity, which makes the study of MKs much easier than purifying these cells from the bone marrow. Gene functions in megakaryopoiesis and thrombopoiesis can be investigated through knocking out or overexpression of these genes in stem cell-derived MKs. Additionally, iPSCs derived from patients with MK/platelet disorders can also be used for disease modeling as these cells carry all the genetic characteristics of the patient and differentiating these cells to MKs/platelets can recapitulate the disease phenotype and reveal interesting mechanisms.

However, ESCs/iPSCs are limited in that their differentiation into MKs recapitulates primitive (embryonic) megakaryopoiesis,[28] so the findings from these models may not be applicable to definitive (adult) megakaryopoiesis. For that, we can utilize adult $CD34^+$ hematopoietic progenitors, which have the limitation of being donor-dependent, but are able to recapitulate definitive megakaryopoiesis.

1.5 Stem Cell-derived Platelets for Transfusions

Other than the study of human MK/platelet biology, another important potential application of stem cell-derived MKs and platelets is the use of these cells for transfusions.

1.5.1 The Clinical Demand for Platelets

Platelet transfusions are used to treat severe thrombocytopenia and bleeding associated with trauma and surgery.[95,96] More than a million platelet transfusions are being performed yearly in the United States alone.[97] Although the clinical demand for platelets has increased over the years, the number of donors has shown a slight decrease, leading to a perpetual shortage of donor platelets for transfusion.[97] Additionally, the quality of human donor platelets is highly variable depending on the donor and there may be issues with immunogenicity, even with matched donors.[98] Donor platelets have to be stored at room temperature,[99] which increases the risk of bacterial contamination. Finally, donor platelets have a short shelf life of 5 days,[99] which means that many platelet units are discarded before they can be used, leading to high wastage.[97]

1.5.2 In Vitro-generated Platelets for Transfusions

The idea of using stem cell-derived platelets to replace or supplement human donor platelets for transfusion is a very attractive one for the following reasons:

1) Since stem cells are self-renewable, we can technically generate unlimited numbers of platelets for transfusion.
2) Since platelets are anucleate, the stem cell-derived platelet product can be irradiated to kill off any contaminating cell types, especially undifferentiated stem cells, which have teratoma-forming potential.

3) Stem cells can be engineered to be human leukocyte antigen (HLA)-deficient to generate "universal" platelets,[90] which can be transfused into any individual without immunogenicity issues.
4) Platelets with enhanced qualities, such as a longer circulating half-life, can be generated through genetic engineering of the parent stem cell.

The first in vitro-generated platelets were described more than 20 years ago.[59] Despite improvements in the efficiency of platelet generation, the in vitro-generated stem cell-derived platelets remain too expensive to be a feasible source for donor platelet replacement in transfusions. Not to mention, the functionality of these in vitro-generated platelets is highly questionable as they have not been rigorously assessed and compared to the gold standard, human donor platelets.

1.5.3 Current Platelet Yields per MK

Thrombopoiesis in vivo is a highly efficient process; each MK release thousands of platelets into the bloodstream.[100] Traditionally, in vitro-generated platelets from static MK cultures are purified using centrifugation methods[89,90,101] (Figure 1.4). Newer and better methods for generating platelets in vitro make use of platelet bioreactors,[102–106] which more accurately mimic the in vivo environment with the incorporation of vascular shear stress, extracellular matrix components and endothelial cell contacts (Figure 1.4). Yet the best in vitro platelet yield per MK is 30,[90] which pales in comparison to the in vivo yield of >1000.[100]

To put things in perspective, a unit of platelets for transfusion contains 3×10^{11} platelets. To get one unit of platelets with the current yield, we need 1×10^{10} MKs. Since each iPSC can give rise to 16 MKs,[90] we would need 625 million iPSCs or approximately 100

6-well plates of iPSCs as starting material to get a unit of platelets. At this efficiency, the process is prohibitively expensive.

1.5.4 Are In Vitro-generated Platelets Functional?

The gold standard assay for assessing platelet functionality is light transmission aggregometry (LTA), which evaluates the kinetics and extent of platelet aggregation in the presence of stimuli. LTA requires a large number of platelets, so low yields from in vitro platelet generation have made it impossible for this technique to be the standard for assessing functionality. Feng et. al.[90] were the first group to achieve sufficient number of in vitro-generated platelets to be tested by LTA. The poor functionality of these platelets was obvious as they had an activation curve similar to cord blood platelets, which were known to be hyporesponsive to physiological agonists as compared to adult platelets.[107–109] Many groups assessed the functionality of in vitro-generated platelets by examining their ability to activate in response to platelet agonists (such as thrombin or adenosine diphosphate (ADP)). The activation response include: 1) changes in conformation of the surface αIIbβ3 receptor, which can be detected by PAC-1 antibody binding[110,111] and 2) surface exposure of P-selectin resulting from alpha-granule release. While human donor platelets show a dramatic shift in PAC-1 binding and P-selectin exposure in these assays, the in vitro-generated platelets showed much weaker responses to the same stimulation,[90–92,112] suggesting subpar functionality.

Another assay to evaluate platelet functionality is to examine their incorporation into a growing thrombus in vivo using a laser injury model. In this assay, a laser injury induced in the arterioles of the mouse's cremaster muscle leads to the formation of a thrombus. When human MKs or platelets are infused prior to the induction of laser injury, the functional human platelets incorporate into the clot through a αIIbβ3 receptor-specific

interaction.[89,90,113] This assay is limited because even human donor platelets show very low incorporation rates into the mouse thrombus due to the overwhelming number of mouse platelets and the poor ability of human platelets to interact with mouse von willebrand factor (VWF),[114] a key process in adhesion.[115] The development of a mouse model expressing VWF with enhanced specificity for human platelets,[114] will be very useful for assessing the functionality of in vitro-generated platelets.

Electron microscopy has also been performed on in vitro-generated platelets to compare their morphology and ultrastructural features to those of human donor platelets.[89,90,92,112] But these studies showcase a few individual platelets, which may not be representative of the whole platelet product.

Last but not least, a strong indication of the poor quality of in vitro-generated platelets is the rapid clearance rate of these platelets by macrophages when infused into immunodeficient mice,[90] presumably because these platelets are pre-activated. In contrast, when human donor platelets are infused into immunodeficient mice, they have a circulating half-life of 12 hours.[113]

The limitations on the yield and functionality of in-vitro generated platelets suggest that there is a lot more to be learned about the biology of megakaryopoiesis and thrombopoiesis so that we can further optimize the process of platelet generation from stem cell sources. While understanding how megakaryopoiesis and thrombopoiesis work in vivo using mouse models is very important, we also need a better understanding of these processes in vitro using human stem cell models.

1.5.5 Platelet Production In Vivo from Infused MKs

An alternative approach to generate platelets is to infuse stem cell-derived MKs into mice or potentially humans and allow them to release platelets in vivo (Figure 1.4). When cultured human MKs are infused into immunodeficient mice, the platelets derived from these MKs circulate with a half-life of 12 hours, similar to infused human donor platelets, suggesting that the platelets produced in vivo following MK infusion are of higher quality than those generated in vitro.[113] The infused MKs get trapped in the lung pulmonary bed and release platelets over a 2-4 hour period.[113] The platelets derived from infused MKs are of similar size to human donor platelets and incorporate into clots following laser injury.[113] These data suggest that MK transfusions may be a possible alternative to platelet transfusions.

In fact, three clinical trials have been performed to assess the safety and feasibility of infusing ex vivo generated MK progenitors into cancer patients.[116–118] These studies showed safety and tolerability of autologous transfusions of MK progenitors differentiated ex vivo from $CD34^+$ hematopoietic progenitors. However, the efficacy of these treatments is unclear as most patients required additional platelet transfusion support and the lag time to platelet recovery was quite long for those that did not require additional platelet transfusions. Although the infusion of MKs or MK progenitors into patients may be possible, we will require more extensive studies for this method to become a clinical reality.

1.6 Overview of Research Goals

The overarching goal of my thesis work is to improve our understanding of the biology of megakaryopoiesis and thrombopoiesis using human stem cell models, as this knowledge is extremely important for the optimization of in vitro platelet generation for

transfusions. The two main approaches I have taken are to: 1) identify and enrich the mature platelet-producing MK population within the heterogeneous, asynchronous human MK culture and 2) elucidate the disease mechanism of TAR syndrome using patient-specific iPSCs as a disease model.

1.6.1 Identification and Enrichment of the Mature Platelet-producing MK Population

One of the difficulties with the manufacture of in vitro platelets is deciding the optimum time frame to harvest the platelets. This is complicated because the in vitro human MK culture is a heterogeneous and asynchronous mixture of MKs at different stages of maturation and platelet release occurs continuously over a certain time frame as the MKs mature. Although we have some idea of the changes that accompany the MK maturation process, we do not have a clear idea of what actually defines a final mature MK that is primed and ready to release platelets. We hypothesize that the mature MK at its prime may be a transient stage that needs to be captured to improve the quality and yield of in vitro platelets, thus my specific goal is to identify and enrich this specific stage of MKs to improve the process of in vitro platelet generation.

1.6.2 Elucidation of the Disease Mechanism of TAR Syndrome Using Patient-Specific Induced Pluripotent Stem Cells (iPSCs)

The growing ease of reprogramming patient samples to iPSCs and the improvements in MK/platelet differentiation protocols has made disease modeling using patient-specific iPSCs a feasible strategy for understanding disease mechanisms and identifying novel key proteins that regulate megakaryopoiesis and thrombopoiesis. As described previously, TAR syndrome has a complicated genetic basis and *RBM8A*/Y14 is the most probable candidate gene/protein responsible for the disease pathogenesis. However, it remains unclear exactly how *RBM8A*/Y14 deficiency results in thrombocytopenia in

these patients. Hence, my specific goal for this project is to use patient-specific iPSCs as a disease model to investigate the role of *RBM8A*/Y14 in the disease mechanism of TAR syndrome. As *RBM8A*/Y14 has no known roles in megakaryopoiesis or thrombopoiesis, elucidating the disease mechanism will provide insights into an unknown area of MK and platelet biology, which may have implications for the treatment of TAR syndrome as well as the in vitro generation of platelets for transfusions.

Figure 1.1

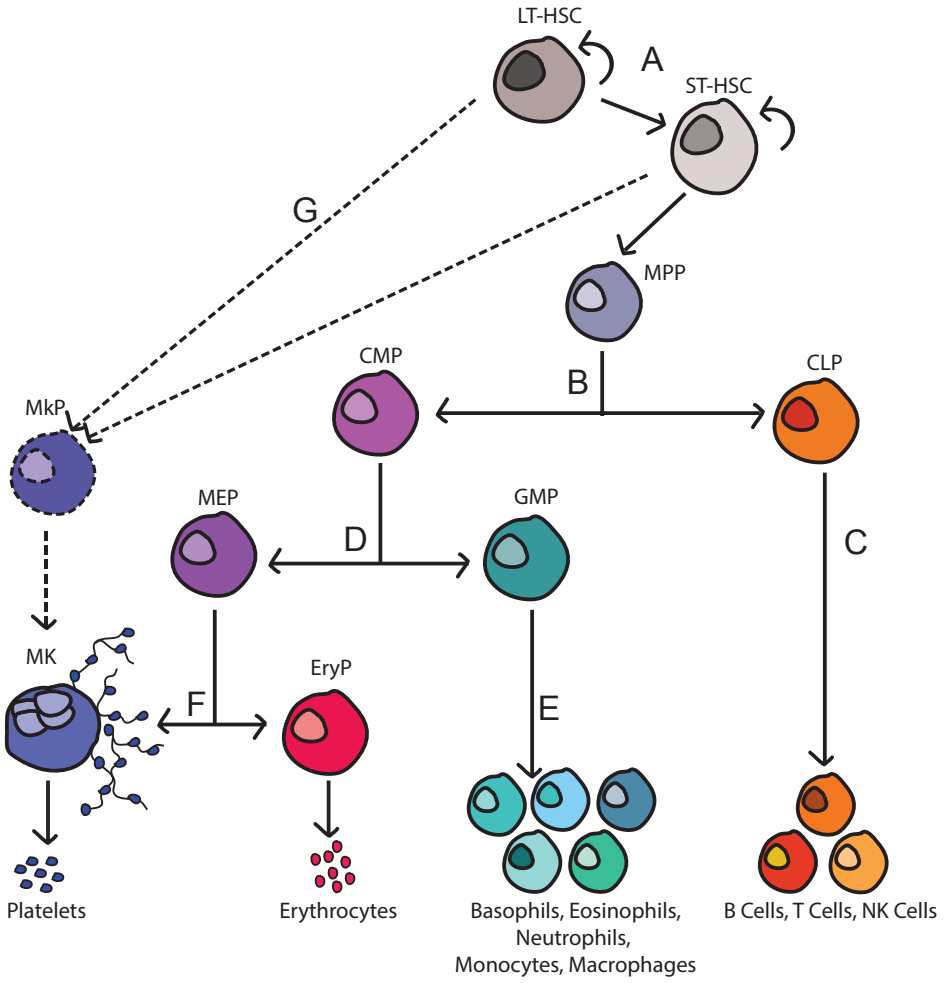

Figure 1.1: Model of Hematopoiesis (A) The long term-hematopoietic stem cell (LT-HSC) and the short term-hematopoietic stem cell (ST-HSC) in the bone marrow are at the top of the hematopoietic hierarchy and give rise to all the blood lineages. (B) The quiescent HSCs can either self-renew or differentiate into proliferative multi-potent progenitors (MPPs), which undergo further differentiation into common myeloid progenitors (CMPs) or common lymphoid progenitor (CLPs), with more restrictive hematopoietic potential. (C) The CLP gives rise to B cells, T cells and natural killer (NK) cells. (D) The CMP can develop into a megakaryocyte-erythroid progenitor (MEP) or a granulocyte-monocyte progenitor (GMP). (E) GMPs give rise to neutrophils, basophils, eosinophils, monocytes and macrophages. (F) MEPs give rise to megakaryocytes (MKs), which produce platelets, and erythrocytes. (G) Within the HSC population, there is a subpopulation is platelet/MK-biased, which can differentiate directly into MK progenitors (MkPs) that give rise to MKs and platelets only.

Figure 1.2

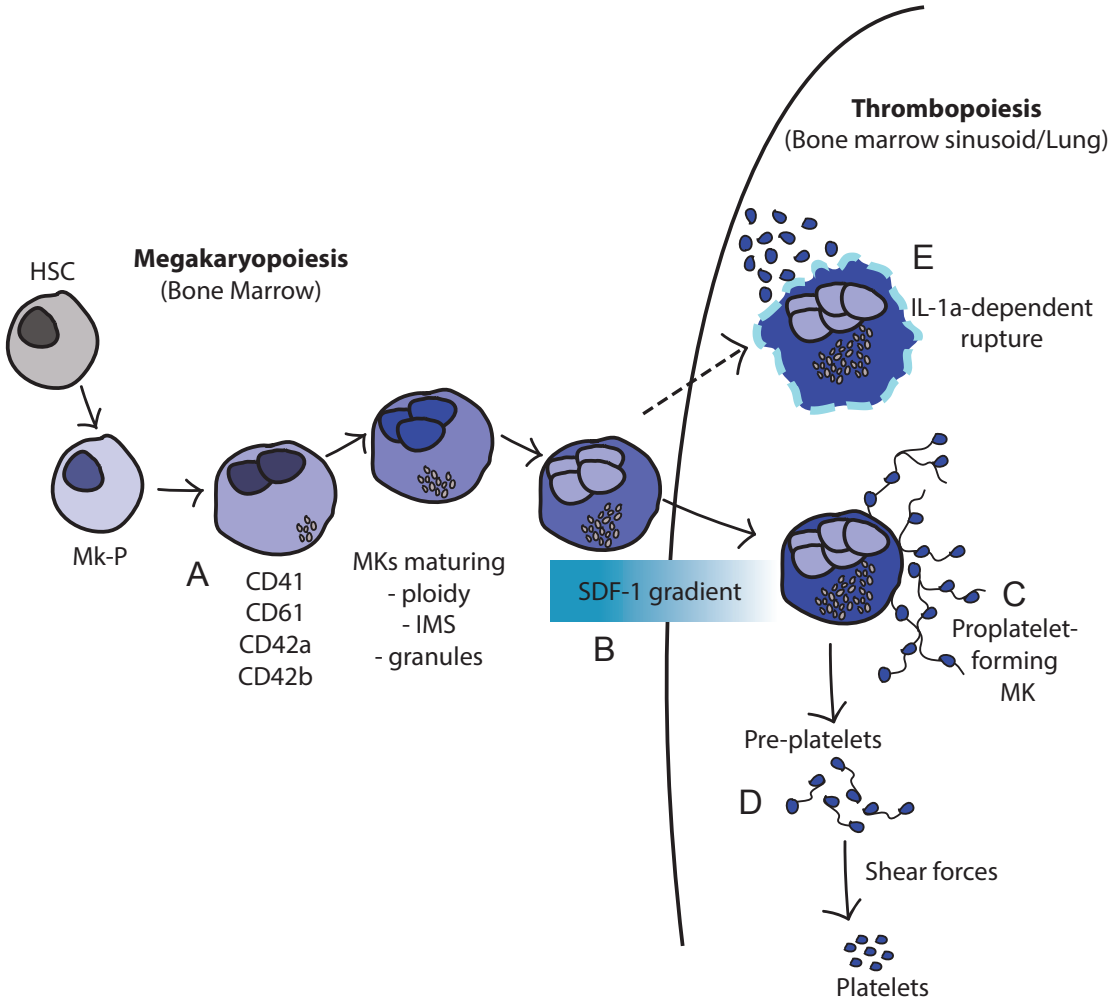

Figure 1.2: Model of Megakaryopoiesis and Thrombopoiesis (A) HSCs give rise to MKs through pathways illustrated in Figure 1.1. As MKs mature, there is an increase in surface expression of MK-specific receptors (CD41, CD61, CD42a, CD42b), an increase in ploidy, granules (alpha granules, dense granules) and granular content, as well as the formation of a complex IMS. (B) The fully mature MK migrates down the stromal-derived factor 1 (SDF-1) gradient from the osteoblastic niche to the vascular niche, where it extends proplatelets (C), which fragment to release pre-platelets into the bone marrow sinusoids. (D) Pre-platelet fragments are further shaped by vascular shear forces to become platelets. Intact mature MKs also migrate out of the bone marrow and release platelets in the lung capillary bed through similar processes. (E) Mature MKs could also undergo IL-1alpha-dependent rupture mechanism to release large numbers of platelets rapidly, potentially when acute needs arise.

Figure 1.3

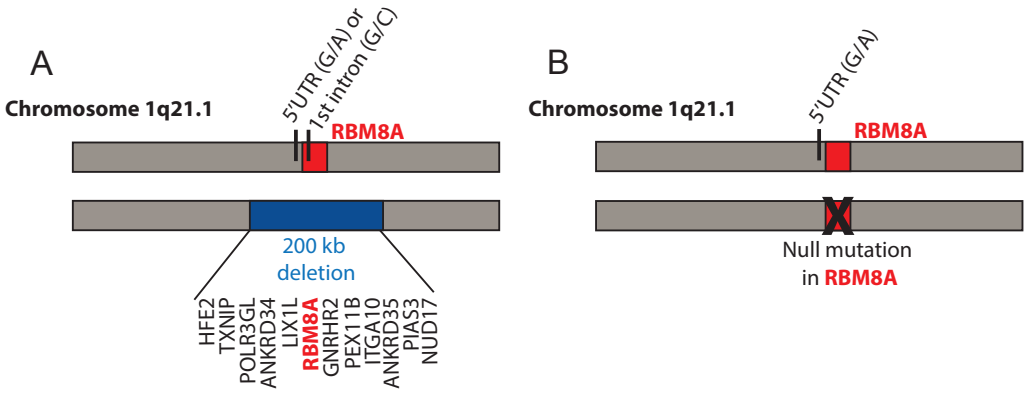

Figure 1.3: The Genetic Basis of TAR Syndrome (A) Most TAR patients have a minimum deletion of 200 kb in the chromosome region of 1q21.1, which results in the loss of one copy of 12 genes, including the *RBM8A* gene. They also have a SNP in the 5' UTR (G/A) or first intron (G/C). Both the deletion and one of the SNPs must be present for TAR syndrome to occur. (B) 2 TAR patients have been identified to have a null mutation in *RBM8A* on one chromosome and a 5' UTR (G/A) SNP on the intact *RBM8A* allele, a strong indication that *RBM8A* may be the candidate disease gene in TAR syndrome.

Figure 1.4

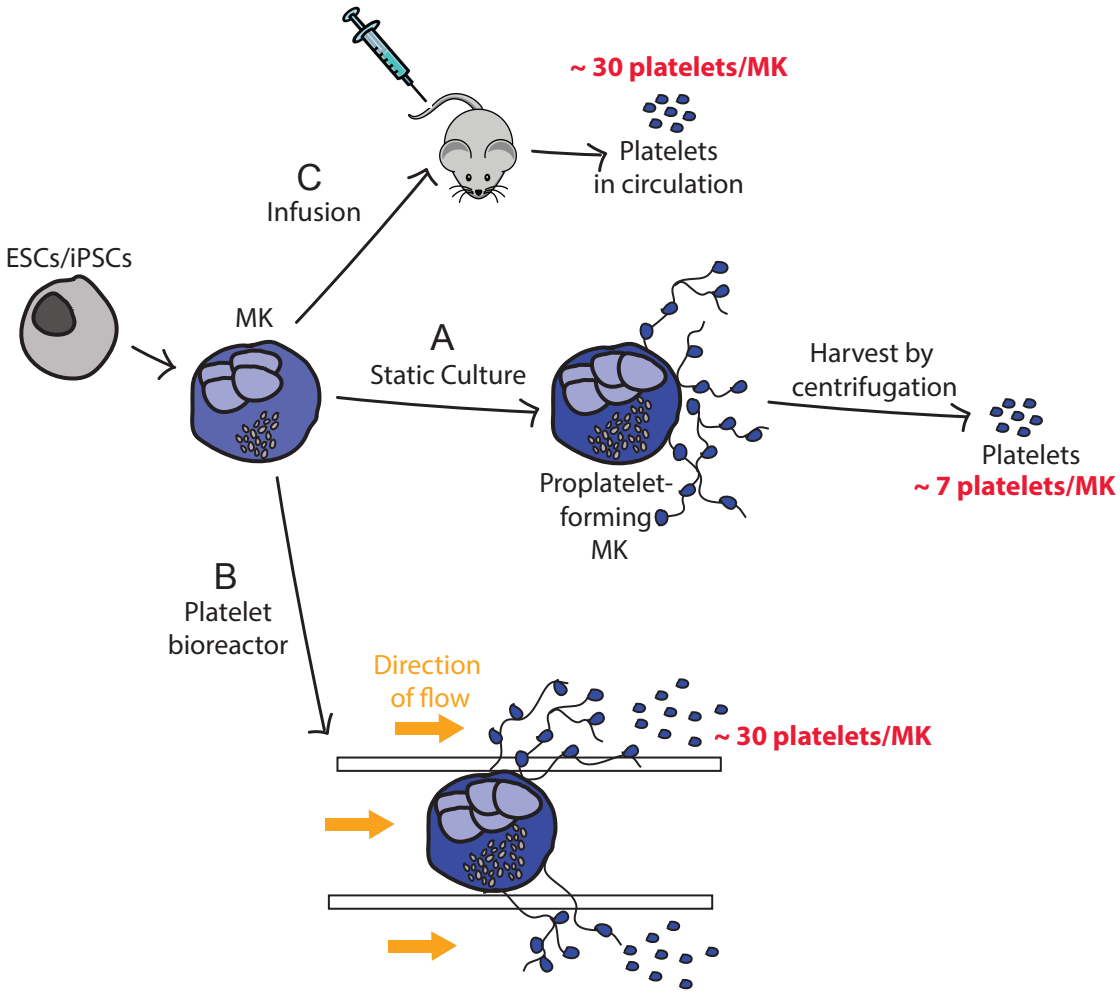

Figure 1.4: Current Methodologies for Generating Stem Cell-derived Platelets (A) MKs differentiated from ESCs and iPSCs in static culture form proplatelets in culture. The platelets that are shed in culture can be purified from the culture medium by centrifugation methods. This method yields approximately 7 platelets per MK. (B) MKs can be infused into a platelet bioreactor, which enhances proplatelet formation with the incorporation of endothelial cell contacts, extracellular matrix components and shear stress, yielding about 30 platelets per MK. (C) MKs infused into immunodeficient mice travel to the lung capillary bed and release platelets into the circulation, yielding about 30 platelets per MK.

CHAPTER 2

Materials and Methods

2.1 Culture and Maintenance of Human iPSCs

TAR syndrome patient-specific iPSC lines (TAR1, TAR2, TAR128) and multiple control iPSC lines from related family members (CTL2, CTL129, CTL130) and unrelated wild-type individuals (CTL3, CHOPWT4, CHOPWT6) were reprogrammed by the Stem Cell Core at the Children's Hospital of Philadelphia (CHOP), using either a lentiviral (TAR1, CHOPWT6) or sendai viral (TAR2, CTL2, CTL3, TAR128, CTL129, CTL130, CHOPWT4) approach.

iPSCs were maintained on irradiated mouse embryonic fibroblasts (MEFs) plated on gelatin-coated 6-well tissue culture plates. The human ES cell maintenance media consists of 85% DMEM/F12, 15% knockout serum replacement, 2 mM glutamine, 50 U/ml penicillin, 50 µg/ml streptomycin, 100 µM non-essential amino acids, 0.075% sodium bicarbonate, 1 mM sodium pyruvate (all from Invitrogen), 10^{-4}M β-mercaptoethanol (Sigma) and 10 ng/ml human recombinant basic fibroblast growth factor (bFGF) (Stemgent). iPSCs were passaged every 4 to 6 days by dissociating with TrypLE™ (Invitrogen) and replating with 10 µM Rho-associated protein kinase (ROCK) inhibitor (Y-27632) (TOCRIS).

2.2 Differentiation of Primary Human CD34$^+$ HPCs into MKs

Human CD34$^+$ HPCs, purchased from the Fred Hutchinson Cancer Research Center, Co-operative Center for Excellence in Hematology Hematopoietic Cell Processing and Repository Core, were differentiated into MKs for 16 days in a MK differentiation media.[93]

2.3 Differentiation of Human iPSCs to HPCs and MKs

iPSCs were differentiated into HPCs as described previously.[119] HPCs were differentiated into erythrocytes in a serum-free differentiation (SFD) medium (75% IMDM (Corning), 25% Hams-F12 (Corning), 50 U/ml penicillin, 50 µg/ml streptomycin, 0.05% BSA, 0.5X B-27 supplement (Gibco) and 0.5X N2 supplement (Gibco)) with recombinant human stem cell factor (SCF) (50 ng/ml) (R&D systems) and erythropoietin (EPO) (2 U/ml) for 5 days before flow cytometric analysis. HPCs were differentiated into MKs in SFD medium with recombinant human SCF (50 ng/ml), interleukin-3 (IL-3) (10 ng/ml) (R&D systems) and thrombopoietin (TPO) (50 ng/ml) (R&D systems) for 5 days before flow cytometric analysis. HPCs can also be differentiated into MKs in the same MK differentiation medium[93] as $CD34^+$ HPCs.

2.4 Fluorescence-activated Cell Sorting (FACS)

Day 14 MKs were stained with CD42a-Phycoerythrin (PE) (BD Pharmingen) in pre-sort media (Iscove's Modified Dulbecco's Medium (IMDM) (Corning), 10% fetal bovine serum (FBS) (Tissue Culture Biologics), 1% DNase (Roche)) on ice for 30 minutes and washed twice prior to sorting. $CD42a^+$ HG and LG MKs were sorted into post-sort media (IMDM, 40% FBS, 1% DNase) and cultured separately for another 6 days.

Day 11 or 14 MKs were pulse labeled with 200 nM of FV-Alexa-647 in MK differentiation media for 1 hour at 37°C. CD42b-PE (BD Pharmingen) antibody was added during the last 20 minutes of the labeling period. MKs were washed twice with pre-sort media prior to sorting. $CD42b^{low}/FV^-$, $CD42b^{high}/FV^-$ and $CD42b^{high}/FV^+$ MKs were sorted into post-sort media and lysed in lysis buffer provided in the RNAeasy micro kit (Invitrogen) before storing at -80°C. Cell sorting was performed using a FACS Aria II (Becton Dickinson).

2.5 Flow Cytometry

Flow cytometry was performed using a FACSCanto II flow cytometer (Becton Dickinson). Flow cytometry data were analyzed using the FlowJo software program (Treestar). The full list of antibodies can be found in Tables 2.1 – 2.3.

For staining of cell surface markers, cells were processed to obtain single cell suspensions. Single cells were stained with the appropriate antibodies in FACS buffer containing Dulbecco's Phosphate Buffered Saline (PBS) (Corning) with 0.1% bovine serum albumin (BSA) (Sigma) and 0.1% sodium azide (Sigma), for 15 minutes at room temperature (RT), in the dark. Cells were washed twice in FACS buffer post-staining before flow cytometric analysis.

For Annexin V staining, cells were stained in Annexin-binding buffer (10 mM HEPES, 140 mM NaCl and 2.5 mM $CaCl_2$, pH7.4) for 15 minutes at RT in the dark and diluted with Annexin-binding buffer before flow cytometric analysis. To detect DNA fragmentation, TUNEL staining was performed on MKs using the APO-DIRECT kit (BD Pharmingen) according to manufacturer's instructions.

For intracellular staining of alpha-granule proteins, cells were fixed in 1.6% paraformaldehyde (PFA) (Electron Microscopy Sciences) at 37°C for 30 minutes, then washed twice with FACS buffer to remove PFA. Fixed cells were stored in FACS buffer at 4 °C. Fixed cells were permeabilized and stained in saponin buffer (Biolegend) with the appropriate primary antibodies at RT for 30 minutes. Cells were washed twice in saponin buffer post-staining and incubated with the appropriate secondary antibodies at RT for 30 minutes. Finally, cells were washed twice in saponin buffer and resuspended in FACS buffer before flow cytometric analysis.

To determine RNA content, thiazole orange (TO) staining was performed on day 14 MKs. A stock of TO (1 mg/ml) (Sigma) was prepared by dissolving powdered TO in 100% methanol. MKs were stained with TO (100 ng/ml final concentration) for 15 minutes at room temperature and washed twice before analyzing by flow cytometry.

For ploidy analysis, MKs were stained with Vybrant DyeCycle Violet (Invitrogen) according to manufacturer's instructions.

2.6 Agonist Stimulation of MKs

MKs were centrifuged at 200*g* for 5 minutes and resuspended in Tyrode's salt solution (Sigma) with 0.1% BSA (Sigma) to a final concentration of 1-4 x 10^6 cells/ml. MKs were stained with anti-CD42a, anti-CD42b, PAC-1 (see Table 2.1) and stimulated with 500 ng/ml of convulxin (Enzo) or 50 μM of protease-activated receptor 1 (PAR1) activating peptide in a final volume of 50 μl for 20 minutes at RT in the dark. 450 μl of ice cold Tyrode's salt solution with 0.1% BSA was added to the MKs post-stimulation and kept on ice until flow cytometric analysis.

2.7 Metalloproteinase Inhibitor and Apoptosis Inhibitor Treatment of MKs

MKs were treated with metalloproteinase inhibitor GM6001 (Calbiochem) (100 μM) or pan-caspase inhibitor Q-VD-Oph (ApexBio) (25 μM) continuously from day 8 to 15 of MK differentiation. The effects of these treatments on apoptosis and CD42b shedding on MKs were analyzed using flow cytometry. The effects on platelet production were evaluated by infusing treated MKs into immunodeficient NSG mice (see section 2.10) and by analyzing platelet-like particles produced in vitro (see section 2.11).

2.8 Pulse Labeling of MKs with Coagulation Factor V (FV)

MKs were pulse-labeled with FV by incubating with 200 nM of a previously described FV variant[120] tagged with Alexa-488 or Alexa-647 for 1 hour at 37°C. MKs were washed with 40 mls of IMDM to remove excess FV. MKs were analyzed at specified time points post-incubation. The platelet-generating capability of FV-labeled MKs was evaluated by infusing MKs into NSG mice (see section 2.10) and by analyzing platelet-like particles produced in vitro (see section 2.11).

2.9 Immunofluorescence Staining and Confocal Microscopy of MKs

Day 11 or 14 MKs were adhered to fibronectin-coated glass coverslips. Adherent MKs were incubated with 200 nM of FV-Alexa-488 for 1 hour or 20 nM of FV-Alexa-488 overnight at 37°C. Adherent MKs that were not incubated with FV-Alexa-488 were used as negative controls. Adherent MKs were fixed with 2% PFA in PBS for 20 minutes at RT and washed with sterile PBS prior to staining. MKs were costained with rabbit anti-human von willebrand factor (VWF) (Dako) and goat anti-human CD42b (Santa Cruz) or mouse anti-human CD41 (Millipore) in PBS, 0.2% saponin, 0.1% BSA in the dark for 1 hour at room temperature and washed 3 times with PBS. MKs were then incubated with secondary antibodies in PBS, 0.2% saponin, 0.1% BSA in the dark for 45 minutes at room temperature. Secondary antibodies included donkey anti-rabbit Alexa-647 (Jackson) for VWF, donkey anti-goat Alexa-594 for CD42b (Thermo Fisher) and goat anti-mouse Alexa-594 for CD41 (Thermo Fisher). After secondary antibody incubation, MKs were washed with PBS before nuclear staining with DAPI in PBS, then washed again with PBS. A few drops of Vectashield was added to protect the fluorescence. Confocal imaging of MKs was performed using a DMi8 microscope (Leica Biosystems) equipped with a 63x Plan Apochromat objective (1.4NA) and a Hamamatsu Photonics

ORCA-Flash4.0 sCMOS digital camera. Images were acquired in z-stacks using a 0.2-micron step size with VisiView (Visitron Systems) software.

2.10 MK Infusion Studies in Immunodeficient Mice

NSG mice were produced at the CHOP using breeders from Jackson Laboratory. Cultured human MKs (2-7 x 10^6) were infused through the tail vein into NSG male mice between 8-12 weeks of age. 10 µl of fresh whole blood was collected retro-orbitally from the same mouse at specified time points following the infusion of human MKs. To detect the presence of human platelets in the mouse circulation, whole blood was stained using mouse anti-human CD42a-PB and CD42b-APC antibodies (see Table 2.1). CHOP's Institutional Animal Care and Use Committee approved all animal experiments. To determine the effect of Q-VD-Oph treatment on platelet production post-infusion, MKs were treated with Q-VD-Oph as described in section 2.7. To determine if FV-labeled MKs generated FV-labeled platelets when infused into NSG mice, day 11 MKs were labeled with FV as described in section 2.8.

2.11 Analysis of In Vitro Platelet-like Particles

To analyze in vitro platelet production from FV-labeled MKs, day 11 or 14 MKs were labeled with 200 nM of FV-Alexa-647 for 1 hour at 37 °C, washed twice and resuspended in fresh MK differentiation media. In vitro platelet-like particles were collected 24 hours post-labeling for analyses. To collect in vitro platelet-like particles, MKs were centrifuged at 335*g* for 3 minutes. The supernatant containing platelet-like particles was collected and 1 µM of prostaglandin E1 (PGE1, Sigma) was added to inhibit the activation of platelet-like particles during centrifugation. The supernatant was then centrifuged at 1455*g* for 8 minutes. The pellet of platelet-like particles was resuspended in final resuspension buffer made up of Tyrode's buffer with 0.2% bovine

serum albumin (BSA, Sigma). CD42a, CD42b expression and Annexin V binding of platelet-like particles were analyzed by flow cytometry. Activation of platelet-like particles was performed with 50 μM of PAR1-activating peptide in final resuspension buffer and analyzed by flow cytometry. Human donor platelets were prepared as control.

2.12 Cremaster Laser Injury Model for Thrombus Formation In Vivo

To examine released human platelet incorporation into thrombi, laser injuries were induced in the creamster arterioles of NSG mice 30 minutes after the infusion of MKs labeled with FV and calcein and thrombus formation was recorded. Day 11 MKs (2 to 7 x 10^6) MKs were labeled with FV-Alexa-488 as in section 2.8 and 2 μM calcein red-orange (ThermoFisher) for 20 minutes at 37°C before infusing into the jugular vein of NSG mice. To visualize the clot, anti-mouse CD41-Alexa647 Fab fragments (BD Pharmingen) were injected intravenously prior to the induction of laser injuries. All animal studies were approved by CHOP's institutional committee for animal welfare.

2.13 Preparation of Primary Human Bone Marrow Aspirates for Flow Cytometry

20 mls of human bone marrow aspirates were drawn from the hip into syringes containing 5 mls of heparin. Aspirates were filtered through a 70 μm nylon mesh and diluted with Hanks Balanced Salt Solution (HBSS) (ThermoFisher). Diluted aspirates were layered over Percoll (GE healthcare) and spun at 400*g* for 30 minutes with no brake. The second layer from the top, including the red blood cells, was collected. Red blood cell lysis was performed with ammonium chloride (STEMCELL technologies) at a volume:volume ratio of 1:1 and incubated at room temperature for 10 minutes. Aspirates were then washed with HBSS twice and spun down at 400*g* for 5 minutes. Washed aspirates are diluted to 20 x 10^6 cells/ml and stained with anti-CD42a-PB and anti-CD42b-PE antibodies (see Table 2.1) before flow cytometric analysis was performed.

2.14 Genotyping of Human iPSCs

To check for the presence of disease-associated single nucleotide polymorphisms (SNPs) in the 5' untranslated region (UTR) and the 3' UTR, the appropriate regions were amplified by PCR using Platinum® Blue PCR SuperMix (Invitrogen) and then purified using NucleoSpin® Gel and PCR Clean-up (Macherey-Nagel) prior to sequencing. Table 2.4 shows the sequences of primers used to amplify and sequence the specified regions.

2.15 Vector Cloning for Targeting a Doxycycline-inducible System for Transgene Expression into the AAVS1 Locus

Zinc finger nucleases (ZFNs) targeting the intron 1 of the AAVS1 gene[121] were synthesized and subcloned into a Phosphoglycerate kinase (PGK) promoter-driven expression vector: PGK-AAVS1-ZFN-Left (addgene #60915) and PGK-AAVS1-ZFN-Right (addgene #60916). Two targeting vectors with arms of homology to the AAVS1 locus were constructed: 1) AAVS1-SA-2A-NEO-CAG-RTTA3 (addgene #60431) express a reverse tet activator (rtTA) driven by a constitutive chicken-actin (CAG) promoter and confers neomycin resistance and 2) AAVS1-SA-2A-PURO-TRE-RBM8A express *RBM8A* driven by a tet-response element (TRE) and confers puromycin resistance (Figure 2.1). The two targeting vectors are designed to confer dual drug resistance to double-targeted clones. To create the AAVS1-SA-2A-PURO-TRE-RBM8A, the coding cDNA sequence with a 106 base pair (bp) partial 3' UTR of the human *RBM8A* gene (ENST00000583313.6) was cloned into the AAVS1-SA-2A-PURO-TRE-eGFP vector (addgene #22074), replacing the eGFP portion of the vector.

2.16 Targeting a Doxycycline-inducible System for Expressing *RBM8A*/Y14 into the AAVS1 Locus

Matrigel (Corning) diluted 1:3 with Iscove's Modification of DMEM (IMDM) (Corning) (1:3 diluted matrigel) was used to coat 6-well tissue culture dishes prior to the plating of irradiated drug resistant DR4 MEFs (ATCC SCRC-1045.1). TAR1 and TAR2 iPSC lines were plated on 1:3 diluted matrigel-coated plates with DR4 MEFs the day before transfection. 1.5 µg of each targeting vector and 0.2 µg of each expression vector were diluted in IMDM and mixed with 10.2 µl of XtremeGENE9 transfection reagent (Roche) to a final volume of 100 µl. The transfection mixture was left to incubate at room temperature for 20 minutes before it was added drop wise into a single well of iPSCs. Medium was changed the next day to remove the transfection reagent. Double-targeted clones were selected by a two-step drug selection procedure commencing 48 hours after transfection, with 0.5 µg/ml of puromycin (Sigma) for 2 days followed by 40 µg/ml of neomycin (G418) (Life Technologies) for 10 days. Surviving clones were manually picked and screened for integration of both targeting vectors by PCR and Southern blot analysis. A more detailed description of the protocol can be found in Sim X et al.[122]

2.17 PCR Screen for Successful Targeting of the Doxycycline-inducible System into the AAVS1 Locus

Genomic DNA from surviving clones post-drug selection was isolated using the DNeasy Blood and Tissue kit (Qiagen). PCR was performed on genomic DNA using Platinum® Blue PCR SuperMix (Invitrogen). 3 sets of screening primers were used to check for the successful integration of both targeting vectors into the AAVS1 locus. The locations of the 3 screening primer sets are shown in Figure 2.1. The sequences of the primer sets, expected band sizes and the purposes of each primer sets are described in Table 2.5.

2.18 Southern Blot

Southern blot analysis was performed to detect any off-target integration of targeting vectors into random regions of the genome. Genomic DNA from surviving clones post-drug selection was isolated using the DNeasy Blood and Tissue kit (Qiagen). 5-10 µg of genomic DNA was digested overnight at 37°C using restriction enzyme SPH1-HF (New England Biolabs). Separation of digested genomic DNA was performed on a 0.7% agarose gel by electrophoresis. The separated genomic DNA was then transferred onto an Amersham Hybond-N^+ membrane (GE Healthcare) using an upward capillary transfer method under alkaline conditions and cross-linked to the membrane by ultraviolet radiation. The membrane was blocked by incubating with for an hour with PerfectHyb™ Plus hybridization buffer (Sigma) in a rotating tube in a hybridization oven set at 62 °C. A 480 bp fragment digested from the targeting vector AAVS1-SA-2A-PURO-RBM8A using restriction enzyme BamHI (New England Biolabs) was used as the probe. The probe was radioactively labeled with ^{32}P-α-dCTP using Prime-It II Random Primer Labeling kit (Agilent) prior to overnight hybridization with the membrane at 62 °C. The membrane was processed through a series of low stringency wash steps using 2X saline sodium citrate (SSC) buffer with 0.2% sodium dodecyl sulfate (SDS) at 25 °C, followed by high stringency wash steps using 0.2X SSC buffer with 0.2% SDS at 62 °C. The resulting membrane was exposed to BioMax MS film (Sigma) for 24 hours before developing. If the AAVS1 locus is correctly targeted with both constructs for the doxycycline inducible transgene expression system, the resulting film should show two bands that are 3.4 kb and 3.7 kb (Figure 2.1).

2.19 Genome Editing Using CRISPR/Cas9 System

Given *RBM8A*'s role in critical cellular functions, knocking out *RBM8A* is likely to be lethal, thus gene editing was carried out in the TAR2 iPSC line, which has doxycycline-

inducible expression of *RBM8A* from the AAVS1 locus (referred to as TAR2 TRE-RBM8A). Doxycycline (1 µg/ml) was added throughout the course of gene editing to maintain a basal level of *RBM8A* expression, in case knocking out *RBM8A* is lethal.

To knock out *RBM8A* using CRISPR/Cas9 technology, guide RNAs (gRNAs) were designed to cut around the 5' UTR/ ATG start site border of *RBM8A* such that it will not cut the *RBM8A* cDNA sequence that was previously targeted into the AAVS1 locus. A 200 bp oligo repair template carrying arms of homology to the region around the cut site and also encoding a frameshift mutation that creates a stop codon 5 amino acids downstream from the starting methionine residue was designed. Homology-directed repair using the oligo repair template will result in a null *RBM8A* allele and the introduction of a XhoI restriction enzyme site, which can be used for screening successfully edited clones (Figure 2.2).

The gRNA sequence: 5'-ATCTCGATCGAAGGCGAGATGG-3' was cloned into an expression vector (addgene #41824) using the Gibson Assembly® cloning kit (New England Biolabs) as described in Mali et. al..[123] TAR2.1 DT67 iPSCs were plated on 1:3 diluted matrigel-coated 6-well plates with MEFs a day prior to transfection. 0.5 µg CAS9-GFP plasmid (Addgene #44719), 0.5 µg gRNA expression plasmid and 1 µg oligo repair template were diluted with IMDM and mixed with 3 µl of XtremeGENE9 transfection reagent (Roche) to a final volume of 100 µl. The transfection mixture was incubated at room temperature for 20 minutes before it was added dropwise to 1 well of iPSCs. 18-24 hours post-transfection, iPSCs were trypsinized and GFP^+ cells were sorted and plated at low density (<10,000 cells per 10 cm dish) in human ES cell maintenance media with ROCK inhibitor (Y-27632) (TOCRIS) on 1:3 diluted matrigel-coated 10 cm dishes with MEFs. Single colonies that emerge after 10-12 days of culture were manually picked and

screened for mutations in *RBM8A*. Genomic DNA for mutation screening was isolated using the DNeasy Blood and Tissue kit (Qiagen). PCR primers were used to amplify a 733 bp fragment, which will be cut by XhoI restriction enzyme into 579 bp and 154 bp fragments if the oligo repair template was integrated into the *RBM8A* locus. Table 2.6 contains the list of primers used for screening and sequencing.

2.20 Western Blot

To determine Y14 protein expression, western blotting was performed on protein harvested from iPSCs. Confluent wells of iPSCs were treated with Accutase (Life Technologies) and passaged 1:1 into 6-well low cluster plate to deplete MEFs and to form embryoid bodies. iPSCs were cultured as embryoid bodies for 2 days before they were trypsinized into single cells and frozen as cell pellets in -80 °C. A 2X Sodium dodecyl sulfate (SDS) sample buffer stock, composed of 187.5 mM Tris-HCl (pH 6.8), 6% SDS, 30% glycerol and 0.03% bromophenol blue, was prepared for protein extraction. Frozen cell pellets were lysed in 1X SDS sample buffer for protein extraction at a concentration of 2.5 x 10^6 cells per ml. Protein lysates were sonicated in pulsed mode for 10 seconds then boiled at 95 °C for 5 minutes and kept on ice until they were ready to be loaded onto the gel. 20 µl of protein lysate was loaded into each well of a NuPAGE® Novex 12% Bis-Tris gel (Invitrogen) and separated by electrophoresis in 1X NuPAGE® MOPS buffer (Invitrogen) and then transferred onto a polyvinylidene fluoride (PVDF) membrane (Thermo Fisher). The membrane was blocked in 5% nonfat dry milk in PBS for at least 3 hours at 4 °C before incubating with primary antibodies against Y14 (4C4) (Santa Cruz) and beta actin (Santa Cruz) diluted in 1% nonfat dry milk in PBS with 0.1% Tween-20 (Sigma) (PBS-T) overnight at 4 °C. Anti-Y14 primary antibody was used at 1:200 dilution while anti-beta actin antibody was used at 1:500 dilution. Following primary antibody incubation, the membrane was washed twice for 10 minutes with PBS-

T before it was incubated with goat-anti-mouse-horse radish peroxidase (HRP) secondary antibody (Biorad) (1:5000 dilution) in 1% milk/PBS-T at RT on a rocker for 2 hours. The membrane was washed thrice for 5 minutes with PBS-T and then incubated with Pierce™ enhanced chemilumescent (ECL) substrates (Thermo Fisher) before exposure to Hyblot CL autoradiography film (Denville Scientific) for developing.

2.21 Reverse Transcription and Quantitative Real Time Polymerase Chain Reaction (qRT-PCR)

Cells were lysed in lysis buffer provided in the RNAeasy micro kit (Invitrogen) and stored at -80 °C. Total RNA was extracted using the RNAeasy micro kit according to manufacturer's instructions. Reverse transcription of total RNA to cDNA was performed using the SuperScript™ III Reverse Transcriptase kit (Invitrogen). qRT-PCR reactions were performed using SYBR-GreenER qPCR Master Mix (Roche) on a LightCycler 480 II (Roche). TATA box binding protein (TBP) was used as the housekeeping gene to determine relative gene expression.[124] The primers used for qRT-PCR are listed in Table 2.7.

2.22 Colony Assays to Determine the Hematopoietic Potential of HPCs

HPCs were plated in a methylcellulose-based medium, Methocult™ H4435 Enriched (STEMCELL technologies) in 35 mm dishes according to manufacturer's instructions. 5 – 10 x 10^3 HPCs were plated per 35 mm dish. Colonies are counted 12-14 days after plating.

2.23 MK Colony Assays to Determine the Megakaryocytic Potential of HPCs

HPCs were plated in a collagen-based medium, MegaCult™-C (Invitrogen) in double chamber slides according to manufacturer's instructions. 5 – 10 x 10^3 HPCs were plated

per slide. Slides were fixed and stained to identify MK colonies after 12 days of culture. MK colonies are enumerated.

2.24 Statistical Analysis

All data are represented as mean ± standard error of the mean (SEM). Differences are analyzed using the Student's *t* test in GraphPad Prism 5 and are considered significant if the *p* value is smaller than 0.05.

Table 2.1: Conjugated Antibodies for Flow Cytometry

Fluorophore	Antibody	Dilution	Company
Phycoerythrin (PE)	CD41a	1:50	BD Pharmingen
	CD42a	1:20	BD Pharmingen
	CD42b	1:20	BD Pharmingen
	PF4	1:100	LSBio
	SSEA4	1:2000	Biolegend
Fluorescein Isothiocyanate (FITC)	CD43	1:50	Biolegend
	CD91 (LRP1)	1:20	BD Pharmingen
	AnnexinV	1:20	Biolegend
	PAC-1	1:10	BD Pharmingen
Pacific Blue(PB)	CD42a	1:20	eBioscience
	CD45	1:100	Biolegend
Allophycocyanin (APC)	CD18	1:20	BD Pharmingen
	CD42b	1:20	Biolegend
	CD235a	1:10000	BD Pharmingen
Alexa647	CD309 (KDR)	1:100	Biolegend
	SSEA3	1:50	Biolegend
	AnnexinV	1:20	LifeTechnologies
PECy7	CD31	1:100	Biolegend

Table 2.2: Unconjugated Primary Antibodies for Flow Cytometry

Antibody	Species	Dilution	Company
Basic Fibroblast Growth Factor (bFGF)	Rabbit IgG	1:20	Abcam
Vascular Endothelial Growth Factor (VEGF)	Rabbit IgG	1:20	Abcam
Endostatin (Col18A)	Mouse IgG2b	1:100	Santa Cruz

Table 2.3: Secondary Antibodies for Flow Cytometry

Antibody	Dilution	Company
Goat anti-rabbit-Alexa647	1:400	Jackson Immunoresearch
Goat anti-mouse IgG2b-Alexa488	1:400	Jackson Immunoresearch
Goat anti-mouse IgG1-Alexa488	1:400	Jackson Immunoresearch

Table 2.4: Primers for amplifying and sequencing SNPs in the 5' and 3' UTR

Purpose	Sequence
Amplify 280 bp fragment in the 5' UTR	Forward: 5'-CAATTTGCGTGTTTTTACCGTGCAG-3' Reverse: 5'-ATTTTCCTATTATAGCCTTCTCTCG-3'
Sequence 5' UTR SNP	Forward: 5'-CTTGACTGGCGACCTTTCCC-3' Reverse: 5'- CCCAGCCTCGTGAAGATCTA-3'
Amplify 402 bp fragment in the 3' UTR	Forward: 5'-GGTCCACCAAAAGGCAAGAG-3' Reverse: 5'-CCATACAGCCTTGCTATGCTTT-3'
Sequence 3' UTR SNP	Forward: 5'-AGGGCAAATACTGTCTGGGTG-3' Reverse: 5'-CGCAACTCAAATACTACGCAT-3'

Table 2.5: Screening Primers for Generating a Doxycycline-Inducible *RBM8A* Expression System

Primer Set and Purpose	Sequence	Expected Band Size
WT-- Screen for the absence of WT band	Forward: 5'-CCCCTATGTCCACTTCAGGA-3' Reverse: 5'-CAGCTCAGGTTCTGGGAGAG-3'	500 bp
AAVS1-CAG -- Screen for the integration of the CAG-RTTA3 plasmid	Forward: 5'-GAGCATCTGACTTTGGCTAATA- 3' Reverse: 5'-GAAGGATGCAGGACGAGAAA-3'	1,920 bp
AAVS1-TRE -- Screen for the integration of TRE-RBM8A plasmid	Forward: 5'-GCAATAGCATCACAAATTTCAC-3' Reverse: Same as AAVS1-CAG-Reverse	1,380 bp

Table 2.6: Screening and Sequencing Primers for Generating *RBM8A* Knockout iPSCs

Primer set	Sequence
RBM8A knock out screening primers	Forward: 5'-CCAACCGTATTGCAACCAAG-3' Reverse: 5'-GTTCCTCGATTCCCATCCTT-3'
RBM8A knockout sequencing primers	Forward: 5'-ATTGGTCAGCTTGACTGGC-3' Reverse: 5'-AGCCTTCTCTCGCACCTTC-3'

Table 2.7: qRT-PCR primers

Gene	Primer sequence
C-MYC	Forward: 5' –CAAATGCAACCTCACAACCTTGGC-3' Reverse: 5'- GCCCAAAGTCCAATTTGAGGCAGT-3'
GATA1	Forward: 5'-CGAAACCGCAAGGCATCTGGAAA-3' Reverse: 5'-GCCACCACCATAAAGCCACCA-3'
NFE2	Forward: 5'- GGGTGGAACTGCTGATGGGATTT-3' Reverse: 5'- GTTGCCATTGTCATCCTCTTCTGG-3'
PF4	Forward: 5'- ACTGGAAGGACAGCCGGGAATAAA-3' Reverse: 5'- TCAGTGCTCAGTGCGATGGGAAA-3'
RBM8A	Forward: 5'- TTCATCTCAACCTCGACAGGCGAA-3' Reverse: 5'-ATAGCAGCCTGGGCTTCCTTGTAT-3'
TBP	Forward: 5'-TTGCTGAGAAGAGTGTGCTGGAGATG-3' Reverse: 5'-CGTAAGGTGGCAGGCTGTTGTT-3'
TUBB1	Forward: 5'- GGATGGGCACTCTGCTCATGAAC-3' Reverse: 5'- GTTGTAGGGCTCCACCACAGTG-3'
VWF	Forward: 5'-CTGTGATGAGAACGGAGCCAATG-3' Reverse: 5'-GCTGCACAGTCCATTCCTGAAC-3'

Figure 2.1

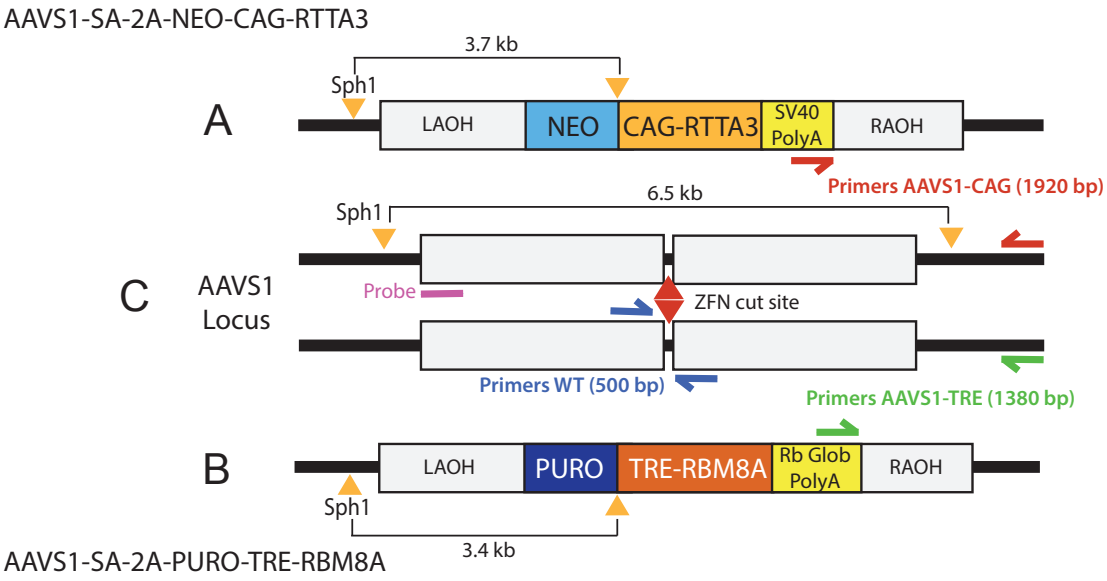

Figure 2.1 Design of Targeting Vectors and Screening Strategy for Generating a Doxycycline-Inducible Transgene Expression System Two targeting constructs AAVS1-SA-2A-NEO-CAG-RTTA3 (A) and AAVS1-SA-2A-PURO-TRE-RBM8A (B) are targeted into the AAVS1 locus (C). The two constructs carry arms of homology to the AAVS1 locus. The left and right arms of homology (LAOH and RAOH) are shown. The approximate locations of the 3 screening primer sets and the expected sizes of the PCR products are indicated. For Southern blotting, SphI restriction enzyme is used to digest the DNA. SphI restriction sites in the constructs and the endogenous locus and the expected sizes of the fragments detected by the probe are shown.

Figure 2.2

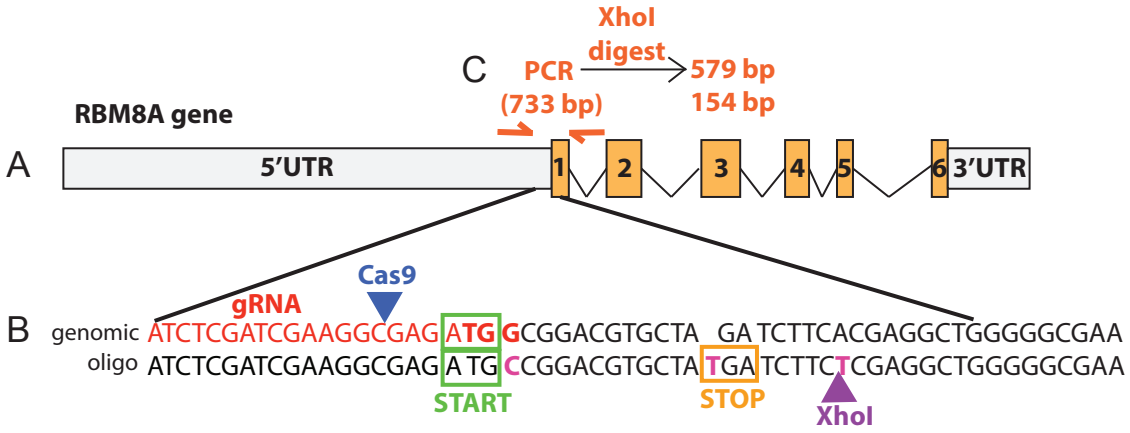

Figure 2.2: Strategy for Generating *RBM8A* Knock-out iPSCs (A) The *RBM8A* gene consists of 6 exons as labeled. (B) (Top) Partial genomic sequence of the *RBM8A* gene between the 5' UTR and exon 1. The guide RNA (gRNA) sequence used to target Cas9 to the *RBM8A* gene is labeled in red. The PAM sequence (TGG) is shown in bold. The Cas9 cut site is indicated as shown. The ATG start site is highlighted with the green box. (Bottom) The partial sequence of the 200 bp oligo repair template is shown. Mutations to the original genomic sequence are shown in pink. The G/C mutation at the PAM sequence prevents re-cutting of the repair template after incorporation into the *RBM8A* locus. A T insertion creates a stop codon as shown. An A/T mutation creates an XhoI restriction enzyme site for screening purposes. (C) Approximate locations of the PCR screening primers are shown. The 733 bp PCR product is digested with XhoI restriction enzyme. If the oligo repair template is successfully integrated into the *RBM8A* locus, the PCR product will be digested into 579 bp and 154 bp fragments.

CHAPTER 3

Factor V Uptake as a Marker of Mature Human Stem Cell-derived Megakaryocytes

3.1 Introduction

The first report of in vitro-generated platelets[59] raised the possibility that stem cell-derived platelets may be produced to complement or displace donor-derived platelets clinically.[125–127] Although considerable progress has been made in the generation of platelets from HSCs,[92–94] ESCs and iPSCs,[87–89,91,128] there remain important challenges to overcome before we can realize the goal of transfusing stem cell-derived platelets into humans. Low platelet yield and poor functionality have been important challenges in the field.[129–132] In part, these unresolved challenges stem from gaps in a detailed understanding of MK maturation in vitro, including defining the mature MKs that are optimally primed to release platelets and directing cultured MKs to this stage.

MK maturation is accompanied by an increase in cell size, ploidy, granular components, MK-specific surface receptors, and the formation of an IMS. [33,35,36,133,134] Whether these changes occur sequentially or as a continuum is unclear as is a definition of a mature MK that is primed for thrombopoiesis.

Human bone marrow MKs have been classified into 4 developmental stages based on size and ploidy: stage I MKs are 10-15 μm (2N/4N), stage II MKs are 14-20 μm (4N/8N), and stage III/IV MKs are 20-40 μm (8N-128N).[135] The ultrastructural features at these stages have been described qualitatively using electron micrographs of primary human bone marrow MKs, but these MKs differ greatly from the in vitro-generated MKs, which are significantly smaller and with a ploidy that rarely exceeds 16N.[25,136] The gene expression profiles of MKs of different ploidy have been compared,[45,46] but gave little

insights into what defines a mature MK primed for thrombopoiesis when infused into a bioreactor[102,103,137] or into mice.[113,138] We hypothesize that there may be a transient stage of MK development that is highly efficient in undergoing thrombopoiesis and that selective harvesting and/or optimizing the yield of these MKs may enhance functional platelet yield.

We examined cell size and granularity changes during human MK differentiation in vitro and identified discrete MK maturation stages with distinct granularity, which we termed the low granular (LG) and high granular (HG) MKs. We further demonstrated that the immature LG MKs give rise to mature HG MKs, which are subdivided into a functional $CD42b^+$ population that produces platelets in vitro and after infusion into immunodeficient mice, and an apoptotic, non-functional $CD42b^-$ population. Moreover, using a labeled coagulation factor V (FV) variant, we showed that the HG/$CD42b^+$ MKs endocytose FV into alpha-granules and release functional platelets with similar size distribution as human donor platelets. Additionally, treatment of MKs with a pan-caspase inhibitor, Q-VD-Oph, prevented both apoptosis and CD42b shedding, and enriched the functional FV^+/$CD42b^+$ population. These studies further our understanding of megakaryopoiesis and thrombopoiesis and may have implications for optimizing the production of stem cell-derived platelets for transfusion.

3.2 Results

3.2.1 Identification of Distinct MK Populations During In Vitro Megakaryopoiesis

Identification of the mature, platelet-producing MKs within the heterogeneous, asynchronous MK culture would allow us to find novel ways of improving the yield and quality of stem cell-derived platelets. Thus, one goal is to determine if we can identify distinct maturation intermediates within the MK culture and if there is a specific

maturation intermediate that is primed for thrombopoiesis. Key changes associated with MK maturation include: increase in cell size, ploidy, alpha-granule content, RNA and the formation of an IMS.[33,35,36,133,134] These features lead to increased size and internal cellular complexity, which can be detected as increased forward scatter (FSC) and side scatter/granularity (SSC) respectively by flow cytometry. By examining these two parameters during the differentiation of human $CD34^+$ HPCs into MKs, we identified two MK populations distinguishable by their granularity, LG and HG MKs (Figure 3.1A). We hypothesize that these novel MK populations represent distinct developmental stages.

The LG MKs appeared around day 7, followed by HG MKs around day 10, with their percentage changing over time (Figure 3.1A). Since HG MKs appeared later and had high granularity suggestive of cytoplasmic changes associated with maturation, we hypothesized that the LG MKs give rise to HG MKs. We tested this hypothesis by sorting LG and HG MKs and examined how the granularity of these sorted populations changed with further culture. We found that the LG MKs became HG MKs upon further culture (Figure 3.1B, top), while the HG MKs remained high granular (Figure 3.1B, bottom), confirming that HG MKs came from LG MKs.

3.2.2 A Subpopulation of HG MKs Show Signs of Injury

We further characterized these two MK populations by examining a panel of known MK markers. We found surface CD42b is selectively lost from the HG population, but not the LG population (Figure 3.2A). These data further divided the cells into 3 subpopulations: LG MKs, HG/$CD42b^+$ MKs and HG/$CD42b^-$ MKs. On platelets, the loss of surface CD42b is due to metalloproteinase cleavage of the extracellular glycocalicin domain of CD42b,[139,140] and is associated with platelet activation, apoptosis and clearance.[140–144] We predict that CD42b shedding on HG MKs also signaled damage, thus we examined

the MKs for signs of apoptosis. Indeed, 80-90% of the HG/CD42b$^-$ MKs were Annexin V$^+$ and positive for terminal deoxynucleotidyl transferase dUTP nick-end labeling (TUNEL$^+$) (Figure 3.2B), indicating that these cells were apoptotic. In contrast, <20% of the LG MKs and HG/CD42b$^+$ MKs were apoptotic (Figure 3.2B). Over time, the percentage of LG MKs and HG/CD42b$^+$ MKs decreased gradually with a concomitant accumulation of apoptotic HG/CD42b$^-$ MKs (Figure 3.2C), suggesting a progression of viable MKs to a non-physiological terminal state that would likely decrease in vitro platelet yield.

As LG MKs progressed to HG/CD42b$^+$ MKs, we observe an increase in ploidy (Figure 3.2D) and some alpha-granule proteins (Figure 3.2E), most notably platelet factor 4 (PF4), a known MK maturation marker.[145] In contrast, HG/CD42b$^-$ MKs lost alpha-granule proteins and most of its RNA content (Figure 3.2E), consistent with their transition to a damaged state.

A feature of mature MKs is their ability to respond to platelet agonists.[146] To assess the responsiveness of these MK subpopulations, we analyzed the percentage of activated MKs following stimulation with platelet agonists, convulxin[147] or protease-activated receptor 1 (PAR1)-activating peptide.[148] Activation causes conformational changes in the surface glycoprotein IIb/IIIa, detectable by PAC-1 antibody.[110,111] While 70-80% of HG/CD42b$^+$ MKs activated in response to stimulation, only 20-30% of LG MKs and virtually none of apoptotic HG/CD42b$^-$ MKs responded (Figure 3.2F). These data suggested that HG/CD42b$^+$ MKs may be nearing their peak of maturation and that CD42b shedding indicated an undesirable decline of these mature MKs to an apoptotic, non-functional state.

To determine if these distinct MK populations are present in the human bone marrow, we examined the size and granularity of primary MKs from marrow aspirates. Primary MKs form a continuum of maturing MKs with increasing cell size and granularity (Figure 3.3A). Since surface CD42a and CD42b are known to increase with maturation, we compared the size and granularity of $CD42a^{high}CD42b^{high}$ MKs and $CD42a^{low}CD42b^{low}$ MKs. We observed that the mature $CD42a^{high}CD42b^{high}$ MKs in the bone marrow were both larger and more granular than $CD42a^{low}CD42b^{low}$ MKs (Figure 3.3B, top). In contrast, the cultured $CD42a^{high}CD42b^{high}$ MKs were more granular, but not bigger than the $CD42a^{low}CD42b^{low}$ MKs (Figure 3.3B, bottom). We also did not detect the presence of $CD42a^{+}CD42b^{-}$ MKs in bone marrow (Figure 3.3A). These differences between marrow MKs and cultured MKs will be further discussed.

3.2.3 FV Uptake Labels Mature, Undamaged MKs

Human coagulation FV is synthesized by the liver and circulates in the plasma.[149,150] While mouse MKs produce FV endogenously[151], human MKs endocytose FV from their surroundings and package it into alpha-granules.[42,152–154] However, the specific stage of maturation when human MKs endocytose FV is unknown.[155] The HG/$CD42b^{+}$ MKs have many characteristics of mature MKs and may be the population that is primed to release platelets. We hypothesized that the HG/$CD42b^{+}$ MKs may be able to endocytose FV and that FV uptake may be a marker of fully mature MKs.

A putative receptor for FV endocytosis is the low-density lipoprotein receptor related protein 1 (LRP1),[156] which is upregulated on the surface of mature MKs.[157] HG/$CD42b^{+}$ MKs showed higher surface LRP1 expression as compared to LG MKs (Figure 3.4A). FV uptake by MKs, as assayed by pulse-labeling MKs with a fluorescently-labeled FV variant,[120] correlated with ploidy, suggesting that FV endocytosis increased with

maturation (Figure 3.4B). Correspondingly, the HG/CD42b^{+} MKs endocytose more FV than the LG MKs (Figure 3.4C). To determine if the kinetics of FV endocytosis change over time, we pulse-labeled MKs with fluorescently-labeled FV on days 11 and 15 of the differentiation. On day 11, LG MKs showed negligible FV uptake while HG/CD42b^{+} exhibited greater FV uptake (Figure 3.4C). By day 15, both MK populations matured over time and took up FV, but the HG/CD42b^{+} MKs still endocytosed FV more efficiently than the LG MKs.

To correlate FV uptake with gene expression changes during MK maturation, we sorted CD42b^{low}/FV^{-} MKs, CD42b^{high}/FV^{-} MKs and CD42b^{high}/FV^{+} MKs (Figure 3.4D) and compared the expression of MK maturation genes in these populations. CD42b^{low}/FV^{-} MKs correspond to LG MKs, while CD42b^{high}/FV^{-} MKs correspond to the smaller HG/CD42b^{+} MKs and CD42b^{high}/FV^{+} MKs correspond to the larger HG/CD42b^{+} MKs (Figure 3.4E), consistent with FV uptake being a marker of mature MKs. We found that the expression of MK maturation genes peak as MKs gain CD42b, with little or no increase as MKs acquire the ability to endocytose FV (Figure 3.4F). These data suggest that the ability to endocytose FV is only acquired in the most mature MKs with peak expression of known MK maturation markers, indicating that FV uptake could be one of the final markers of a fully mature MK primed for thrombopoiesis.

To determine if FV localized to the alpha-granules following endocytosis, we performed immunofluorescence studies on FV-labeled MKs, co-staining for the MK surface marker (CD41 or CD42b) and an alpha-granule marker (von willebrand factor (VWF)). CD42b^{+} MKs showed a punctate distribution of intracellular FV, which partially co-localized with VWF in granules (Figure 3.5A). In contrast, we observed that CD42b^{-} MKs were associated with a very high level of FV fluorescence distinctly localized to the cell

surface (Figure 3.5B-C). We believe that this was due to FV binding to phosphatidylserine (PS) on the surface of apoptotic MKs.[120]

To confirm that the damaged HG/CD42b$^-$ MKs came from the HG/CD42b$^+$ population, we pulse-labeled MKs on day 11, when all the HG MKs are CD42b$^+$. Forty-eight hours later, the newly generated HG/CD42b$^-$ MKs had the same level of FV fluorescence as the HG/CD42b$^+$ MKs post-labeling (Figure 3.5D), indicating that the HG/CD42b$^-$ MKs came from the HG/CD42b$^+$ population and that prevention of this damage may enhance platelet yield.

3.2.4 FV-Labeled MKs Release Platelets When Infused into Immunodeficient Mice

To determine if FV-labeled HG/CD42b$^+$ MKs preferentially generated functional platelets in vivo, we infused FV-labeled MKs into NSG mice. We previously demonstrated that human donor platelets infused into NSG mice could be detected in the blood and were ~10-fold larger than mouse platelets.[113] When cultured human MKs were infused into NSG mice, we observed two distinct populations of human platelet events: (1) platelet-like particles (PLPs) with a broad size-range that have limited half-life and functionality, and (2) platelets released from pulmonary-entrapped MKs that have similar size distribution, half-life and functionality as donor platelets.[113] These data suggest that size can be used as a discriminatory factor to examine if the human platelet events detected in the circulation are more like non-functional PLPs or functional platelets.

For these studies, we used day 11 MKs to avoid the HG/CD42b$^-$ subpopulation that accumulates over time and binds FV non-specifically (Figure 3.2C and Figure 3.5B-C). Following the infusion of FV-labeled MKs, we detected both FV$^+$ and FV$^-$ human platelet events in the circulation post-infusion (Figure 3.6A-B). We observed that all FV$^+$ platelet

events were MK-derived platelets, with sizes similar or larger than donor platelets, as early as 5 minutes post-infusion and at all time points following (Figure 3.6C-E). In contrast, the FV^- platelet events had a broad range of sizes initially, indicating that they were a mixture of PLPs and MK-derived platelets, but by 1-4 hours, the short-lived PLPs were cleared, leaving mostly the MK-derived platelets in circulation (Figure 3.6C-E). These data suggest that although both FV^+ and FV^- MKs release platelets, FV^+ MKs appear primed to release platelets as soon as they encounter the right in vivo environment.

3.2.5 FV^+ Platelets Are Incorporated into Thrombi Following Laser Injury

To examine the functionality of FV^+ platelets, we performed laser injury studies following the infusion of MKs double-labeled with FV-Alexa-488 and calcein red-orange. To visualize the clot, we labeled mouse platelets with mCD41-Alexa-647 (blue). We detected both FV^+ (yellow) and FV^- (red) human platelets/PLPs in the clots (Figure 3.7A). Given that the MKs infused were 33 ± 3% FV^+ and the circulating platelets/PLPs were 29 ± 2% FV^+, the observation that FV^+ particles were present at 74 ± 6% in the clot (Figure 3.7B-C) support that FV^+ platelets were preferentially incorporated over FV^- particles, suggesting that FV^+ platelets had better functionality than FV^- platelets/PLPs.

3.2.6 FV-Labeled MKs Generate FV-Labeled PLPs In Vitro That Are Partially Functional

To determine whether FV-labeled MKs generate FV-labeled PLPs in vitro, we analyzed in vitro PLPs from day 11 FV-labeled MKs 24 hours post-labeling. All $CD42b^+$ PLPs in vitro were FV-labeled (Figure 3.8A), indicating that they came from FV-labeled HG/$CD42b^+$ MKs. There was a small but distinct subpopulation of $CD42b^-$ PLPs that were FV^{high} (Figure 3.8A), which likely came from apoptotic HG/$CD42b^-$ MKs that bind FV

through their surface PS. Consistent with published data,[89,158] the FV-labeled CD42b$^+$ PLPs were slightly larger than human donor platelets (Figure 3.8B). The FV-labeled CD42b$^+$ platelets were Annexin V^{low} and activated in response to agonist stimulation, although not as well as human donor platelets (Figures 3.8C-E), suggesting that they are partially functional. In contrast, the CD42b$^-$ PLPs were smaller than donor platelets, Annexin V^{high} and did not respond to agonist stimulation (Figures 3.8B-E), indicating that they are likely non-functional cellular debris.

3.2.7 Metalloproteinase Inhibition Protects MKs From CD42b Shedding, but Not Apoptosis

Metalloproteinase cleavage of CD42b on platelets occurs following activation, apoptosis or improper storage,[141–144,159] thus CD42b surface expression is a key parameter for assessing platelet quality. Metalloproteinase inhibitors like GM6001 prevent CD42b shedding on platelets and improve the hemostatic function and recovery of platelets post-infusion.[139] These drugs have also been used to protect in vitro-generated platelets from damage.[90,160] Since CD42b shedding and apoptosis are intricately linked events in platelets and the regulation of apoptosis in MKs is crucial for platelet formation, we examined whether inhibiting CD42b shedding can enrich the HG/CD42b$^+$ subpopulation.

Treatment of MKs with GM6001 preserved CD42b expression, but did not affect apoptosis (Figures 3.9A-B). Importantly, although the percentage of CD42b$^+$ MKs increased following treatment, many of these MKs remained apoptotic and fewer CD42b$^+$ MKs responded to agonist stimulation (Figure 3.9C), indicating that the preservation of CD42b on MKs is insufficient to preserve MK viability.

3.2.8 Apoptosis Inhibition Protects MKs From Both Apoptosis and CD42b Shedding

To examine whether apoptosis inhibition can enrich the HG/CD42b$^+$ subpopulation, we treated MKs with a pan-caspase inhibitor, Q-VD-Oph.[161,162] Q-VD-Oph inhibited both apoptosis and CD42b shedding (Figure 3.10A), resulting in a 90% reduction in the percentage of apoptotic CD42b$^-$ MKs and a 50% increase in the percentage of CD42b$^+$ MKs (Figure 3.10B). More specifically, Q-VD-Oph enriched the HG/CD42b$^+$ MKs (Figure 3.10C). These data suggested that CD42b shedding occurred downstream of apoptosis. To determine if Q-VD-Oph affected the localization of ADAM17, the metalloproteinase responsible for CD42b shedding,[140] we analyzed ADAM17 surface expression on MKs. We found that ADAM17 surface expression was upregulated with maturation and was unaffected by Q-VD-Oph (Figure 3.10D). However, the ADAM17's activity require PS exposure,[163] thus ADAM17 is poised to cleave CD42b on mature MKs, but is unable to do so unless PS is exposed following apoptosis. This also explains why CD42b shedding occurs only on HG MKs, but not on LG MKs. Therefore, we posit that by inhibiting apoptosis and PS exposure, Q-VD-Oph also prevents CD42b shedding.

Importantly, apoptosis inhibition by Q-VD-Oph did not affect ploidy or responsiveness to agonists (Figure 3.10E-F) and led to a small increase in FV uptake by the HG/CD42b$^+$ MKs (Figure 3.10G). When Q-VD-Oph-treated MKs were infused into NSG mice, we detected increased number of human platelets post-infusion (Figure 3.10H). However, Q-VD-Oph treatment led to a decrease in the yield of CD42b$^+$ PLPs in vitro (Figure 3.10I).

3.2.9 Distinct MK Populations Can Also Be Found in iPSC-Derived MK Cultures

To determine whether these MK subpopulations were present in MK cultures derived from a different stem cell source, studies were repeated with human iPSC-derived MKs. LG, HG/CD42b^{+} and HG/CD42b^{-} MK populations were present within iPSC-derived MK cultures (Figure 3.11A-B). Similarly, HG/CD42b^{+} MKs endocytosed more FV than LG MKs (Figure 3.11C). When we inhibited apoptosis with Q-VD-Oph, iPSC-derived MKs showed decreased apoptosis and CD42b shedding (Figure 3.11D). Thus, these distinct MK maturation stages are present in MK cultures derived from two different stem cell sources.

3.3 Discussion

Despite advances in the understanding of megakaryopoiesis and thrombopoiesis, it remains unclear what defines a MK that is primed to release platelets. Our studies addressed this important question through developmental staging of human stem cell-derived MKs beginning with the idea that MKs increase in size and granularity with maturation.[133] We identified distinct stages of MK differentiation with an initial maturation phase leading to a transient, functional stage, followed by a declining phase characterized by apoptosis, CD42b shedding and a loss of RNA and alpha-granule proteins (Figure 3.12). These stages are not clearly distinguishable in primary marrow MKs as mature MKs exit the marrow to shed platelets in the circulation,[54] thus, normally few or no MKs undergo apoptosis and/or CD42b shedding in the marrow. These insults may be more apparent in clinical settings like myelodysplastic syndromes and immune thrombocytopenia purpura, where intramedullary MKs fail to exit the marrow and/or undergo apoptosis.[164–167] The loss of RNA and alpha-granule proteins may be due to degranulation, typically observed in idiopathic myelofibrosis, where growth factors released from MK alpha-granules promote marrow fibrosis.[168–170] Collectively, apoptosis,

CD42b shedding and degranulation are associated with pathological clinical outcomes, suggesting that protecting cultured MKs from such insults may be important for producing high quality stem cell-derived platelets. Additionally, while primary marrow MKs increase in size and granularity as they mature, in vitro-derived MKs increase in granularity, but not in size as they mature. This result correlates with published observations that cultured MKs do not achieve high ploidy like those in vivo,[25,133,136] reiterating the idea that the size and ploidy of in vitro-grown MKs may limit platelet yields.

Unlike murine MKs, which express FV endogenously[151], human MKs endocytose FV from the surroundings. We examined if the FV uptake into alpha-granules would be a useful marker of mature, functional human MKs. When we pulse-labeled the heterogeneous MK culture with fluorescently-labeled FV, the mature HG/CD42b$^+$ MKs preferentially internalized the FV. The FV$^+$ MKs released functional platelets with a size range similar or larger than human donor platelets almost immediately post-infusion. Since newly released young platelets and pre-platelets are larger than circulating old platelets,[158,171,172] FV$^+$ platelets are likely young platelets released in vivo by infused FV-labeled MKs. Moreover, FV$^+$ platelets are overrepresented in clots following laser injury, an indication of better functionality over FV$^-$ platelets. Additionally, all functional, CD42b$^+$ in vitro PLPs are derived from the FV$^+$ MKs, reaffirming that FV$^+$ MKs are primed for platelet formation. With these new insights into the specific stage of MK maturation when FV endocytosis occurs, we can use this model to address the mechanisms of FV endocytosis and trafficking in human MKs, which is critical as mouse models do not accurately reflect human physiology in regard to FV uptake.

The heterogeneous and asynchronous nature of MK cultures makes it difficult to purify the mature MKs that are primed for platelet production. To improve the efficiency of in vitro platelet generation, we propose that FV labeling could be a tool to harvest the transient, mature MKs for platelet bioreactor use[102,103,137], particularly since MK's ability to endocytose FV is acquired after peak expression of many maturation genes. Genome-wide studies to compare $CD42b^{high}/FV^{-}$ and $CD42b^{high}/FV^{+}$ MKs may lead to the identification of novel MK maturation markers, potentially cell surface receptors that could be useful substitutes for FV for the purification of mature MKs. Alternatively, FV^{+} MKs may be infused into patients with the anticipation that they would release a large number of platelets rapidly after infusion. Apart from FV, MKs also endocytose other proteins like fibrinogen[43,52,173] and immunoglobulins.[51] Whether endocytosis of these proteins by MKs occurs at the same stage of maturation and whether they could substitute for FV uptake is presently unclear.

We also found that CD42b shedding occurs downstream of apoptosis, likely due to ADAM17 activation by exposed PS on the MK following apoptosis, thus apoptosis inhibition also prevented CD42b shedding and enriched the mature FV-labeled MKs. The role of apoptosis in platelet formation is controversial.[174] Initial studies supporting the requirement of apoptosis in platelet formation showed that caspase inhibition blocked proplatelet formation in culture and that compartmentalized activation of caspases is necessary for cytoskeletal rearrangements during platelet shedding.[175,176] However, later studies showed that mice deficient in various components of the intrinsic and extrinsic apoptotic pathways shed platelets normally.[177,178] In fact, apoptosis regulation is crucial for keeping MKs alive during platelet formation.[179] We observed increased in vivo platelet yield following infusion of Q-VD-Oph-treated MKs, but decreased in vitro yield of PLPs from the same MKs. This may be due to differences in

platelet formation in vitro and in vivo. It is tempting to speculate that in vitro PLPs may arise through an apoptotic-related process while platelet formation in vivo occurs through a different mechanism. Future studies examining in vitro and in vivo platelet formation from human MKs deficient in various components of the apoptotic pathways may shed more light on the relationship between survival, apoptosis and platelet formation.

In conclusion, we have identified distinct maturation stages within the in vitro MK culture. Within these stages, a transient, mature, functional HG/CD42b^{+} MK population becomes damaged and apoptotic over time. MKs at peak maturation endocytose FV, and this ability to endocytose FV correlates with readiness to release functional platelets when infused into immunodeficient mice. Additionally, we found that apoptosis inhibition protects the mature, platelet-producing MKs and results in increased platelet yield in vivo, but not in vitro. These studies provide new insights into megakaryopoiesis and thrombopoiesis, and offer new tools that may be beneficial for improving platelet production from cultured MKs and to study human-specific MK physiology.

Figure 3.1

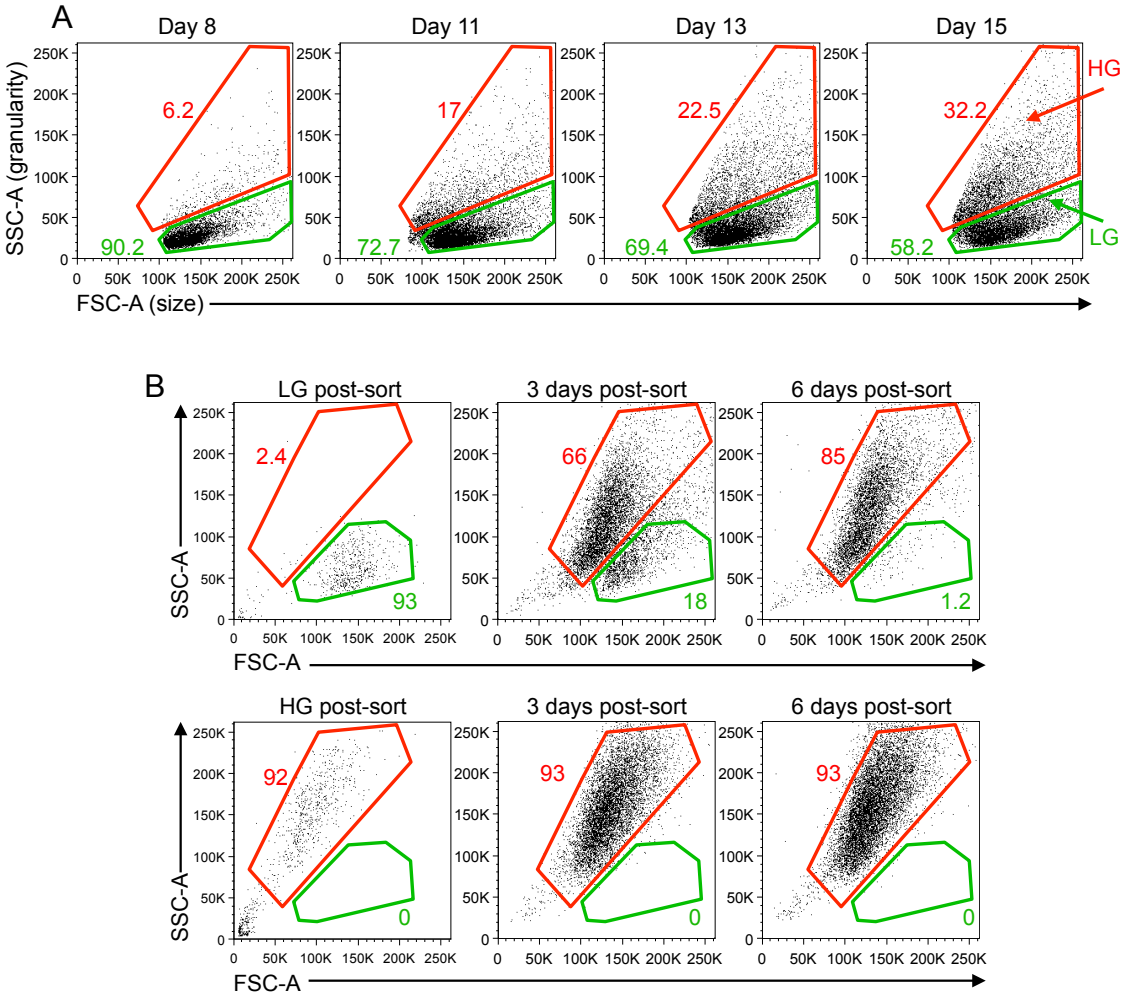

Figure 3.1. Two MK Populations with Distinct Granularity are Present in the In Vitro Human Stem Cell-derived MK Culture Representative size (FSC-A) and granularity (SSC-A) profiles of $CD42a^+$ MKs at specified time points during the differentiation of human $CD34^+$ hematopoietic progenitors. LG and HG MKs are gated as shown. (B) (Top) Day 14 LG $CD42a^+$ MKs were sorted and cultured for another 6 days. Size and granularity of MKs 3 days and 6 days post-sort are shown. (Bottom) Day 14 HG $CD42a^+$ MKs were similarly sorted and cultured. Profiles shown are representative of three independent studies.

Figure 3.2

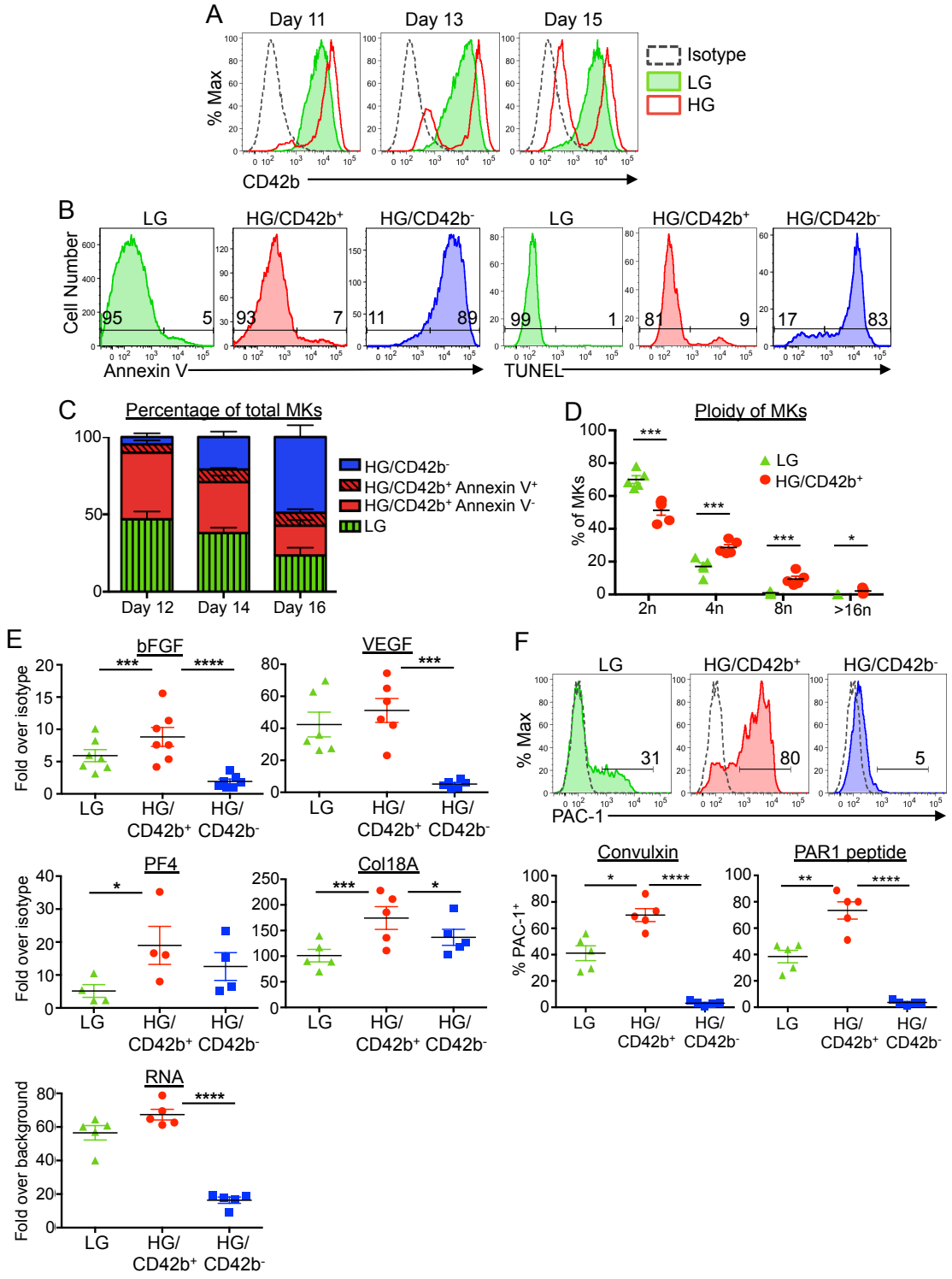

Figure 3.2. HG/CD42b$^+$ MKs Have Characteristics of Mature MKs (A) Representative flow plots of CD42b expression on LG (green) and HG (red) MKs at specified time points of the differentiation. (B) Representative flow plots of Annexin V staining (left) and TUNEL staining (right) on day 14 MK cultures. (C) The percentage ± 1 SEM for each MK subpopulation at specified time points of the differentiation are shown of four independent studies. (D) Graph quantifying the percentages of MKs in each ploidy class ± 1 SEM of five independent studies. (E) Expression of alpha-granule proteins (bFGF, VEGF, PF4, Col18A) and total RNA content of day 14 MKs were determined by intracellular staining and TO staining, respectively. Graphs quantifying the fold changes in mean fluorescence intensity over isotype/background ± 1 SEM are shown. (F) Day 14 MKs were stimulated with convulxin (500 ng/ml) or PAR-1-activating peptide (50 μM) for 20 minutes at RT. (Top) Representative flow plots showing percentages of activated (PAC-1$^+$) MKs following convulxin stimulation. Black dotted line histogram indicates background staining in the absence of stimulation. (Bottom) Graph quantifying the percentages of PAC-1$^+$ MKs following convulxin or PAR-1-activating peptide stimulation (n = 5 independent studies). * $p < 0.05$, ** $p < 0.01$, *** $p < 0.005$, *** $p < 0.001$ for all statistical analyses shown. p values are determined by the student's t test.

Figure 3.3

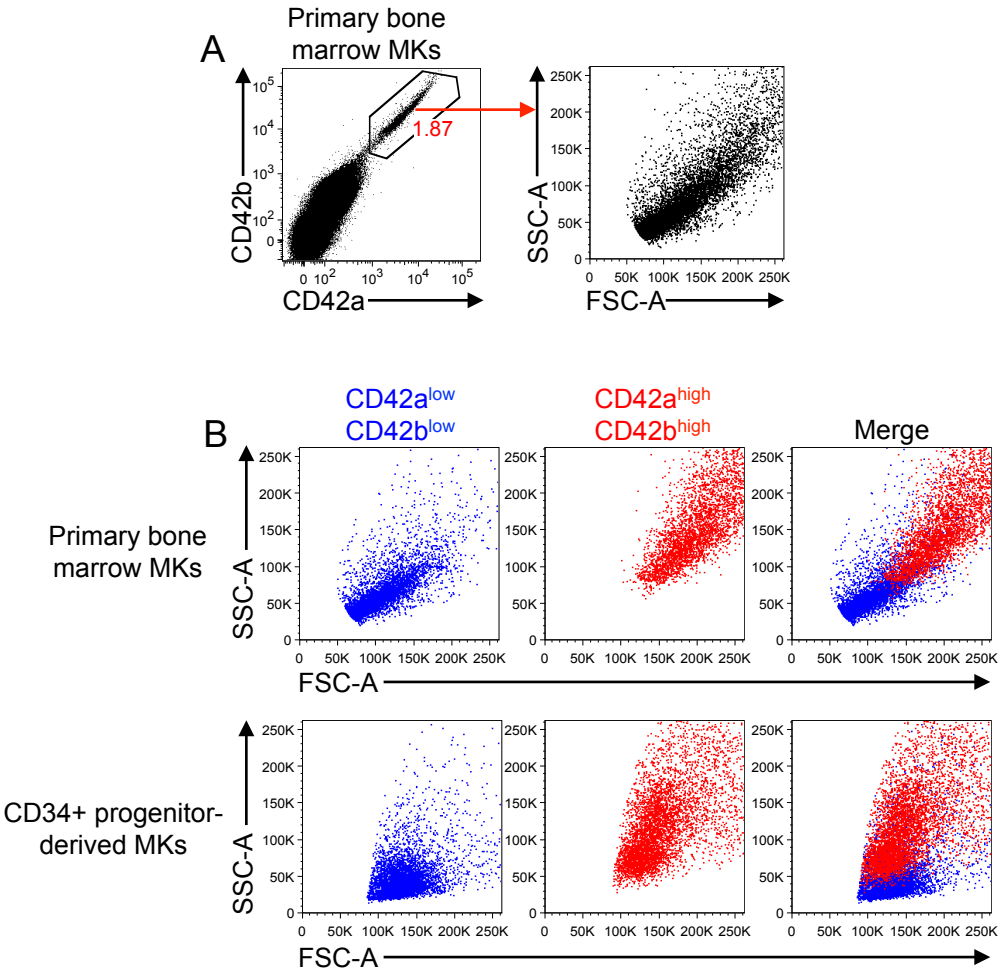

Figure 3.3. Primary Human Bone Marrow MKs Increase in Size and Granularity as They Mature (A) Human bone marrow aspirates were processed through a Percoll density gradient and subjected to red cell lysis treatment before staining for CD42a and CD42b. (Left) Percentage of $CD42a^{+}CD42b^{+}$ MKs detected in the processed human bone marrow aspirate. (Right) Size and granularity of $CD42a^{+}CD42b^{+}$ bone marrow MKs. (B) Representative size and granularity profiles of $CD42a^{low}CD42b^{low}$ (blue) and $CD42a^{high}CD42b^{high}$ (red) MKs from human bone marrow and from cultured $CD34^{+}$ hematopoietic progenitors. Profiles are representative of three independent studies.

Figure 3.4

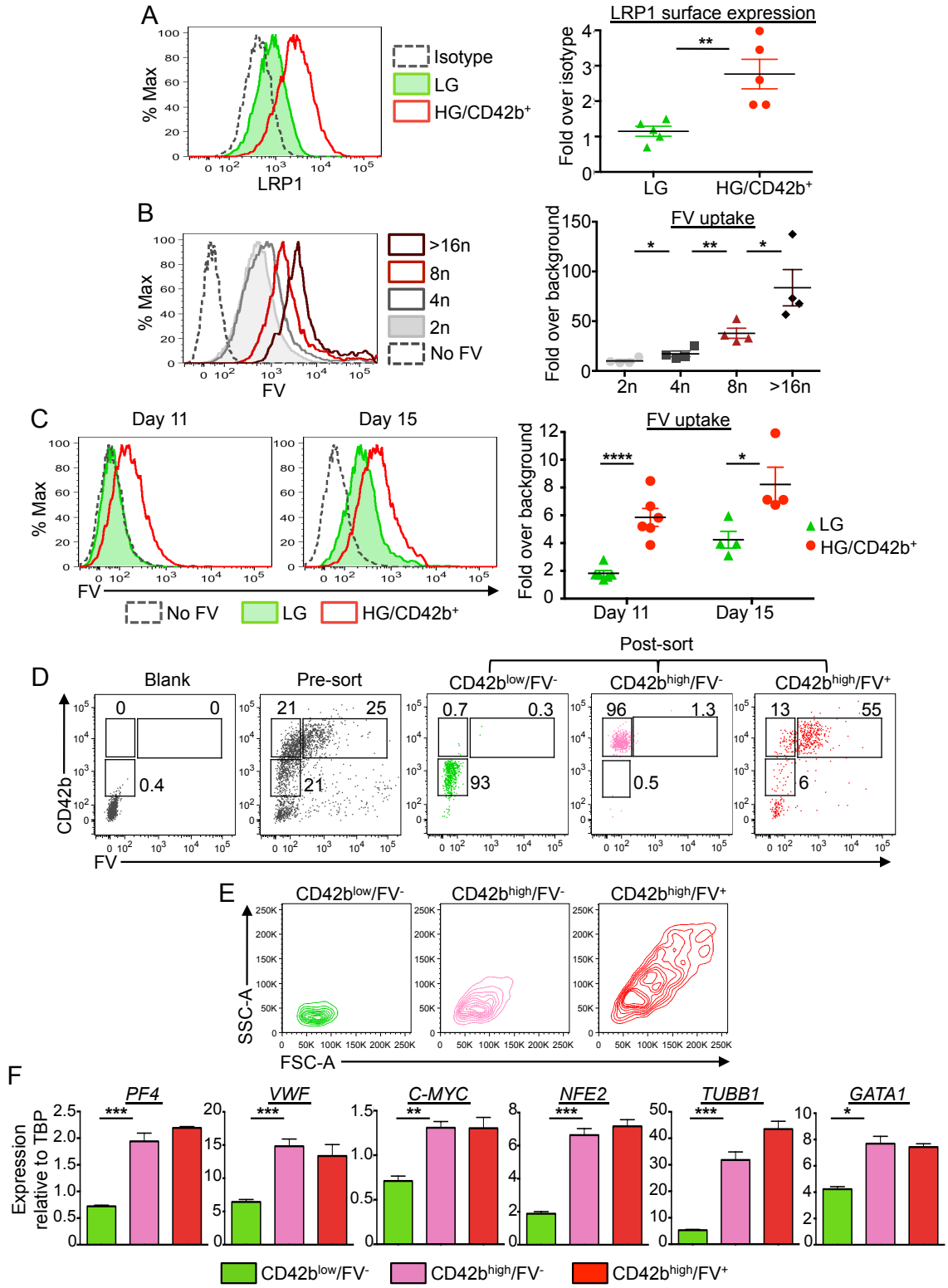

Figure 3.4. FV Uptake Correlates with Maturation (A) Surface expression of LRP1 receptor on day 14 MKs. (Left) Representative flow plot of LRP1 surface expression on LG and HG/CD42b^{+} MKs. (Right) Graph quantifying median fluorescence intensity of LRP1 expression over isotype for LG and HG/CD42b^{+} MKs. Mean ± 1 SEM are shown (n = 5 independent studies). (B) Day 14 MKs were pulse labeled with 200 nM FV-Alexa-488 or Alexa-647 for 1 hour at 37°C. (Left) Representative flow plot of FV uptake by CD42b^{+} MKs of different ploidy classes. (Right) Graph quantifying median FV fluorescence over background associated with MKs of different ploidy classes (n = 4 independent studies). (C) Day 11 or day 15 MKs pulse labeled with FV as in (B). (Left) Representative flow plot of FV uptake by LG and HG/CD42b^{+} MK populations are shown. (Right) Graph quantifying median FV fluorescence over background associated with LG and HG/CD42b^{+} MKs on days 11 and 15. (D) Day 11 or 14 MKs were pulse-labeled with 200 nM of FV-Alexa-647 for 1 hour and stained with CD42b-PE antibody for 20 minutes at 37°C and washed twice prior to sorting. (Left) Representative plots of CD42b expression and FV fluorescence of unlabeled (blank) and labeled (pre-sort) MKs prior to sorting. Three populations were sorted for comparison: CD42b^{low}/FV^{-}, CD42b^{high}/FV^{-} and CD42b^{high}/FV^{+}. (Right) Representative plots of CD42b expression and FV fluorescence of sorted populations of 4 independent studies. (E) Representative FSC-A (size) and SSC-A (granularity) profiles of sorted populations. (n = 4) (F) Expression of late MK markers were examined in sorted MKs from (D) by qPCR. mRNA expression of late MK markers (*PF4, VWF, C-MYC, NFE2* (nuclear factor, erythroid 2), *TUBB1* (Tubulin Beta 1), *GATA1* (Gata binding protein 1)) relative to housekeeping gene TBP in sorted CD42b^{low}, CD42b^{high}/FV^{-} and CD42b^{high}/FV^{+} populations are shown. * $p < 0.05$, ** $p < 0.01$, *** $p < 0.005$, *** $p < 0.001$ for all statistical analyses. p values are determined by the student's t test.

Figure 3.5

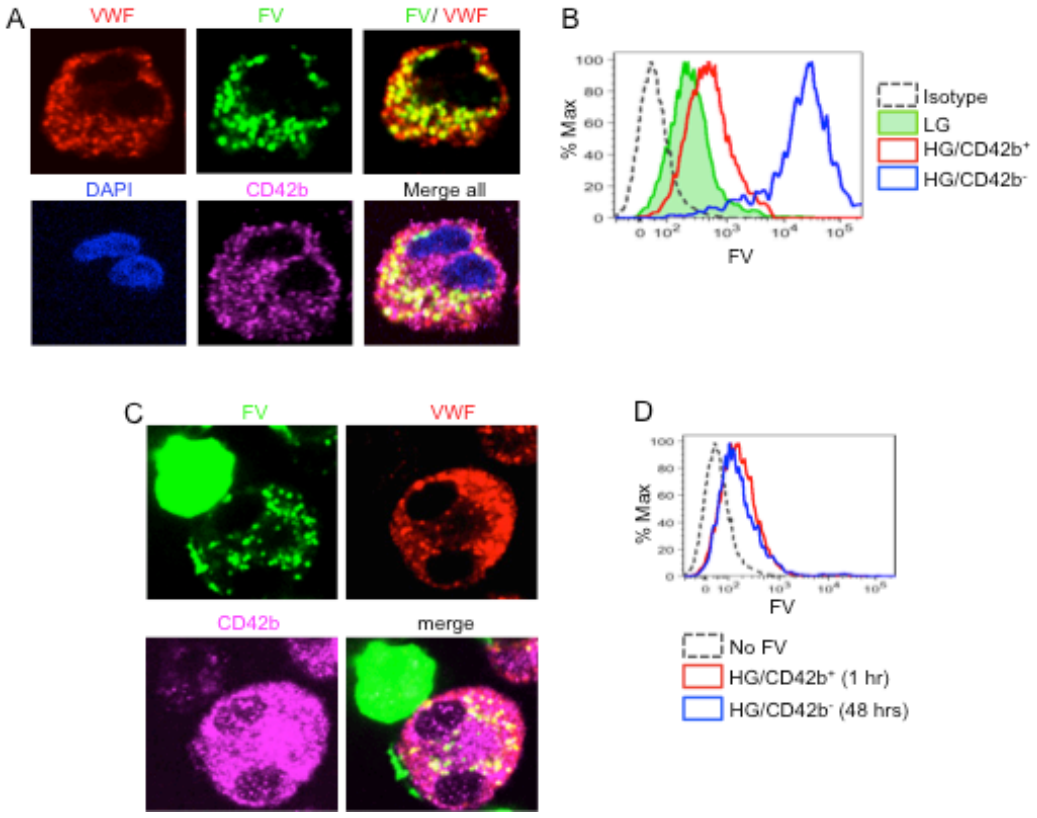

Figure 3.5. Mature MKs Endocytose FV into Their Alpha-granules (A) Immunostaining of CD42b and VWF was performed on day 14 FV-labeled MKs that were adhered to fibronectin-coated glass cover slips. Confocal images of the MKs show FV colocalizing with VWF in alpha-granules. Images were acquired using a DMi8 microscope (Leica Biosystems) equipped with a 63x Plan Apochromat objective (1.4NA) and a Hamamatsu Photonics ORCA-Flash4.0 sCMOS digital camera. (B) Day 14 MKs were pulse labeled with 200 nM of FV-Alexa-488 for 1 hour at 37°C. Representative flow plots showing the FV fluorescence associated with each MK subpopulation. (C) FV-labeled MKs were immunostained with VWF and CD42b. $CD42b^+$ MKs showed punctate staining of intracellular FV, which colocalized with alpha-granule marker VWF, while $CD42b^-$ MKs showed surface staining of FV. (D) Day 11 MKs were pulse labeled with FV as in (B). Excess FV was removed by washing, and MKs were followed for 48 hours. Representative flow plot showing that the intensity of FV fluorescence associated with $HG/CD42b^+$ MKs 1 hour post-labeling is the same as that associated with $HG/CD42b^-$ MKs 48 hours later, indicating that $HG/CD42b^+$ MKs give rise to $HG/CD42b^-$ MKs.

Figure 3.6

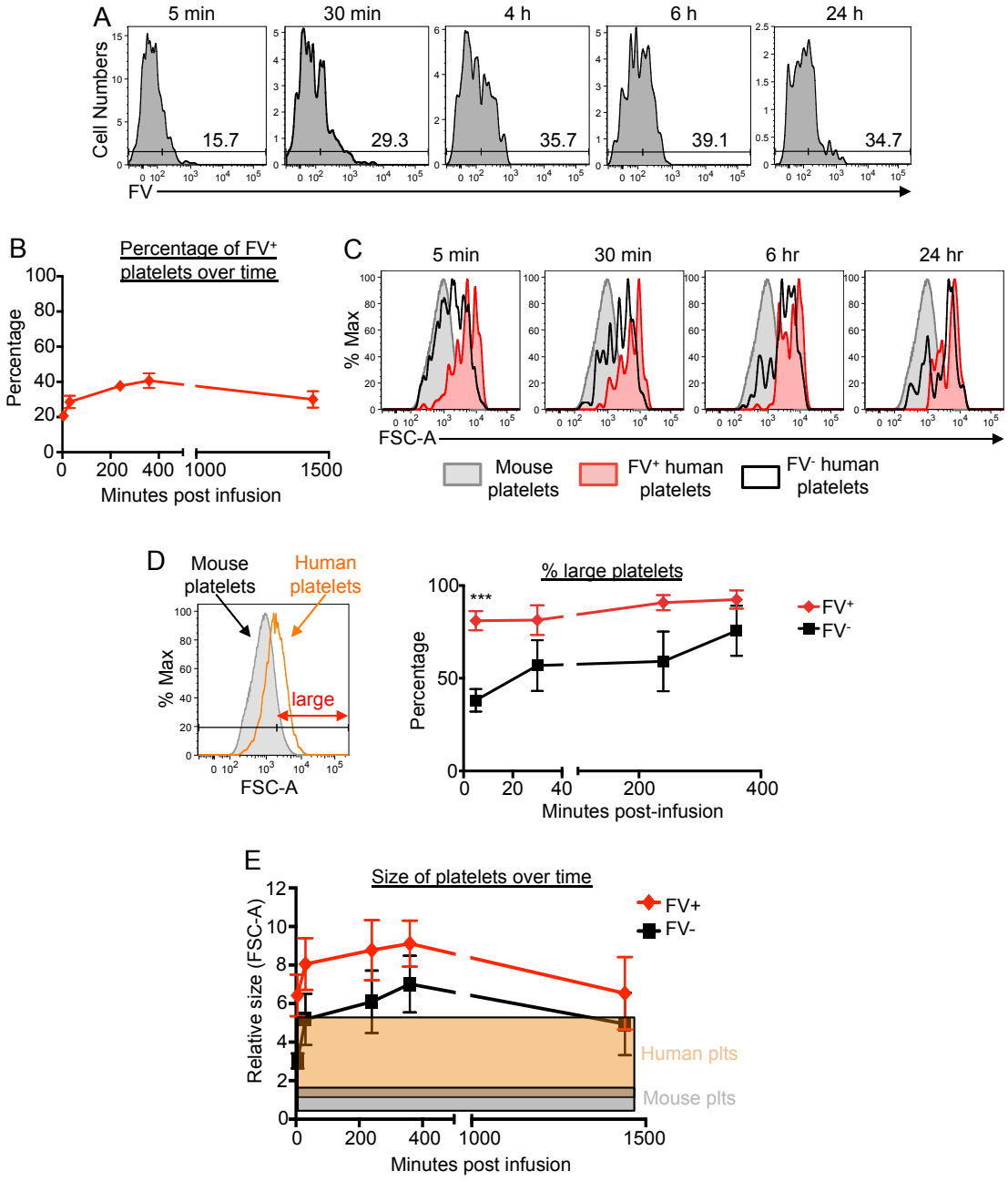

Figure 3.6. FV-labeled MKs Generate FV^+ Platelets in the Circulation of NSG Mice Post-infusion Day 11/12 MKs were incubated with 200 nM FV-Alexa-488 for 1 hour at 37°C prior to infusion into NSG mice. (A) Representative flow plots showing the FV fluorescence of $CD42a^+CD42b^+$ human platelet events detected in the circulation at the specified time points post-infusion. Percentages of FV^+ platelet events are displayed. (B) Graph quantifying the percentage of $CD42a^+$ $CD42b^+$ FV^+ human platelet events in the circulation over time post-infusion. Mean ± 1 SEM are shown for 4 independent studies. (C) Representative flow plots showing the sizes of $CD42a^+CD42b^+$ FV^+ (red) and FV^- (black) human platelet events detected in the circulation of mice at the specified time points after the infusion of FV-labeled MKs. The sizes of mouse platelets are shown in grey. (D) (Left) Relative sizes of endogenous mouse platelets and infused human donor platelets. Platelets were considered large if their FSC-As are larger than 90% of the mouse platelets' FSC-As. (Right) Percentage of FV^+ (red) and FV^- (black) platelets that were large at the various time points post-infusion. Mean ± 1 SEM are shown. (n = 4) *** $p < 0.005$, as determined by the student's t test. (E) Graph showing the relative sizes of FV^+ and FV^- platelets over time. Mean ± 1 SEM are displayed for 4 independent studies. The size ranges of infused human donor platelets (orange) and mouse platelets (grey) are shown for comparison.

Figure 3.7

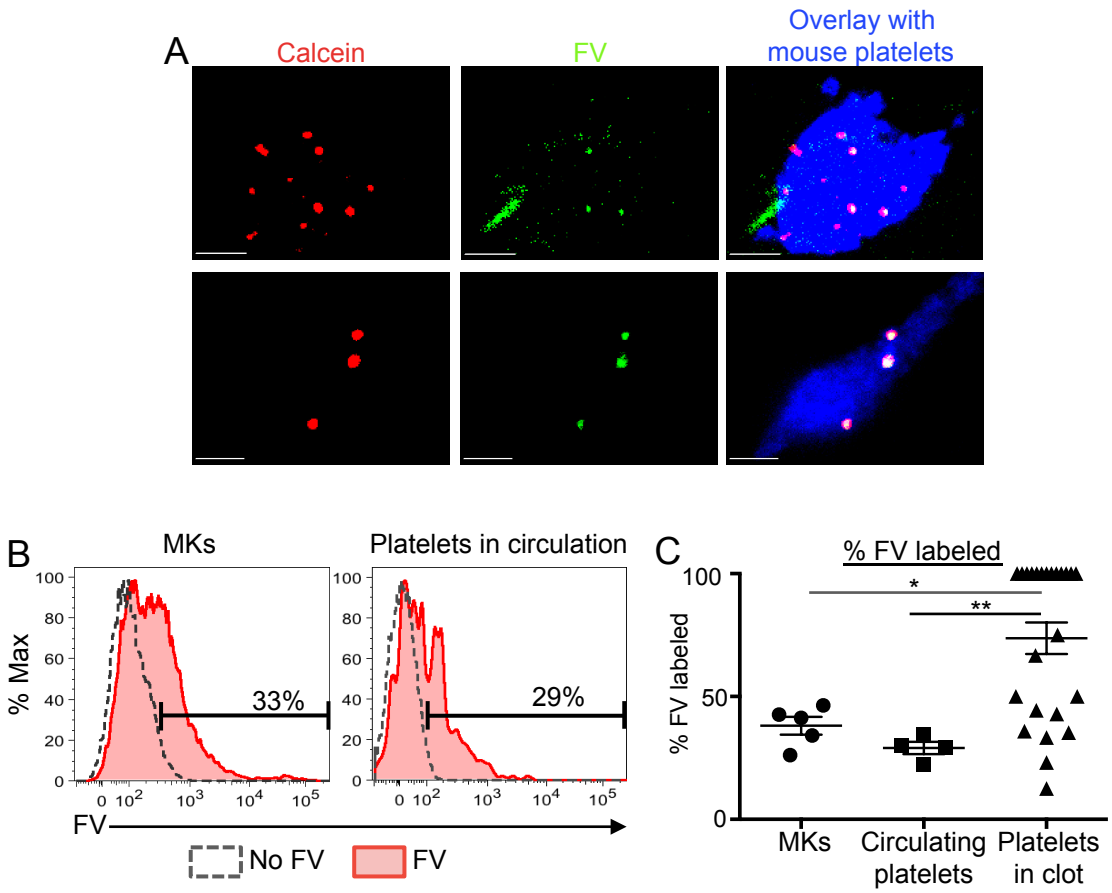

Figure 3.7. FV$^+$ MKs Release Functional FV$^+$ Platelets In Vivo (A) Day 11 MKs double-labeled with calcein red orange (red) and FV-Alexa-488 (green) were infused into NSG mice 30 minutes prior to the induction of the first cremaster arteriole laser injury. Representative confocal images of clots formed after laser injury are shown. Mouse platelets are labeled with CD41-Alexa-647 (blue). All human platelets derived from infused MKs are calcein-labeled (red). FV-labeled (green) human platelets appear yellow in the overlay. Scale bars shown are 10 μm. (B) Representative flow plots showing the percentage of FV-labeled MKs that were infused (left) and FV-labeled human platelets circulating in mice post-infusion (right). (C) Quantification of the percentages of FV-labeled MKs that were infused with 5 independent studies, FV-labeled human platelets detected in the circulation post-infusion (n=4) and FV-labeled platelets detected in the clot (n = 25). *p < 0.05, ** p < 0.01, *** p < 0.005 for all statistical analyses. p values are determined by the student's t test.

Figure 3.8

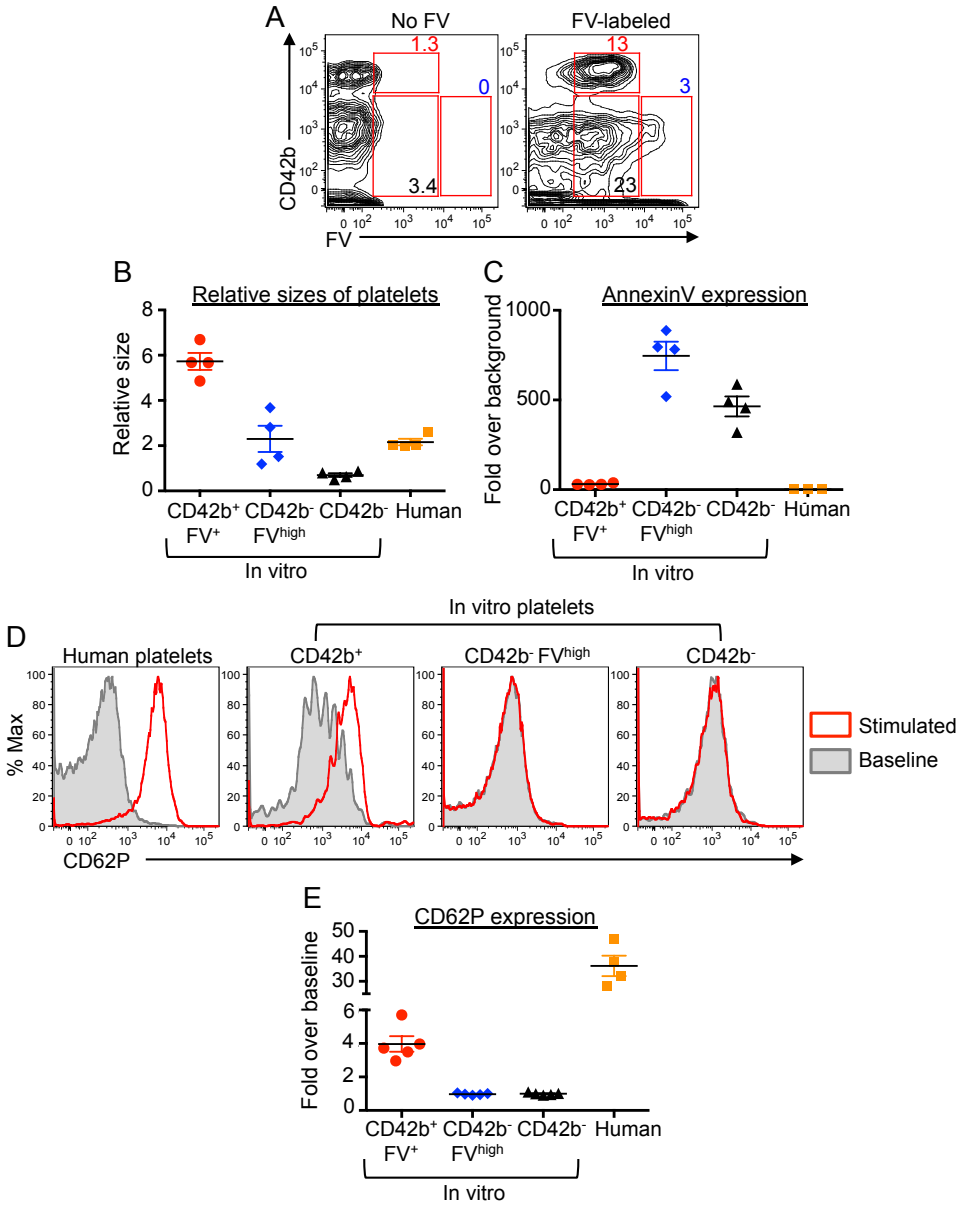

Figure 3.8. FV-labeled MKs Give Rise to Functional CD42b$^+$ Platelets In Vitro Day 11 MKs were pulse labeled with FV, washed and resuspended in fresh medium. In vitro platelets were harvested 24 hours later for analysis. (A) CD42b and FV expression of CD42a$^+$ platelet-sized particles harvested from non-labeled (left) and FV-labeled (right) MKs. CD42b$^+$FV$^+$, CD42b$^-$ FV^{high} and CD42b$^-$ particles were gated as shown. (B) Relative sizes of platelet-sized particles in vitro compared to human donor platelets. (C) Quantification of Annexin V staining on platelet-sized particles in vitro compared to human donor platelets. (D) In vitro platelets and human donor platelets are stimulated with PAR1-activating peptide (25 μM) for 20 minutes at 37°C. Platelet activation is indicated by the increase in surface CD62P expression. (E) Graph quantifying the fold change in CD62P expression over baseline when in vitro platelet-sized particles and human donor platelets are stimulated.

Figure 3.9

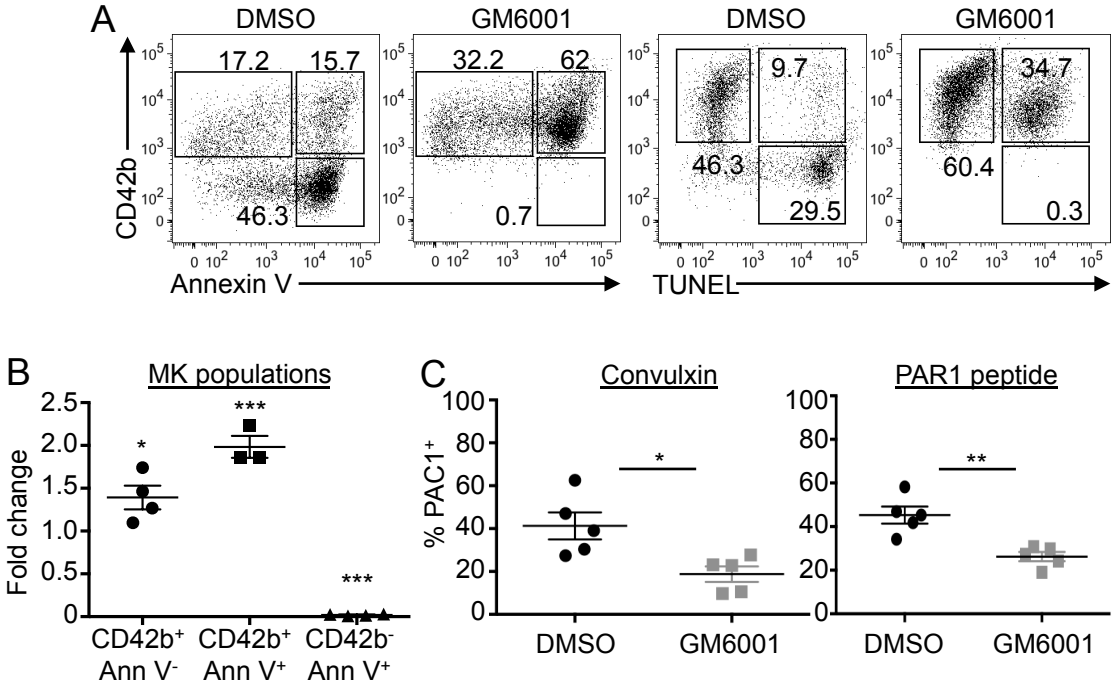

Figure 3.9. Effect of Metalloproteinase Inhibition on MKs. MKs were treated with GM6001 (100 μM) or DMSO (control) from day 8 to day 15 and analyzed on day 15. (A) Representative flow plots showing CD42b expression versus Annexin V binding or TUNEL positivity in MKs treated with GM6001 or DMSO. (n = 5) (B) Graph quantifying the fold changes in the percentages of MK subpopulations with GM6001 treatment relative to DMSO. Mean ± 1 SEM is shown. (n ≥ 3) (C) Quantification of the percentages of $CD42b^+$ MKs that are $PAC\text{-}1^+$ after convulxin (left) or PAR1-peptide (right) activation of GM6001 or DMSO treated MKs. Mean ± 1 SEM is shown for 5 independent studies. *p < 0.05, ** p < 0.005, *** p < 0.001 for all statistical analyses. p values are determined by the student's t test.

Figure 3.10

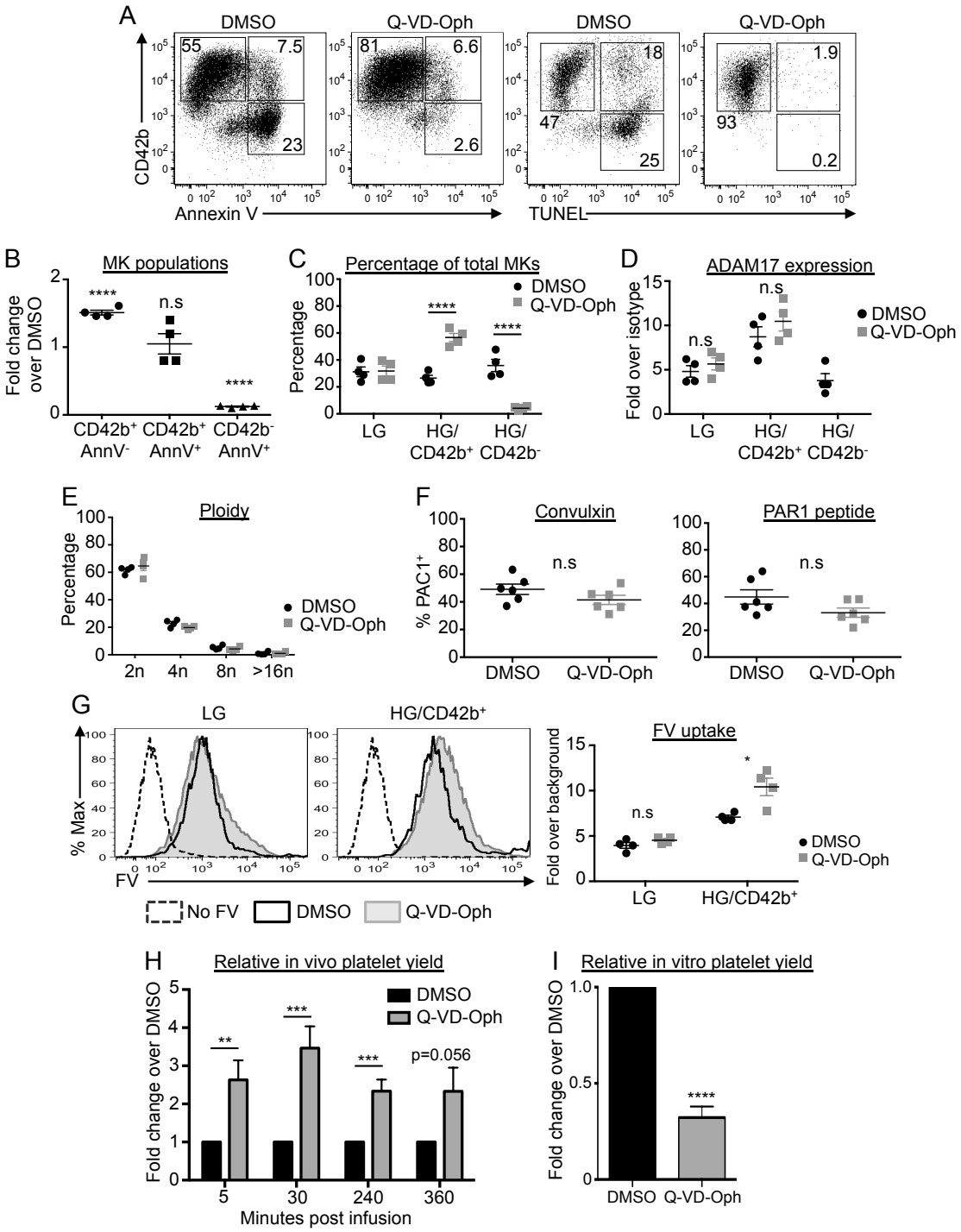

Figure 3.10. Effect of Apoptosis Inhibition on MKs and Platelet Production MKs were treated with Q-VD-Oph (25 μM) or DMSO (control) from day 8 to day 15 and analyzed on day 15. (A) Representative flow plots showing CD42b expression versus Annexin V binding or TUNEL positivity in MKs treated with DMSO or Q-VD-Oph. (B) Graph quantifying fold changes in the percentages of MK subpopulations with Q-VD-Oph treatment relative to DMSO. Mean ± 1 SEM are shown for 4 independent studies. (C) Quantification of the percentages of MK subpopulations with DMSO or Q-VD-Oph treatment. Mean ± 1 SEM are shown for 4 independent studies. (D) Graph quantifying the mean fluorescence intensity of ADAM17 expression over isotype on DMSO or Q-VD-Oph-treated day 15 MKs. Mean ± 1 SEM are shown. (E) Graph quantifying the percentages of $CD42b^+$ MKs in each ploidy class with DMSO or Q-VD-Oph treatment. Mean ± 1 SEM are shown for 4 independent studies. (F) Quantification of the percentages of $CD42b^+$ MKs that are $PAC\text{-}1^+$ after convulxin (left) or PAR1-peptide (right) activation of DMSO or Q-VD-Oph-treated MKs. Mean ± 1 SEM are shown for 6 independent studies. n.s. = not significantly different between treatment arms. (G) DMSO and Q-VD-Oph treated MKs were pulse labeled with FV. (Left) Representative plot showing FV uptake by LG and HG/$CD42b^+$ MKs treated with DMSO or Q-VD-Oph. (Right) Quantification of FV uptake by DMSO and Q-VD-Oph treated MKs. Mean ± 1 SEM are shown for 4 independent studies. (H) Graph quantifying the relative platelet production at specified time points following the infusion of Q-VD-Oph or DMSO-treated MKs into immunodeficient mice. Platelet production is normalized to DMSO control at each time point. Mean ± 1 SEM are shown for 6 independent studies. (I) Graph quantifying the relative in vitro platelet yield from DMSO or Q-VD-Oph treated MKs for 5 independent studies. n.s. = not significantly different between treatments for all statistical analyses. *$p < 0.05$, ** $p < 0.01$, *** $p < 0.005$, **** $p < 0.001$ for all statistical analyses. p values are determined by the student's t test.

Figure 3.11

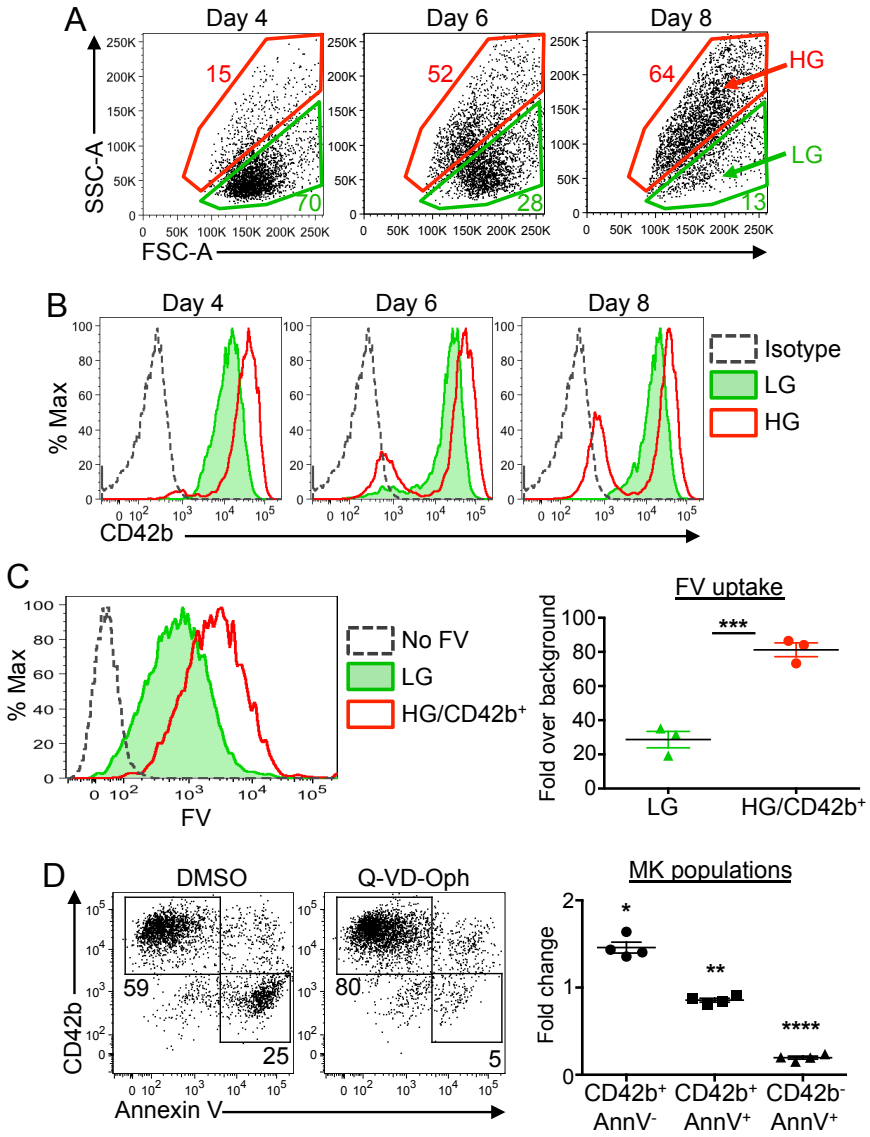

Figure 3.11. LG and HG MK Populations Are Present in iPSC-derived MK Cultures (A) Representative size and granularity profiles of iPSC-derived CD42a$^+$ MKs at specified time points of the differentiation. LG and HG MKs are gated as shown. (B) Representative flow plots showing CD42b expression of LG and HG MKs at specified time points of the differentiation. (C) Day 4 MKs were incubated with 200 nM of FV-Alexa-647 for 1 hour at 37°C. (Left) Representative flow plot showing FV uptake by LG and HG/CD42b$^+$ MKs. (Right) Graph quantifying FV uptake by LG and HG/CD42b$^+$ MKs. Mean ± 1 SEM are shown for 3 independent studies. (D) MKs were treated with Q-VD-Oph (25 μM) or DMSO from day 4 to day 7 of the differentiation. (Left) Representative flow plots showing CD42b expression and Annexin V binding of day 7 MK cultures with DMSO or Q-VD-Oph treatment. (Right) Graph quantifying the fold changes in the percentages of MK subpopulations with Q-VD-Oph treatment relative to DMSO. Mean ± 1 SEM are shown for 4 independent studies. * $p < 0.05$, ** $p < 0.01$, *** $p < 0.005$ and **** $p < 0.001$ for all statistical analyses. p values are determined by the student's t test.

Figure 3.12

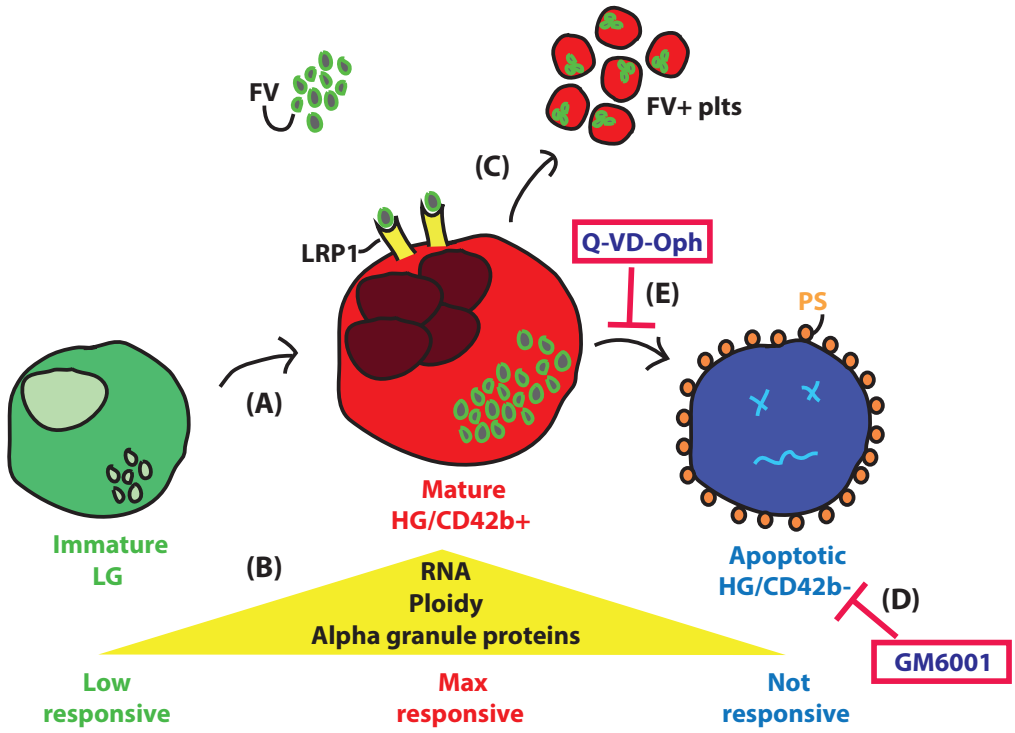

Figure 3.12. Developmental Staging of In Vitro-generated MKs Schematic representation of the stages as immature human MKs mature and then undergo injury. (A) The immature LG MK population has low ploidy and few internal granules and show limited response to agonist stimulation. These LG MKs mature to become the HG/CD42b$^+$ MK population. (B) The mature HG/CD42b$^+$ MKs have increased ploidy, RNA and alpha-granular content as compared to the immature LG MKs. They are also maximally responsive to stimulation by various agonists. (C) Mature HG/CD42b$^+$ MKs take up fluorescently-labeled FV into their alpha granules and release FV-labeled platelets in vitro and in the circulation of mice when infused. The FV-labeled platelets are similar in size or larger than human donor platelets. FV-labeled platelets are incorporated into clots and activate in response to agonist stimulation, suggesting that they are functional. (D) GM6001 inhibits CD42b shedding from MKs, but does not prevent apoptosis or improve MK functionality. (E) On the other hand, blocking apoptosis also prevents CD42b shedding, and redirects MKs to increase the number of CD42b$^+$ MKs that take up FV and release functional platelets.

CHAPTER 4

Elucidating the Disease Mechanism of TAR Syndrome Using Patient-Specific iPSCs

4.1 Introduction

TAR Syndrome is a rare congenital disorder characterized by low platelet count, bilateral absence of the radius bone, other skeletal abnormalities and cardiac lesions. The low platelet count in TAR patients is likely due to defects in MK development and maturation as 1) TAR patients have severely reduced number of mature MKs in their bone marrow[71,73] and 2) hematopoietic/MK progenitors isolated from TAR patients show defects in the growth of colony-forming units (CFU)-MK and differentiate poorly into MKs in vitro.[71–73]

In 2012, Albers et. al. uncovered the genetic basis of TAR syndrome as the compound inheritance of a low frequency SNP with a rare null mutation in the *RBM8A* gene. The null mutation in *RBM8A* gene in TAR patients is most commonly due to a deletion of at least 200 kb in the chromosome region of 1q21.1 while the SNPs are either in the 5' UTR (G/A) or the first intron (G/C) of the intact *RBM8A* allele. Since the SNPs are in the non-coding regions of the protein, a hypomorphic mechanism is proposed, in which the loss of one copy of *RBM8A* (due to the deletion/null mutation) is exacerbated by further reductions in *RBM8A* expression by noncoding SNPs on the remaining copy. Thus, the reduction of *RBM8A* expression below a certain threshold level may be responsible for TAR syndrome. *RBM8A* codes for the Y14 protein, which forms part of the EJC involved in enhancing the translation of spliced mRNAs and regulating the nonsense-mediated decay of mRNAs with premature stop codons. It remains unclear how suboptimal expression of *RBM8A*, which is ubiquitously expressed in all cells and performs essential cellular functions, targets megakaryopoiesis and thrombopoiesis.

Investigating the disease mechanism of TAR syndrome has been a challenge due to the difficulties in isolating primary MKs from patients, since MKs are very rare in the bone marrow and even rarer in TAR patients. With the growing ease of reprogramming patient samples to iPSCs and the improvements in differentiation protocols, it is now possible to use patient-specific iPSCs as a disease model to study the mechanism of TAR syndrome.

We reprogrammed fibroblast and blood samples from TAR patients into iPSCs and differentiated iPSCs into HPCs, which can be further differentiated into various hematopoietic lineages in colony assays and liquid cultures. We verified that TAR patient-specific iPSCs have the genotypes described by Albers et. al. previously and also identified a novel 3' UTR SNP that is also associated with TAR syndrome. We found that a clear reduction in *RBM8A* mRNA expression by at least 50% in TAR patient-derived iPSCs and HPCs as compared to wild type (WT). Interestingly, minor differences in Y14 protein expression between TAR iPSCs and WT iPSCs are observed.

TAR HPCs showed decreased propensity to form MKs and other hematopoietic colonies in colony assays compared to WT, but were able to differentiate normally into MKs and erythrocytes in liquid culture. When *RBM8A* expression is restored in TAR iPSCs using a doxycycline-inducible transgene expression system in the AAVS1 safe harbor locus, we saw minimal effect on hematopoiesis and megakaryopoiesis, which suggests that *RBM8A* expression in TAR iPSCs may be sufficient for normal primitive hematopoiesis and megakaryopoiesis. Thus to determine if *RBM8A* plays any role in hematopoiesis/megakaryopoiesis, we went further to knock out *RBM8A* completely in iPSCs and found that complete deficiency of *RBM8A* is lethal for iPSCs as well as all differentiated hematopoietic lineages.

Overall, we were able to recapitulate a partial phenotype of TAR syndrome in vitro using patient-derived iPSCs and demonstrate that a basal level of *RBM8A* expression is necessary for the survival of all cell types. Unfortunately, the mystery of whether and how *RBM8A*/Y14 contribute to the disease pathogenesis of TAR syndrome remained unresolved. The limitations of our current differentiation system in elucidating the disease mechanism of TAR syndrome and how we can address these limitations are discussed.

4.2 Results

4.2.1 TAR Syndrome Patient-Specific iPSCs Carry a Deletion in the Chromosome Region 1q21.1 and a SNP in the 5' or 3' UTR of the *RBM8A* Gene

Most TAR patients have a minimum deletion of 200 kb in the chromosome region 1q21.1, which results in the loss of 1 copy of the *RBM8A* gene.[75,76] They also have a low frequency SNP in the 5' UTR (G/A) or first intron (G/C) of the intact *RBM8A* allele.[75] To verify that the TAR patient-derived iPSCs have these genetic characteristics, we performed copy number variance analysis and sequencing on genomic DNA isolated from TAR iPSCs and various control iPSCs from patient's family members and unrelated WT individuals.

All TAR iPSCs (TAR1, TAR2 and TAR128) from 3 different TAR patients carry the 1q21.1 deletion, with TAR 128 having the biggest deletion in the region (Figure 4.1A). CTL2, reprogrammed from the sister of TAR2, and CTL129, reprogrammed from the mother of TAR128, carry the same deletion as the patients, but these family members are not affected with TAR syndrome because they do not have the disease-associated SNPs (Figure 4.1A and B). TAR1 and TAR2 iPSC lines have the (G/A) 5' UTR SNP associated with TAR syndrome (Figure 4.1B). Interestingly, instead of the 5' UTR or first

intronic SNP, TAR128 has a (C/G) SNP in the 3' UTR, 6 nucleotides from the stop codon, which is the prevalent SNP in the African American TAR patient population (V. Horner, personal communication). A summary of the genotypes of the iPSC lines and who they are derived from is found in Figure 4.1C.

4.2.2 TAR iPSCs and HPCs Have Decreased *RBM8A* mRNA Expression

To determine if the 1q21.1 deletion and SNPs result in a decrease in *RBM8A*/Y14 expression, we differentiated TAR iPSCs into HPCs and MKs (Figure 4.2) and analyzed *RBM8A*/Y14 expression at various stages of the differentiation.

All TAR iPSCs showed > 50% reduction in *RBM8A* expression as compared to WT iPSCs and this difference is maintained when they are differentiated towards mesoderm and HPCs (Figure 4.3A-C). CTL2 and CTL129 iPSCs, mesoderm and HPCs also showed decreased *RBM8A* expression similar to TAR lines (Figure 4.3A-C), suggesting that the bulk of this decrease in expression is due to the loss of one copy of the *RBM8A* gene in the deleted 1q21.1 region. Due to the difficulties in obtaining sufficient numbers of HPCs and MKs for western blotting, we only analyzed Y14 protein expression in TAR and control iPSCs (Figure 4.3D). Interestingly, only TAR1 iPSCs showed a significant decrease in Y14 expression as compared to WT iPSCs (Figure 4.3D), and even this decrease is smaller than expected based on *RBM8A* mRNA expression, suggesting that Y14 may be regulated differently at the protein and at the mRNA level.

4.2.3 TAR iPSCs Showed Decreased MK Colony Formation and Abnormal Hematopoietic Potential

To determine if TAR iPSCs showed defective hematopoiesis or megakaryopoiesis, we differentiated TAR iPSCs into HPCs, which can be further expanded in liquid culture to

MKs, or cultured in methocult or megacult assays to evaluate the hematopoietic colony forming potential, or MK colony-forming potential, respectively (Figure 4.2).

TAR HPCs gave rise to fewer MK colonies than WT and CTL HPCs, suggestive of defective megakaryopoiesis (Figure 4.4A). However, megakaryopoiesis seemed relatively unaffected when we differentiated TAR HPCs in liquid culture (Figure 4.4B). Surprisingly, CTL2 HPCs also exhibited defective MK colony formation even though it is not derived from a patient (Figure 4.4A).

In terms of hematopoietic potential, while TAR1 and TAR128 gave rise to fewer hematopoietic colonies across the board, TAR2 preferentially gave rise to erythroid colonies (Figure 4.4C). However, this preference to differentiate towards the erythroid lineage is not seen when we differentiated TAR2 HPCs in liquid culture (Figure 4.4B).

The discrepancies in hematopoietic/megakaryocytic potential of TAR HPCs using different assays may be due to differences in the composition of megacult and methocult assays versus liquid culture. The nutrient-rich medium used in the liquid culture may provide extra stimulatory factors that can overcome some of the defects in megakaryopoiesis/hematopoiesis and mask the subtle phenotype.

4.2.4 Restoring *RBM8A* Expression in TAR iPSCs Using a Doxycycline-inducible System Has Little or No Effect on Megakaryopoiesis

Comparing the differentiation potential of TAR with WT iPSCs has its caveats: the genetic background of iPSCs affect their differentiation potential and this potential varies even amongst different WT iPSC lines. Thus, to better elucidate the TAR phenotype and the role in which *RBM8A* plays in hematopoiesis and megakaryopoiesis, we generated

isogenic corrected iPSC lines, where *RBM8A* expression is restored in TAR iPSC lines using a doxycycline-inducible system, which we will refer to as TAR TRE-RBM8A iPSCs. By comparing the differentiation of TAR TRE-RBM8A iPSCs with and without doxycycline addition, we can determine whether restoring *RBM8A* expression improves hematopoiesis or megakaryopoiesis and reveal subtle phenotypes, which are difficult to detect by comparing TAR iPSC lines with WT lines.

To generate the TAR TRE-RBM8A iPSCs, we targeted two constructs into the AAVS1 safe harbor locus. The first construct carries a constitutive promoter driving reverse tetracycline-controlled transactivator (RTTA) and the second construct carries a tet-response element (TRE) driving *RBM8A* expression (Figure 2.1). In the presence of doxycycline, RTTA will bind to the TRE to drive *RBM8A* expression. The advantage of this system is that we can control the timing and level of *RBM8A* expression by the adding the appropriate concentration of doxycycline at the desired time.

When doxycycline is added to TAR TRE-RBM8A iPSCs, we saw an increase in *RBM8A*/Y14 expression to a level that is comparable or greater than that in WT iPSCs (Figure 4.5A and B). However, when we compared the differentiation of TAR TRE-RBM8A HPCs into MKs and erythrocytes in liquid culture with and without doxycycline, there were no significant changes in MK and erythrocyte numbers (Figure 4.5C). Similarly, there was no significant increase in MK colony formation when TAR TRE-RBM8A HPCs were cultured in megacult with doxycycline (Figure 4.5D). These data suggest that increasing *RBM8A* expression in TAR HPCs does not affect hematopoiesis or megakaryopoiesis, thus it remains unclear whether decreased *RBM8A* expression is the cause of megakaryopoiesis defects in TAR syndrome.

4.2.5 Complete Deficiency of *RBM8A* is Lethal in iPSCs, HPCs, Erythrocytes and MKs

To determine whether *RBM8A* plays a role in hematopoiesis/megakaryopoiesis, we examined whether a complete deficiency of *RBM8A* will block hematopoiesis or selectively affect megakaryopoiesis. Since *RBM8A* is part of the EJC, which is involved in essential cellular functions such as, enhancing the translation of spliced mRNAs and regulating nonsense mediated decay, it is highly likely that a complete deficiency of *RBM8A* will be lethal. Thus, we decided to knock out *RBM8A* in TAR TRE-RBM8A iPSCs in the presence of doxycycline, to maintain a basal level of *RBM8A* for survival during the gene knock out process, in case knocking out *RBM8A* is lethal. Additionally, since TAR TRE-RBM8A iPSCs only have 1 endogenous *RBM8A* allele (the other allele is deleted), it will be easier to knock out *RBM8A* in these cells.

We generated the *RBM8A* knock out iPSCs using CRISPR/Cas9 technology and incorporated an oligo template for homology directed repair. The integration of the repair template into the *RBM8A* locus will lead to a premature stop codon 6 amino acids from the start site (Figure 2.2 and 4.6A) and thus, a truncated, non-functional *RBM8A* protein. We incorporated an XhoI restriction site into the repair template for screening purposes and mutated the PAM sequence to prevent re-cutting by the guide RNA (Figure 2.2 and 4.6A).

As expected, a complete deficiency of *RBM8A* is lethal to iPSCs. *RBM8A* knock-out iPSCs have to be cultured in the presence of doxycycline (minimum concentration: 0.03 μg/ml) to maintain a basal level of *RBM8A* expression for survival. *RBM8A* expression in *RBM8A* knock-out iPSCs and hematopoietic cells correspond to the concentration of doxycycline present in the system (Figure 4.6B). Interestingly, even though we saw

significant decreases in mRNA expression as we titrate down the concentration of doxycycline, we did not observe a similar decrease at the protein level even when doxycycline concentration is titrated down to 0.05 µg/ml, suggesting that Y14 is highly regulated at the protein level (Figure 4.6C). However, when doxycycline is completely withdrawn from iPSCs for 16 and 48 hours, we see a rapid loss in Y14 protein (Figure 4.6C), indicating that Y14 turns over quickly in cells. In these *RBM8A* knock-out iPSCs, Y14 expression is maintained by the continued presence of doxycycline driving constant transcription and translation of Y14.

When *RBM8A* knock-out HPCs are differentiated to MKs and erythrocytes under various concentrations of doxycycline, viability of all cells decrease drastically with decreasing doxycycline concentrations (Figure 4.6D), suggesting that both MKs and erythrocytes are highly sensitive to reductions in *RBM8A* levels. Thus, a complete deficiency of *RBM8A* is lethal for all cell types, ranging from undifferentiated iPSCs to HPCs, MKs and erythrocytes.

4.3 Discussion

We used a pioneering approach to investigate the disease pathogenesis of TAR syndrome using patient-derived iPSCs from 3 different patients. We verified that all 3 TAR iPSC lines carry a 1q21.1 deletion of varying lengths and a SNP in the non-coding region of the intact *RBM8A* allele. Based on the genotype of TAR patients, we predicted that TAR iPSCs and HPCs would have decreased *RBM8A*/Y14 expression. Although we found a consistent, significant reduction in *RBM8A* mRNA expression in TAR iPSCs and HPCs compared to their control/WT counterparts, it was unclear whether Y14 protein expression was lower in the TAR iPSCs. Albers et. al. showed decreased Y14 protein expression in platelet lysates obtained from TAR patients as compared to controls/WT.[75]

Thus, it is possible that Y14 protein expression may be regulated differently in undifferentiated cells versus differentiated hematopoietic cells, but due to technical difficulties in obtaining large numbers of pure MKs for western blotting, we were unable to determine whether Y14 protein expression is reduced in TAR MKs versus control/WT MKs.

When we compared the hematopoietic and megakaryocytic potential of HPCs derived from TAR iPSCs and control/WT iPSCs, we observed a defect in MK colony forming ability, which was consistent with published literature.[71–73] However, we did not find significant defects in MK differentiation when TAR HPCs were expanded in liquid culture, thus it remained unclear if there is a real defect in megakaryopoiesis in these cells. Since the genetic background of iPSCs has an important impact on its differentiation potential, we should ideally compare isogenic lines with the same genetic background. We reasoned that, if subthreshold *RBM8A*/Y14 expression were the underlying cause of the megakaryopoiesis defect in TAR syndrome, restoring *RBM8A*/Y14 expression would boost megakaryopoiesis in TAR HPCs and may also reveal subtle defects that we might have missed when comparing TAR HPCs to WT HPCs. Thus, we generated isogenic TAR TRE-RBM8A iPSC lines by restoring *RBM8A* expression in TAR iPSC lines by targeting a doxycycline-inducible transgene expression system into the AAVS1 safe harbor locus. We were able to restore *RBM8A* expression during hematopoiesis and megakaryopoiesis by adding doxycycline to TAR TRE-RBM8A iPSCs, but we did not observe any significant improvement in MK differentiation or MK colony forming ability. These results suggest that basal *RBM8A*/Y14 expression in TAR TRE-RBM8A iPSCs may be sufficient for megakaryopoiesis and that any further increase in expression does not further improve megakaryopoiesis.

To determine if *RBM8A* plays any role in hematopoiesis or megakaryopoiesis, we decided to take a step further and knock out *RBM8A* completely. Unsurprisingly, a complete deficiency of *RBM8A* is lethal to iPSCs, HPCs and differentiated hematopoietic cells. We titrated different concentrations of doxycycline to vary *RBM8A* expression levels to determine if MKs are more sensitive to *RBM8A* levels than other hematopoietic cells, e.g., erythrocytes. We found that the viability of MKs and erythrocytes decrease drastically with decreasing levels of doxycycline/*RBM8A* expression and that MKs and erythrocytes are both equally sensitive to *RBM8A* levels.

In conclusion, we were not able elucidate the role of RBM8A in TAR syndrome or fully recapitulate the TAR syndrome phenotype using patient-derived iPSCs. An interesting feature of TAR syndrome is that platelet counts in patients usually recover to near normal levels over time, suggesting that the defect in megakaryopoiesis/ thrombopoiesis is perhaps specific to fetal/neonatal stage of life. The differentiation of iPSCs into the various hematopoietic lineages in vitro recapitulates yolk sac primitive hematopoiesis, which occurs during the embryonic phase of life. It is possible that the MKs during the embryonic stage of development are less sensitive to *RBM8A* levels or that *RBM8A* expression is regulated differently at that stage. Differentiation protocols to direct iPSCs towards definitive/fetal hematopoietic progenitors and MKs may be necessary to elucidate the TAR syndrome phenotype. Alternatively, additional genes affected by the deletion in TAR syndrome may also contribute to the observed phenotype in patients.

Figure 4.1

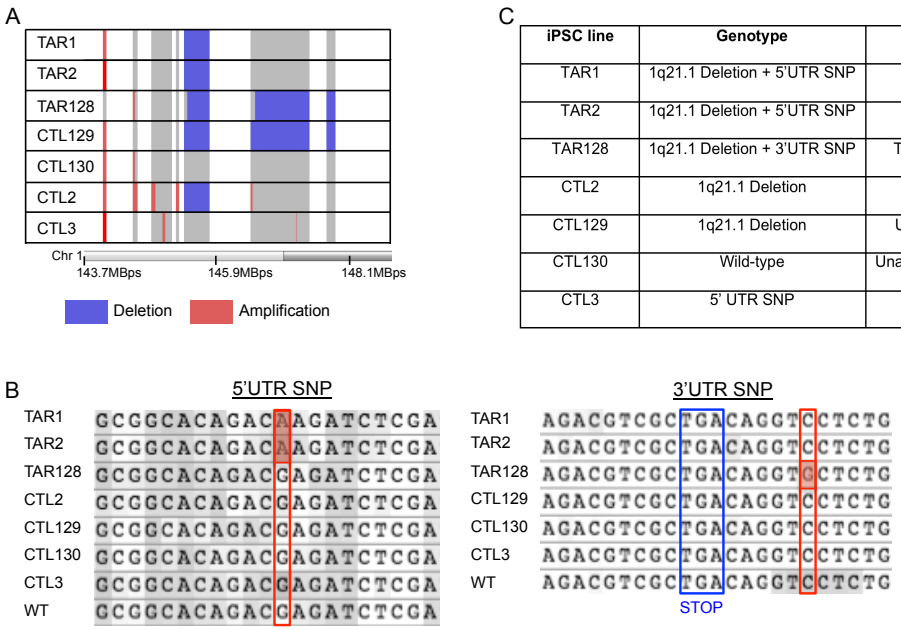

C

iPSC line	Genotype	Notes
TAR1	1q21.1 Deletion + 5'UTR SNP	TAR patient
TAR2	1q21.1 Deletion + 5'UTR SNP	TAR patient
TAR128	1q21.1 Deletion + 3'UTR SNP	TAR patient, African American
CTL2	1q21.1 Deletion	Unaffected sister of TAR2
CTL129	1q21.1 Deletion	Unaffected mother of TAR128
CTL130	Wild-type	Unaffected grandmother of TAR128
CTL3	5' UTR SNP	Wild-type individual

Figure 4.1: TAR iPSC Lines Carry a Deletion in the Chromosome Region 1q21.1 and a SNP in the 5' UTR or 3' UTR of the Intact *RBM8A* Allele (A) Copy number variance analysis comparing TAR and control (CTL) iPSC lines. Deletion (blue) and amplification (red) of regions in chromosome region 1q21.1 are shown. (B) Partial sequences of TAR and control iPSC lines in the 5' UTR (left) and 3' UTR (right) of *RBM8A* gene. The disease-associated SNPs are highlighted in red. The STOP codon is highlighted in blue. (C) Summary of the genotypes of iPSC lines and who they are derived from.

Figure 4.2

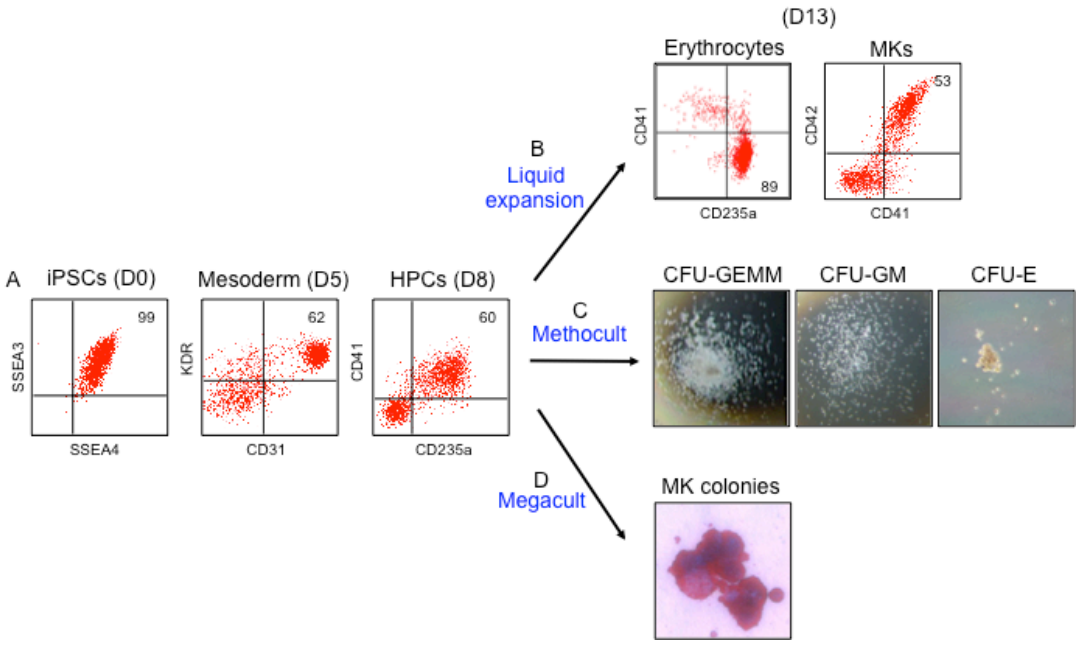

Figure 4.2: Differentiation Schematic for iPSCs (A) Representative flow cytometric profiles for iPSCs ($SSEA3^+$ $SSEA4^+$), mesoderm (KDR^+, $CD31^+$) and HPCs ($CD41^+$, $CD235a^+$) on days 0, 5 and 8 of hematopoietic differentiation. D8 HPCs can be expanded in liquid culture (B) or further differentiated in methocult (C) or megacult (D) assays for evaluation of hematopoietic or megakaryocytic potential respectively. (B) Representative flow cytometric profiles for $CD41^-CD235a^+$ erythrocytes and $CD41^+$ $CD42^+$ MKs after 5 days of differentiation. (C) Representative images of hematopoietic colonies after 12 days of culture in methocult: Colony forming unit-granulocyte, erythrocyte, monocyte, megakaryocyte (CFU-GEMM), Colony forming unit-granulocyte, monocyte (CFU-GM), Colony forming unit-erythrocyte (CFU-E). (D) Representative image of MK colony post-fixation and staining after 12 days of culture in megacult.

Figure 4.3

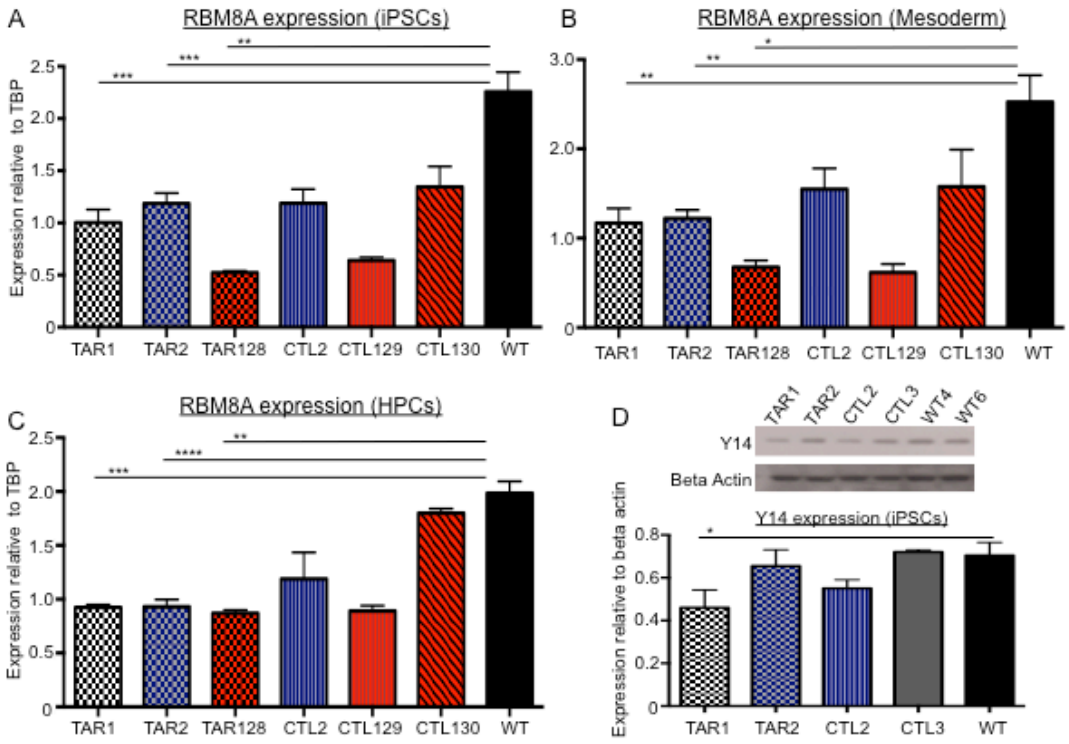

Figure 4.3: *RBM8A* mRNA and Y14 Protein Expression in TAR, CTL and WT iPSCs and Differentiated Cells *RBM8A* mRNA expression in (A) TAR and control iPSCs (n ≥ 2), (B) mesoderm derived from TAR and control iPSCs.(n ≥ 2), (C) HPCs derived from TAR and control iPSCs. (n ≥ 2). (D) (Top) Representative western blot showing Y14 and beta actin protein expression in TAR and control iPSCs. (Bottom) Quantification of Y14 protein expression in TAR and control iPSCs (n ≥ 2) *p < 0.05, **p < 0.01, ***p<0.001, ****p<0.0001 comparing *RBM8A*/Y14 expression in WT versus TAR as indicated.

Figure 4.4

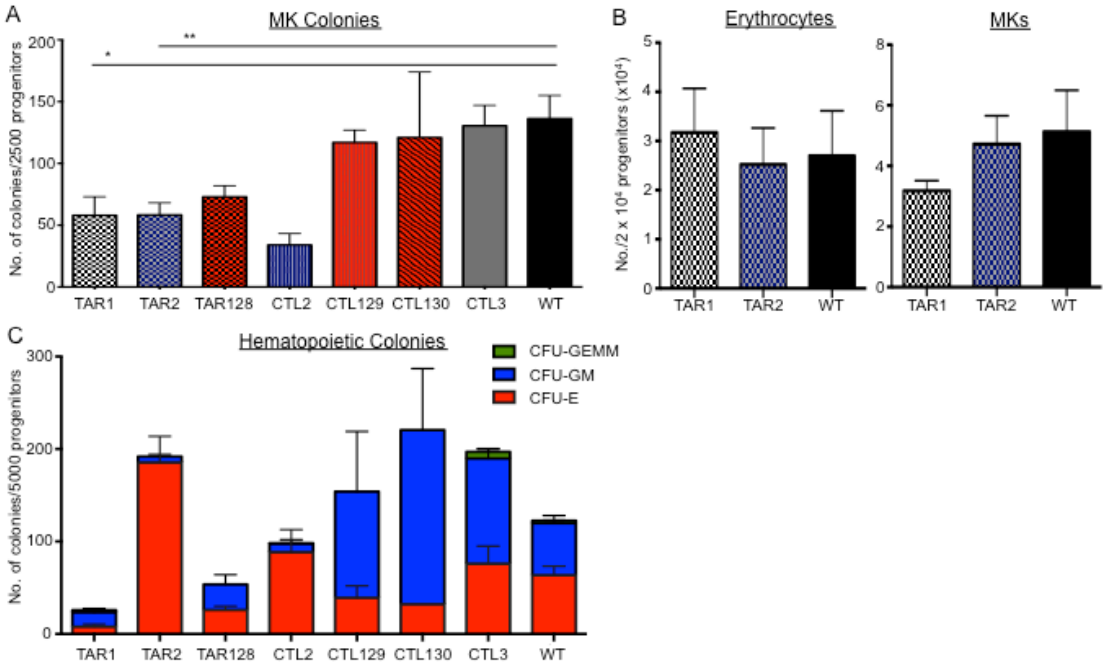

Figure 4.4: Hematopoietic Phenotype of TAR iPSCs (A) Day 8 HPCs were plated in Megacult^{TM} collagen-based medium for MK colony formation. Number of MK colonies were enumerated after 12 days in culture. *$p < 0.05$ comparing TAR1 versus WT and **$p<0.01$ comparing TAR2 versus WT. ($n \geq 2$). (B) Day 8 HPCs were differentiated into erythrocytes and MKs in liquid culture. Bar graph shows the quantification of the number of erythrocytes and MKs after 5 days in culture. ($n \geq 4$). Differences between TAR versus WT were not significant. (C) Day 8 HPCs were plated in Methocult^{TM} methylcellulose medium for hematopoietic colony formation. Number and types of colonies were enumerated after 12 days in culture. CFU-GEMM: colony forming unit-granulocyte, erythrocyte, monocyte, megakaryocyte; CFU-GM: colony forming unit-granulocyte, monocyte; CFU-E: colony forming unit-erythrocyte. ($n \geq 2$).

Figure 4.5

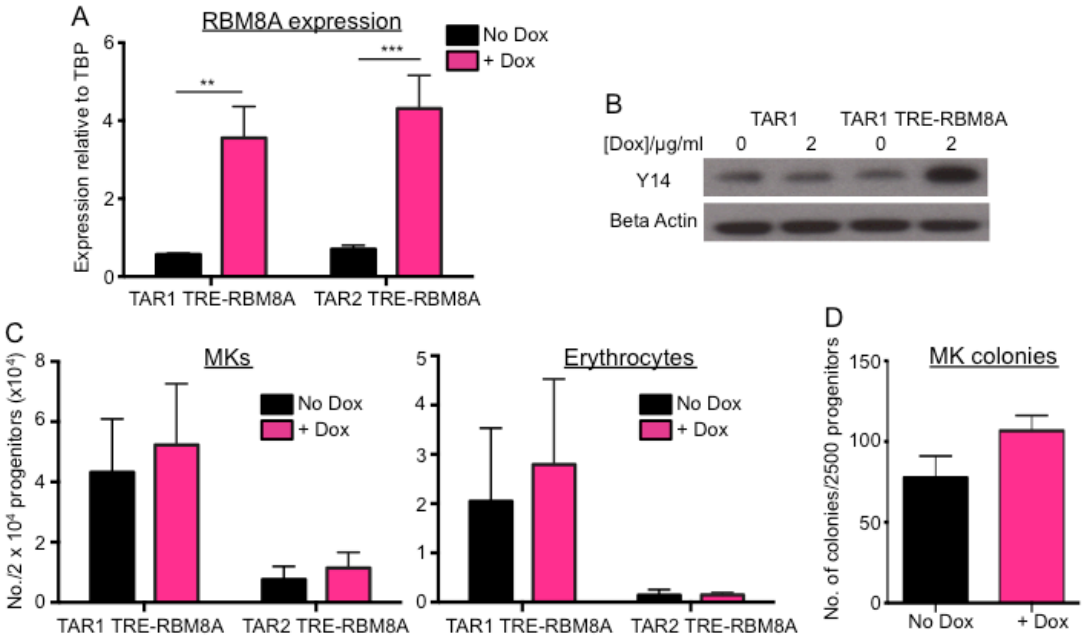

Figure 4.5: Restoring *RBM8A* Expression in TAR iPSCs Using a Doxycycline-inducible Transgene Expression System (A) *RBM8A* mRNA expression in TAR iPSC lines with doxycycline (dox)-inducible *RBM8A* expression (TAR1 TRE-RBM8A and TAR2 TRE-RBM8A) in the absence (black) or presence (pink) of 2 µg/ml of dox. **$p < 0.01$ and ***$p<0.001$ comparing *RBM8A* expression with and without the addition of dox. ($n \geq 9$) (B) Representative western blot showing Y14 and beta actin protein expression in TAR1 and TAR1 TRE-*RBM8A* iPSCs in the presence and absence of dox. (C) Day 8 HPCs were differentiated into MKs and erythrocytes for 5 days in liquid culture. Bar graph shows the quantification of the number of MKs and erythrocytes in the absence (black) and presence (pink) of 2 µg/ml of dox. Differences between conditions with and without dox were not significant. ($n \geq 3$) (D) Day 8 HPCs were plated in Megacult^{TM} assay in the absence (black) or presence (pink) of 2 µg/ml of dox for MK colony formation. Bar graph quantification of the number of MK colonies after 12 days is shown. The differences between conditions with and without dox were not significant. ($n = 2$)

Figure 4.6

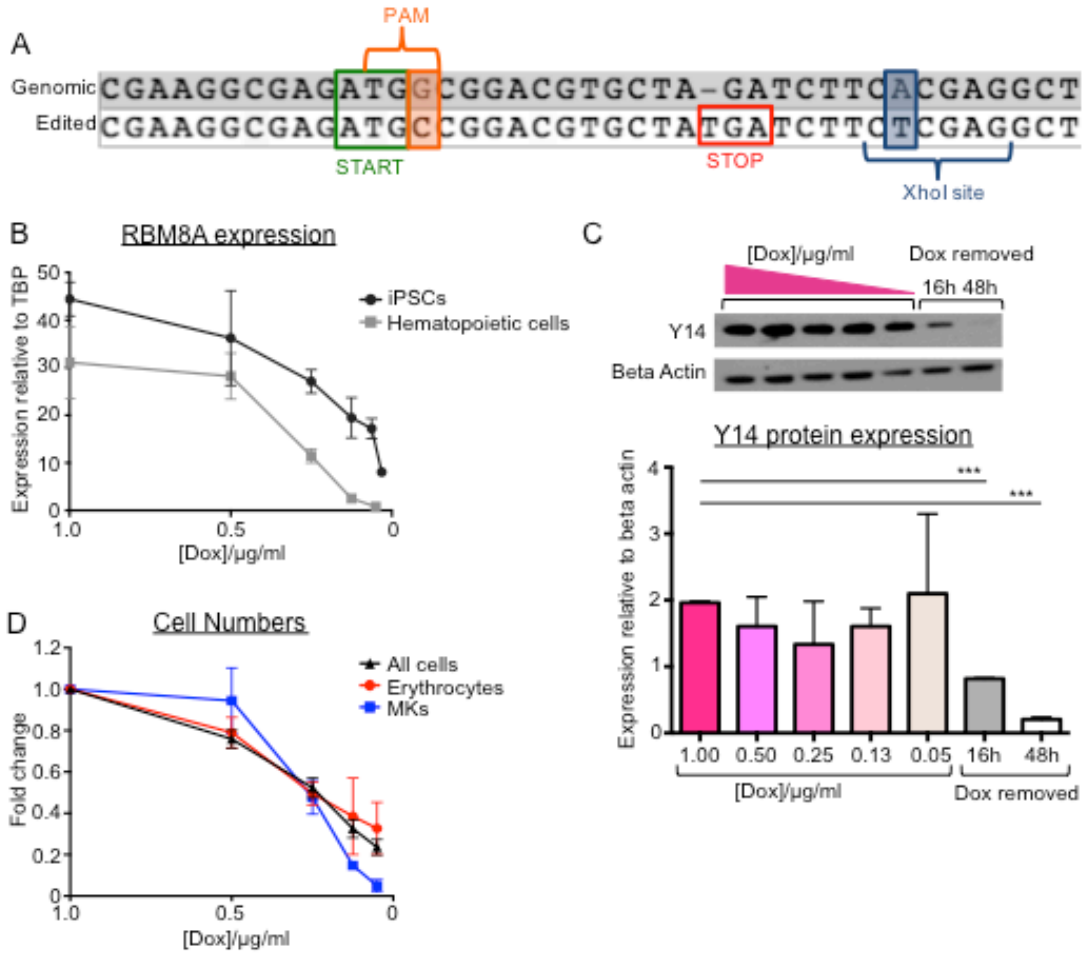

Figure 4.6: A Complete Deficiency of *RBM8A* is Lethal to Both iPSCs and Hematopoietic Cells (A) The CRISPR/Cas9 system was used to knock out *RBM8A* in TAR2-TRE-*RBM8A* iPSCs. The genomic sequence of *RBM8A* aligned with the edited sequence is shown. The ATG start site is marked in green. The PAM sequence (orange) is mutated to prevent recutting by Cas9. A STOP codon (red) is created by the insertion of a single base T. An XhoI restriction site (blue) is created for screening by a single base substitution from A to T. (B) *RBM8A* mRNA expression in RBM8A-knockout (RBM8A-KO) iPSCs and hematopoietic cells derived from these iPSCs at various doxycycline (dox) concentrations. (n = 3) (C) (Top) Representative western blot showing Y14 and beta actin protein expression of *RBM8A* knockout iPSCs cultured under decreasing dox concentrations and when dox was removed for 16 and 48 hours. (Bottom) Bar graph quantifying Y14 protein expression of *RBM8A* knockout iPSCs under these conditions. ***p < 0.001 comparing Y14 protein expression in the presence of 1 µg/ml of dox and when dox was removed for 16 and 48 hours. p value was determined by the student's t test. (D) RBM8A-KO iPSCs were differentiated into HPCs with 2 µg/ml of dox. Day 8 HPCs were differentiated into MKs and erythrocytes in liquid culture at various dox concentrations. Graph quantifying the total number of live cells (black triangles), MKs (blue squares) and erythrocytes (red circles) after 5 days in culture is shown. (n = 3)

CHAPTER 5

Conclusions and Future Directions

In conclusion, we have used human stem cell-derived MKs to address two important questions in the field of megakaryopoiesis and thrombopoiesis: 1) to define the features of a mature MK optimally primed to release platelets, 2) to understand the disease mechanism of TAR syndrome. We showed that the ability to take up FV is a defining feature of mature MKs that are ready to release platelets and that this transient mature population can be enriched by protecting them from apoptosis. Next, we recapitulated a partial phenotype of TAR syndrome using patient-specific iPSCs but did not find a specific role for *RBM8A* in primitive (embryonic) hematopoiesis or megakaryopoiesis. These results form the basis for future work, which will help refine our understanding of megakaryopoiesis and thrombopoiesis, and in turn, improve the efficiency of generating stem cell-derived platelets for transfusions.

5.1 Using FV-labeled MKs as a Tool to Uncover New Maturation Markers and Mechanisms

Traditionally, mature MKs are defined by high surface CD42b expression,[33] increased expression of maturation genes (e.g. *NFE2, TUBB1, PF4*),[34] high ploidy,[35] high alpha-granule and RNA content.[37,39–41] We can now go one step further and define mature platelet-ready MKs as those that can take up FV efficiently, as this ability is acquired after peak expression of the known maturation markers mentioned above.

Purifying the mature MKs from the heterogeneous, asynchronous culture is important for several reasons: 1) we can improve the efficiency of platelet production by infusing only the mature platelet-ready MKs into a platelet bioreactor or potentially a person, and

allowing the immature MKs more time to develop; 2) we can purify the mature MKs for gene expression analysis and further functional analysis to improve the characteristics of this specific population. Although mature MKs can be purified from bulk culture by sorting for MKs that have internalized FV, the stress of cell sorting may compromise its functionality in downstream assays, for instance platelet release in a platelet bioreactor. A better strategy would be to isolate them based on cell surface receptors, which will allow gentler methods of purification like magnetic bead sorting. Thus, moving forward, transcriptome studies to compare $CD42b^{high}/FV^{-}$ and $CD42b^{high}/FV^{+}$ MKs may be useful for identifying novel surface markers on $CD42b^{high}/FV^{+}$ MKs that are not present on $CD42b^{high}/FV^{-}$ MKs. Moreover, such studies may also reveal additional late markers of MK maturation, beyond what we already know.

Potential cell surface markers for isolating mature MKs would include receptors involved in FV internalization as their expression levels are likely to increase as MKs acquire the ability to endocytose FV. We found that LRP1 surface expression is upregulated on mature HG/$CD42b^{+}$ MKs as compared to immature LG MKs, which correlates well with the idea that LRP1 is the putative receptor for FV endocytosis.[156] However, LRP1 surface expression is too low to be a useful surface marker for purifying mature MKs. If we can generate a reporter line, which expresses enhanced green fluorescent protein under the LRP1 promoter, this could potentially improve the LRP1 signal and the ease of isolating $LRP1^{high}$ MKs.

Another potential marker is galectin-8, which has recently been identified as a glycoprotein expressed on MKs that interacts specifically and directly with FV.[180] Additionally, blockage of this glycoprotein by antibodies impair FV endocytosis, suggesting that it plays an important role in FV endocytosis, perhaps by binding FV and

transferring it to LRP1 for endocytosis.[156,180] Examining the surface expression of galectin-8 in mature and immature MKs and correlating its expression levels with the ability to internalize FV would be the first step to determine if galectin-8 could be a suitable cell surface receptor for isolating mature MKs that are capable of taking up FV.

We have demonstrated that FV^+ MKs releases functional FV^+ platelets in vivo when infused and gives rise to partially functional FV^+ platelet-like particles in vitro. Going further, it would be interesting to infuse FV-labeled MKs into a platelet bioreactor to see if FV^+ MKs preferentially release functional platelets as compared FV^- MKs. Several versions of platelet bioreactors have been developed over the years, which are known to give higher platelet yields as compared to static MK cultures.[102,103,106,137] These bioreactors incorporate elements to mimic the bone marrow microenvironment including endothelial cell contacts, extracellular matrix components and shear stress to stimulate and enhance platelet production.[102,103,106,137] Examining platelet release from FV-labeled MKs using these improved systems may give additional insights, in particular, it will be interesting to see if these systems generate FV^+ platelets of higher quality and functionality.

To examine platelet formation from FV-labeled MKs in its natural, physiological environment, we can use techniques like two photon intravital microscopy to directly visualize proplatelet formation in the bone marrow sinusoids or in the lung following the infusion of FV-labeled MKs into immunodeficient mice. The hypothesis is that FV^+ MKs will release platelets quickly in the lung or bone marrow sinusoids post-infusion while FV^- MKs may linger and release platelets much later. Assessing the functionality of FV-labeled MKs in platelet bioreactors, in the bone marrow sinusoids and in the lung will give further validation to our idea that FV uptake defines mature platelet-ready MKs.

Demonstrating that we can detect fluorescently-labeled FV in the alpha-granules of human stem cell-derived MKs established a unique human model system for studying the mechanism of protein endocytosis by human MKs, which is critical since the murine model is not optimum for these studies as mouse MKs produce FV endogenously. Since human MKs are known to endocytose other proteins such as immunoglobulins or fibrinogen,[43,51,52,173] we can potentially label these proteins with fluorescent probes and analyze whether uptake of these molecules occur at the same stage of maturation and whether they are sorted into the same or different compartments.

Mechanistic studies on the uptake, trafficking and packaging of FV and other proteins within MKs and how they are eventually distributed into platelets may provide new insights into alpha-granule biology in MK and platelets. For instance, incubation of MKs with different variants of FV may reveal specific FV regions or amino acid residues that are crucial for the binding interaction and subsequent endocytosis. Knocking out or mutations of LRP-1 and/or galectin-8 in human stem cell-derived MKs by CRISPR/Cas9 system will further crystallize the involvement of these receptors in the endocytosis of FV. A detailed time course looking at the colocalization of FV with various known proteins important for alpha-granule biogenesis at different time points following incubation of FV with MKs may give additional insights to the specific trafficking route of FV through the cell following endocytosis.

In human plasma, FV concentrations range from 12 – 42 nM, with a mean concentration of 20 nM. In our initial optimization studies, we titrated FV concentrations ranging from 20 nM to 200 nM over a period of 1 hour to 24 hours and found that FV uptake increases with the external concentration of FV and the amount of time MKs were exposed to FV, suggesting that FV uptake by MKs may be regulated simply by its exposure to FV in the

natural environment. This means that to make truly functional platelets with the right amount of FV, we need to more carefully quantify the kinetics of FV uptake by MKs, the amount of FV taken up by MKs under various incubation conditions and the amount of FV required in platelets for normal function. Similar assays are also needed for other proteins that are endocytosed by MKs like fibrinogen and immunoglobulins.

5.2 Exploring the Role of Apoptosis in Platelet Formation In Vitro and In Vivo Using Human Stem Cell Models

The question of whether apoptosis plays a role in platelet formation remains controversial as there are evidences for both sides of the story. Initial studies supporting the role of apoptosis in platelet formation demonstrated that treatment of human stem cell-derived MKs with pharmacological inhibitors of apoptosis led to decreased proplatelet formation in vitro[175,176] and that Fas ligand-induced extrinsic apoptosis in MK cell lines or primary murine MKs increases the yield of PLPs in vitro.[176]

However, studies from mice with MK-specific or hematopoietic-specific deletions of the key mediators of intrinsic apoptosis Bax and Bak or caspase 9 showed that the inability to activate intrinsic apoptosis did not affect platelet counts.[177,179] Furthermore, mice deficient in pro-survival protein B cell lymphoma-extra large (BCL-X_L) displayed increased MK apoptosis and failed to shed platelets, suggesting that restraining apoptosis is necessary to help MKs survive and shed platelets.[179] More recently, a triple knockout mouse with deficiencies in proteins essential for both intrinsic (Bax and Bak) and extrinsic apoptosis (caspase 8) showed normal platelet production, lending further support to the idea that apoptosis is dispensable for platelet formation at least in mice, in vivo.[178]

In humans, BH3 mimetics, a class of cancer drugs that induce apoptosis in cells through its inhibition on pro-survival proteins such as BCL-X_L, led to thrombocytopenia at high doses[181–183], suggesting that apoptosis may be detrimental to platelet production and survival. A mutation of human cytochrome c that enhances intrinsic apoptosis led to premature release of platelets into the marrow space instead of the sinusoids, resulting in thrombocytopenia.[166] When $CD34^+$ HPCs isolated from patients carrying the mutated cytochrome c were differentiated into MKs and platelets, there was early and enhanced production of $CD41^+$ PLPs,[166] suggesting that PLPs arise through an apoptotic process in vitro. Collectively, the contradictory conclusions from these different studies could be due to differences between in vivo and in vitro systems.

We showed that mature MKs in culture are being damaged by apoptosis and by keeping them viable until they are infused into the right environment in vivo increases platelet yield. However, mature MKs cultured in the presence of apoptosis inhibitor resulted in decreased PLP production in vitro. Based on these results, we may hypothesize that platelet formation in vitro and in vivo may be different and that in vitro PLPs may be products of apoptosis. We can begin to test this hypothesis by knocking out components of the intrinsic and extrinsic apoptotic pathway (Bak, Bax, caspase 9 and 8) singly and in combination in human stem cell-derived MKs using the CRISPR/Cas9 system and examining the effects of these manipulations on MK viability and platelet formation in vitro and in vivo. These experiments are complementary to previously published work and will shed light on whether there is a difference between in vitro and in vivo platelet formation.

In our studies, Q-VD-Oph, a pan-caspase inhibitor,[161,162] was able to restrain apoptosis but could not eliminate it completely. With Q-VD-Oph, MKs were able to maintain their

viability for a longer time but would eventually succumb to apoptosis if they were cultured for an extended period of time. Additionally, the effect this drug is temporary as its removal led to a quick progression of cells towards apoptosis. The limitation of Q-VD-Oph may be due to the fact that it interferes at the level of caspases, which occurs after mitochondrial outer membrane permeabilization (MOMP), often recognized as the "point of no return" in the intrinsic apoptotic cascade.[184] Inhibiting apoptosis before MOMP occurs could be a good way to more permanently or effectively protect the viability of MKs. We tried to inhibit apoptosis using cyclosporine A, Bax inhibiting peptide V5 and mitochondrial division inhibitor-1 (mdivi-1), which block apoptosis at the level of MOMP,[185–187] but surprisingly, these inhibitors were not successful at inhibiting apoptosis at the range of doses that we tested. We and others have found that MKs in culture are not able to reach the size and ploidy of MKs in their natural in vivo environment,[25,136] which may be the limiting factor for platelet yield. We start to see apoptosis in our MK cultures from day 13 and without any intervention, apoptotic MKs quickly take over the culture. We may hypothesize that MKs in culture are not able to achieve high ploidy because they become apoptotic. Although Q-VD-Oph protected the MKs from apoptosis, we did not see an improvement in ploidy, probably due to its late intervention. Future efforts to protect MK viability by preventing MOMP and examining the effect of apoptosis protection on MK ploidy could employ the use of human stem cell-derived MKs genetically modified to knock out proteins necessary for MOMP (e.g. cyclophilin D, Bax and Bak).

5.3 In Vitro Platelet Generation Versus MK Infusion?

There are two potential ways of increasing platelet count in thrombocytopenic patients using stem cell-derived products. We can either infuse stem cell-derived platelets that

are generated in vitro or infuse stem cell-derived MKs that can give rise to platelets in the circulation.

The advantages of infusing in vitro-generated platelets over MKs directly include: 1) better control of the number of platelets that are infused; 2) the platelet product can be irradiated to remove any other contaminating cell types, especially undifferentiated stem cells, which have teratoma-forming potential. However, it is extremely challenging to produce real, functional platelets in vitro because the microenvironment and the signals controlling platelet release are complicated and cannot be easily mimicked even with much improved in vitro systems, like platelet bioreactors. Our studies and others showed that the yield and purity of functional $CD42b^+$ PLPs from a static MK culture is very low.[88,89] Moreover, even the $CD42b^+$ PLPs have limited functionality compared to donor platelets as indicated by a smaller fold change of surface P-selectin, a marker of activation and degranulation in platelets. Presently, the in vitro-generated platelets also lack FV, fibrinogen and immunoglobulins, proteins that are crucial for their function. These proteins, normally endocytosed by MKs in their natural environment and transferred to platelets, are not present in the culture medium. Incubation of MKs with these factors prior to platelet production should be an essential step in the protocol of generating functional in vitro platelets.

In contrast, the advantages of infusing MKs over in vitro-generated platelets include: 1) the potential for sustained release of platelets over an extended period of time, which reduces the need for frequent transfusions, 2) the possibility of building up frozen stocks of expandable MKs for emergency use, and 3) the ability to take advantage of the natural in vivo microenvironment for efficient platelet production.

The greatest concern over infusing MKs as a therapeutic strategy is the potential danger of infused MKs blocking pulmonary capillaries during platelet release. Preliminary studies suggest that infusions of up to 5.45 x 10^6 MK progenitors are safe and tolerable but these treatments did not show substantial evidence of efficacy.[116–118] Perhaps the number of MK progenitors infused need to be further optimized or perhaps mature platelet-ready MKs instead of MK progenitors should be infused to improve efficacy. Recent advances strengthen the model that MKs travel to the lung capillary bed to release platelets into the circulation by providing evidence that thrombopoiesis in the lung accounts for 50% of the total platelet output.[69] If thrombopoiesis naturally occurs in the lung, there should be an excess of pulmonary capillaries such that the small percentage of capillaries blocked by MKs during platelet release at any time,[188] should not significantly affect blood flow. Extensive research would be needed to determine the optimum number of mature MKs to infuse to maximize safety and efficacy.

Additionally, ascertaining the functionality of platelets produced in vivo from infused MKs is also a challenge due to the low yield of platelets and the difficulty of isolating the platelets derived from infused MKs from endogenous platelets for functionality assays. We have demonstrated that platelets derived from infused MKs in immunodeficient mice activate in response to agonists and incorporate into clots following laser injury,[113] which are good preliminary indicators of functionality. However, the laser injury model is imperfect for assessing human platelet functionality as human platelets interact poorly with mouse VWF, thus human platelet incorporation rates into the mouse's thrombus are very low regardless of their functionality. We can improve this model by engineering a mouse model that expresses VWF with enhanced specificity for human platelets.[114] To investigate platelet functionality more extensively, we can also use thrombocytopenic mouse models to see if infused MKs can cause an appreciable increase in platelet

counts to reverse thrombocytopenia. Lastly, platelet yields have to be massively improved before we can even begin to analyze their functionality using assays like LTA, which is the gold standard assessment for platelet functionality.

5.4 Directing iPSCs to Definitive (Adult) HPCs and MKs Could Be Informative for Elucidating the Mechanism of TAR Syndrome

We were unable to fully recapitulate the hematologic features of TAR syndrome by differentiating TAR patient-specific iPSCs into HPCs and MKs, perhaps because these HPCs and MKs are primitive (embryonic) in nature and the developmental defects are only present in the definitive (adult) lineages. No one has successfully generated adult hematopoietic stem cells from iPSCs/ESCs, but advances have been made in protocols to generate early definitive-like hematopoietic progenitors that have broader hematopoietic potentials.[189–191] Using these improved protocols to differentiate TAR patient-specific iPSCs into more definitive-like hematopoietic progenitors may reveal hematologic phenotypes that are more similar to that observed in patients. Recapitulating the patient's phenotype using patient-specific iPSCs will be the first step towards elucidating the disease mechanism and revealing the elusive role of *RBM8A* in megakaryopoiesis and thrombopoiesis. If we can recapitulate the TAR syndrome phenotype starting from more definitive-like hematopoietic progenitors but not from primitive progenitors, this will be an interesting starting point for investigating the differences between primitive (embryonic) MKs and definitive (adult) MKs, an area that is not yet well-understood.

Primitive (embryonic) MKs are more proliferative but have lower ploidy as compared to definitive (adult) MKs. Transcriptome analyses comparing human ESC-derived MKs with primitive yolk sac-derived MKs and definitive fetal liver and definitive adult $CD34^+$ HPCs

derived MKs showed that ESC-derived MKs are most similar to primitive yolk-sac-derived MKs,[24] which is unsurprising since we know that in vitro differentiation of ESCs and iPSCs to HPCs recapitulates primitive hematopoiesis.[28,29] Additionally, more than 1/3 of the genes that were continuously upregulated with MK ontogeny were cytoskeleton proteins and proteins involved in polyploidization, proplatelet formation and platelet functions, an potential explanation for why definitive adult MKs may be better platelet producers than primitive embryonic MKs.[24] Future work to understand the differences in the regulation of primitive and definitive megakaryopoiesis and to recapitulate definitive megakaryopoiesis from ESCs and iPSCs will have important implications for the generation of stem cell-derived platelets and the use of iPSCs for modeling diseases with defects in MK development, maturation and platelet production. Figuring out whether platelets released by primitive MKs function similarly as adult human donor platelets is crucial to determine whether the platelets we get from iPSCs/ESCs will ever be good enough for transfusion without undergoing definitive megakaryopoiesis through a HSC intermediate. Lastly, understanding whether a MK/platelet developmental defect is primitive or definitive in origin will be important to determine what differentiation protocols are needed to recapitulate the phenotype and elucidate the disease mechanism.

Bibliography

1. Pease D. An Electron Microscopic Study of Red Bone Marrow. *Blood*. 1956;11(6):501–526.
2. Nakeff A, Maat B. Separation of Megakaryocytes From Mouse Bone Marrow by Velocity Sedimentation. *Blood*. 1974;43(4):591–595.
3. Bruns I, Lucas D, Pinho S, et al. Megakaryocytes regulate hematopoietic stem cell quiescence via CXCL4 secretion. *Nat. Med.* 2014;20(11):1315–1320.
4. Zhao M, Perry JM, Marshall H, et al. Megakaryocytes maintain homeostatic quiescence and promote post-injury regeneration of hematopoietic stem cells. *Nat. Med.* 2014;20(11):1321–1326.
5. Golebiewska EM, Poole AW. Platelet secretion: From haemostasis to wound healing and beyond. *Blood Rev.* 2015;29(3):153–162.
6. Nurden AT, Nurden P, Sanchez M, Andia I, Eduardo A. Platelets and wound healing. *Front. Biosci.* 2008;13(i):3532–3548.
7. Walsh TG, Metharom P, Berndt MC. The functional role of platelets in the regulation of angiogenesis. *Platelets*. 2014;7104(3):1–13.
8. Ware J, Corken A, Khetpal R. Platelet function beyond hemostasis and thrombosis. *Curr. Opin. Hematol.* 2013;20(5):451–456.
9. Jenne CN, Kubes P. Platelets in inflammation and infection. *Platelets*. 2015;26(4):286–292.
10. Bertozzi CC, Hess PR, Kahn ML. Platelets: Covert regulators of lymphatic development. *Arterioscler. Thromb. Vasc. Biol.* 2010;30(12):2368–2371.
11. Akashi K, Traver D, Miyamoto T, Weissman IL. A clonogenic common myeloid progenitor that gives rise to all myeloid lineages. *Nature*. 2000;404:193–197.
12. Manz MG, Miyamoto T, Akashi K, Weissman IL. Prospective isolation of human clonogenic common myeloid progenitors. *Proc. Natl. Acad. Sci. U. S. A.* 2002;99(18):11872–11877.
13. Debili N, Coulombel L, Croisille L, et al. Characterization of a bipotent erythro-megakaryocytic progenitor in human bone marrow. *Blood*. 1996;88(4):1284–1296.
14. Woolthuis CM, Park CY. Hematopoietic stem/progenitor cell commitment to the megakaryocyte lineage. *Blood*. 2016;127(10):1242–1248.
15. Sanjuan-Pla A, Macaulay IC, Jensen CT, et al. Platelet-biased stem cells reside at the apex of the haematopoietic stem-cell hierarchy. *Nature*. 2013;502(7470):232–6.
16. Shin JY, Hu W, Naramura M, Park CY. High c-Kit expression identifies hematopoietic stem cells with impaired self-renewal and megakaryocytic bias. *J. Exp. Med.* 2014;211(2):217–231.
17. Yamamoto R, Morita Y, Ooehara J, et al. Clonal analysis unveils self-renewing lineage-restricted progenitors generated directly from hematopoietic stem cells. *Cell*. 2013;154(5):1112–1126.
18. Nishikii H, Kanazawa Y, Umemoto T, et al. Unipotent megakaryopoietic pathway bridging hematopoietic stem cells and mature megakaryocytes. *Stem Cells*. 2015;33(7):2196–2207.
19. Tavian M, Péault B. Embryonic development of the human hematopoietic system. *Int. J. Dev. Biol.* 2005;49(2–3):243–250.
20. McGrath KE, Palis J. Hematopoiesis in the yolk sac: More than meets the eye. *Exp. Hematol.* 2005;33(9 SPEC. ISS.):1021–1028.
21. Palis J, Robertson S, Kennedy M, Wall C, Keller G. Development of erythroid and myeloid progenitors in the yolk sac and embryo proper of the mouse. *Development*. 1999;126(22):5073–5084.

22. Xu M J, Matsuoka S, Yang FC, et al. Evidence for the presence of murine primitive megakaryocytopoiesis in the early yolk sac. *Blood*. 2001;97(7):2016–2022.
23. Tober J, McGrath KE, Palis J. Primitive erythropoiesis and megakaryopoiesis in the yolk sac are independent of c-myb. *Blood*. 2008;111(5):2636–2639.
24. Bluteau O, Langlois T, Rivera-Munoz P, et al. Developmental changes in human megakaryopoiesis. *J. Thromb. Haemost.* 2013;11(9):1730–41.
25. Mattia G, Vulcano F, Milazzo L, et al. Different ploidy levels of megakaryocytes generated from peripheral or cord blood CD34+ cells are correlated with different levels of platelet release. *Blood*. 2002;99(3):888–897.
26. Potts KS, Sargeant TJ, Markham JF, et al. A lineage of diploid platelet-forming cells precedes polyploid megakaryocyte formation in the mouse embryo. *Blood*. 2014;124(17):2725–2730.
27. Tober J, Koniski A, McGrath KE, et al. The megakaryocyte lineage originates from hemangioblast precursors and is an integral component both of primitive and of definitive hematopoiesis. *Blood*. 2007;109(4):1433–1441.
28. Murry CE, Keller G. Differentiation of embryonic stem cells to clinically relevant populations: lessons from embryonic development. *Cell*. 2008;132(4):661–680.
29. Klimchenko O, Mori M, DiStefano A, et al. A common bipotent progenitor generates the erythroid and megakaryocyte lineages in embryonic stem cell-derived primitive hematopoiesis. *Blood*. 2009;114(8):1506–1517.
30. Kuter DJ, Beeler DL, Rosenberg RD. The purification of megapoietin: a physiological regulator of megakaryocyte growth and platelet production. *Proc. Natl. Acad. Sci. U. S. A.* 1994;91:11104–11108.
31. Lok S, Kaushansky K, Holly RD, et al. Cloning and expression of murine thrombopoietin cDNA and stimulation of platelet production in vivo. *Nature*. 1994;369:565–568.
32. Kaushansky K, Broudy VC, Lin N, et al. Thrombopoietin, the Mp1 ligand, is essential for full megakaryocyte development. *Proc. Natl. Acad. Sci. U. S. A.* 1995;92(8):3234–3238.
33. Debili N, Issaad C, Massé JM, et al. Expression of CD34 and platelet glycoproteins during human megakaryocytic differentiation. *Blood*. 1992;80(12):3022–3035.
34. Tijssen MR, Ghevaert C. Transcription factors in late megakaryopoiesis and related platelet disorders. *J. Thromb. Haemost.* 2013;11(4):593–604.
35. Vitrat N, Cohen-Solal K, Pique C, et al. Endomitosis of human megakaryocytes are due to abortive mitosis. *Blood*. 1998;91(10):3711–3723.
36. Radley J, Haller C. The demarcation membrane system of the megakaryocyte: A misnomer? *Blood*. 1982;60(1):213–219.
37. Heijnen HF, Debili N, Vainchencker W, et al. Multivesicular bodies are an intermediate stage in the formation of platelet alpha-granules. *Blood*. 1998;91(7):2313–2325.
38. Youssefian T, Cramer EM. Megakaryocyte dense granule components are sorted in multivesicular bodies. *Blood*. 2000;95(12):4004–4007.
39. Fava RA, Casey TT, Wilcox J, et al. Synthesis of transforming growth factor-beta 1 by megakaryocytes and its localization to megakaryocyte and platelet alpha-granules. *Blood*. 1990;76(10):1946–1955.
40. Schick PK, Walker J, Profeta B, Denisova L, Bennett V. Synthesis and secretion of von willebrand factor and fibronectin in megakaryocytes at different stages of maturation. *Arterioscler. Thromb. Vasc. Biol.* 1997;17:797–801.
41. Lambert MP, Meng R, Xiao L, et al. Intramedullary megakaryocytes internalize

released platelet factor 4 and store it in alpha granules. *J. Thromb. Haemost.* 2015;13(10):1888–1899.
42. Suehiro Y, Veljkovic DK, Fuller N, et al. Endocytosis and storage of plasma factor V by human megakaryocytes. *Thromb. Haemost.* 2005;94:585–592.
43. Harrison P, Wilbourn B, Debili N, et al. Uptake of plasma fibrinogen into the alpha granules of human megakaryocytes and platelets. *J. Clin. Invest.* 1989;84(4):1320–1324.
44. Handagama PJ, George JN, Shuman MA, McEver RP, Bainton DF. Incorporation of a circulating protein into megakaryocyte and platelet granules. *Proc. Natl. Acad. Sci. U. S. A.* 1987;84(3):861–865.
45. Raslova H, Roy L, Vourc'h C, et al. Megakaryocyte polyploidization is associated with a functional gene amplification. *Blood*. 2003;101(2):541–544.
46. Raslova H, Kauffmann A, Sekkaï D, et al. Interrelation between polyploidization and megakaryocyte differentiation: a gene profiling approach. *Blood*. 2007;109(8):3225–34.
47. Schulze H, Korpal M, Hurov J, et al. Characterization of the megakaryocyte demarcation membrane system and its role in thrombopoiesis. *Blood*. 2006;107(10):3868–3875.
48. Antkowiak A, Viaud J, Severin S, et al. Cdc42-dependent F-actin dynamics drive structuration of the demarcation membrane system in megakaryocytes. *J. Thromb. Haemost.* 2016;14(6):1268–1284.
49. Rowley JW, Schwertz H, Weyrich AS. Platelet mRNA: the meaning behind the message. *Curr. Opin. Hematol.* 2012;19(5):385–391.
50. Roth GJ, Hickey MJ, Chung DW, Hickstein DD. Circulating human blood platelets retain appreciable amounts of poly (A)+ RNA. *Biochem. Biophys. Res. Commun.* 1989;160(2):705–710.
51. Handagama P, Rappolee DA, Werb Z, Levin J, Bainton DF. Platelet α-Granule fibrinogen, albumin, and immunoglobulin G are not synthesized by rat and mouse megakaryocytes. *J. Clin. Invest.* 1990;86:1364–1368.
52. Handagama P, Scarborough RM, Shuman MA, Bainton DF. Endocytosis of fibrinogen into megakaryocyte and platelet alpha-granules is mediated by alpha IIb beta 3 (glycoprotein IIb-IIIa). *Blood*. 1993;82:135–138.
53. Klement GL, Yip TT, Cassiola F, et al. Platelets actively sequester angiogenesis regulators. *Blood*. 2009;113(12):2835–2842.
54. Avecilla ST, Hattori K, Heissig B, et al. Chemokine-mediated interaction of hematopoietic progenitors with the bone marrow vascular niche is required for thrombopoiesis. *Nat. Med.* 2004;10(1):64–71.
55. Pitchford SC, Lodie T, Rankin SM. VEGFR1 stimulates a CXCR4-dependent translocation of megakaryocytes to the vascular niche , enhancing platelet production in mice. 2012;120(14):2787–2795.
56. Junt T, Schulze H, Chen Z, et al. Dynamic visualization of thrombopoiesis within bone marrow. *Science (80-.).* 2007;317:1767–1770.
57. Zhang L, Orban M, Lorenz M, et al. A novel role of sphingosine 1-phosphate receptor S1pr1 in mouse thrombopoiesis. *J. Exp. Med.* 2012;209(12):2165–2181.
58. Italiano JE, Lecine P, Shivdasani R a., Hartwig JH. Blood platelets are assembled principally at the ends of proplatelet processes produced by differentiated megakaryocytes. *J. Cell Biol.* 1999;147(6):1299–1312.
59. Choi ES, Nichol JL, Hokom MM, Hornkohl AC, Hunt P. Platelets generated in vitro from proplatelet-displaying human megakaryocytes are functional. *Blood*. 1995;85(2):402–413.
60. Behnke O. An Electron Microscope Study of the Rat Megacaryocyte. *J.*

Ultrastruct. Res. 1969;26:111–129.
61. Becker RP, De Bruyn PPH. The transmural passage of blood cells into myeloid sinusoids and the entry of platelets into the sinusoidal circulation; a scanning electron microscopic investigation. *Am. J. Anat.* 1976;145(2):183–206.
62. Thon JN, Montalvo A, Patel-Hett S, et al. Cytoskeletal mechanics of proplatelet maturation and platelet release. *J. Cell Biol.* 2010;191(4):861–874.
63. Nishimura S, Nagasaki M, Kunishima S, et al. IL-1 induces thrombopoiesis through megakaryocyte rupture in response to acute platelet needs. *J. Cell Biol.* 2015;209(3):453–466.
64. Levine R, Eldor A, Schoff P, et al. Circulating megakaryocytes: Delivery of large numbers of intact, mature megakaryocytes to the lungs. *Eur. J. Hematol.* 1993;51:233–246.
65. Zucker-Franklin D, Philipp CS. Platelet production in the pulmonary capillary bed: new ultrastructural evidence for an old concept. *Am. J. Pathol.* 2000;157(1):69–74.
66. Kaufman RM, Airo R, Pollack S, Crosby WH. Circulating megakaryocytes and platelet release in the lung. *Blood*. 1965;26(6):720–731.
67. Pedersen N. Occurrence of megakaryocytes in various vessels and their retention in the pulmonary capillaries in man. *Scand. J. Haematol.* 1978;21(5):369–375.
68. Howell W, Donahue D. The production of blood platelets in the lungs. *J. Expe*. 1937;65(2):177–203.
69. Lefrançais E, Ortiz-Muñoz G, Caudrillier A, et al. The lung is a site of platelet biogenesis and a reservoir for haematopoietic progenitors. *Nature*. 2017;544:105–109.
70. Hall JG, Levin J, Kuhn JP, et al. Thrombocytopenia with absent radius (TAR). *Medicine (Baltimore).* 1969;48(6):411–439.
71. de Alarcon PA, Graeve JA, Levine RF, McDonald TP, Beal DW. Thrombocytopenia and absent radii syndrome: defective megakaryocytopoiesis-thrombocytopoiesis. *Am. J. Pediatr. Hematol. Oncol.* 1991;13(1):77–83.
72. Letestu R, Vitrat N, Massé A, et al. Existence of a differentiation blockage at the stage of a megakaryocyte precursor in the thrombocytopenia and absent radii (TAR) syndrome. *Blood*. 2000;95(5):1633–1641.
73. Homans A, Cohen J, Mazur E. Defective megakaryocytopoiesis in the syndrome of thrombocytopenia with absent radii. *Br. J. Haematol.* 1988;70:205–210.
74. Hedberg VA, Lipton JM. Thrombocytopenia with absent radii. A review of 100 cases. *J. Pediatr. Hematol. Oncol.* 1988;10(1):51–64.
75. Albers C a, Paul DS, Schulze H, et al. Compound inheritance of a low-frequency regulatory SNP and a rare null mutation in exon-junction complex subunit RBM8A causes TAR syndrome. *Nat. Genet.* 2012;44(February):435–9, S1-2.
76. Klopocki E, Schulze H, Strauss G, et al. Complex inheritance pattern resembling autosomal recessive inheritance involving a microdeletion in thrombocytopenia-absent radius syndrome. *Am. J. Hum. Genet.* 2007;80(2):232–240.
77. Le Hir H, Izaurralde E, Maquat LE, Moore MJ. The spliceosome deposits multiple proteins 20-24 nucleotides upstream of mRNA exon-exon junctions. *EMBO J.* 2000;19(24):6860–6869.
78. Kataoka N, Yong J, Kim VN, et al. Pre-mRNA splicing imprints mRNA in the nucleus with a novel RNA-binding protein that persists in the cytoplasm. *Mol Cell*. 2000;6(3):673–682.
79. Kim VN, Yong J, Kataoka N, et al. The Y14 protein communicates to the cytoplasm the position of exon-exon junctions. *EMBO J.* 2001;20(8):2062–2068.
80. Le Hir H, Gatfield D, Izaurralde E, Moore MJ. The exon-exon junction complex

provides a binding platform for factors involved in mRNA export and nonsense-mediated mRNA decay. *EMBO J.* 2001;20(17):4987–4997.
81. Wiegand HL, Lu S, Cullen BR. Exon junction complexes mediate the enhancing effect of splicing on mRNA expression. *Proc. Natl. Acad. Sci. U. S. A.* 2003;100(20):11327–11332.
82. Palacios IM, Gatfield D, Johnston DS, Izaurralde E. An eIF4AIII-containing complex required for mRNA localization and nonsense-mediated mRNA decay. *Nature*. 2004;427(February):753–757.
83. Kim VN, Kataoka N, Dreyfuss G. Role of the nonsense-mediated decay factor hUpf3 in the splicing-dependent exon-exon junction complex. *Science (80-.).* 2001;293(5536):1832–1836.
84. Lykke-Andersen J, Shu MD, Steitz JA. Communication of the position of exon-exon junctions to the mRNA surveillance machinery by the protein RNPS1. *Science (80-.).* 2001;293(5536):1836–1839.
85. Salicioni AM, Xi M, Vanderveer LA, et al. Identification and structural analysis of human RBM8A and RBM8B: two highly conserved RNA-binding motif proteins that interact with OVCA1, a candidate tumor suppressor. *Genomics*. 2000;69(1):54–62.
86. Hachet O, Ephrussi A. Drosophila Y14 shuttles to the posterior of the oocyte and is required for oskar mRNA transport. *Curr. Biol.* 2001;11(21):1666–1674.
87. Gaur M, Kamata T, Wang S, et al. Megakaryocytes derived from human embryonic stem cells: A genetically tractable system to study megakaryocytopoiesis and integrin function. *J. Thromb. Haemost.* 2006;4:436–442.
88. Takayama N, Nishikii H, Usui J, et al. Generation of functional platelets from human embryonic stem cells in vitro via ES-sacs, VEGF-promoted structures that concentrate hematopoietic progenitors. *Blood*. 2008;111(11):5298–5306.
89. Lu S, Li F, Yin H, et al. Platelets generated from human embryonic stem cells are functional in vitro and in the microcirculation of living mice. *Cell Res.* 2011;21:530–545.
90. Feng Q, Shabrani N, Thon JN, et al. Scalable generation of universal platelets from human induced pluripotent stem cells. *Stem Cell Reports*. 2014;3:817–831.
91. Nakamura S, Takayama N, Hirata S, et al. Expandable megakaryocyte cell lines enable clinically applicable generation of platelets from human induced pluripotent stem cells. *Cell Stem Cell*. 2014;14:535–548.
92. Matsunaga T, Tanaka I, Kobune M, et al. Ex vivo large-scale generation of human platelets from cord blood CD34+ cells. *Stem Cells*. 2006;24:2877–87.
93. Pineault N, Robert A, Cortin V, Boyer L. Ex Vivo Differentiation of Cord Blood Stem Cells into Megakaryocytes and Platelets. *Methods Mol. Biol.* 2013;946:205–224.
94. Guerriero R, Testa U, Gabbianelli M, et al. Unilineage megakaryocytic proliferation and differentiation of purified hematopoietic progenitors in serum-free liquid culture. *Blood*. 1995;86(10):3725–3736.
95. Johansson I, Stensballe J, Oliveri R, et al. How I treat patients with massive hemorrhage. *Blood*. 2014;124(20):3052–3059.
96. Kaufman RM, Djulbegovic B, Gernsheimer T, et al. Platelet transfusion: A clinical practice guideline from the AABB. *Ann. Intern. Med.* 2015;162(3):205–213.
97. Whitaker B, Rajbhandary S, Kleinman S, Harris A, Kamani N. Trends in United States blood collection and transfusion: results from the 2013 AABB Blood Collection, Utilization, and Patient Blood Management Survey. *Transfusion*. 2016;56(9):2173–2183.

98. Stroncek DF, Rebulla P. Platelet transfusions. *Lancet*. 2007;370(9585):427–438.
99. Tynngård N. Preparation, storage and quality control of platelet concentrates. *Transfus. Apher. Sci.* 2009;41(2):97–104.
100. Stenberg P, Levin J. Mechanisms of platelet production. *Blood Cells*. 1989;15:23–47.
101. Robert A, Cortin V, Garnier A, Pineault N. Megakaryocyte and platelet production from human cord blood stem cells. *Methods Mol. Biol.* 2012;3:91–100.
102. Thon JN, Mazutis L, Wu S, et al. Platelet bioreactor-on-a-chip. *Blood*. 2014;124(12):1857–1867.
103. Nakagawa Y, Nakamura S, Nakajima M, et al. Two differential flows in a bioreactor promoted platelet generation from human pluripotent stem cell-derived megakaryocytes. *Exp. Hematol.* 2013;41:742–748.
104. Sullenbarger B, Bahng JH, Gruner R, Kotov N, Lasky LC. Prolonged continuous in vitro human platelet production using three-dimensional scaffolds. *Exp. Hematol.* 2009;37(1):101–110.
105. Avanzi MP, Oluwadara OE, Cushing MM, et al. A novel bioreactor and culture method drives high yields of platelets from stem cells. *Transfusion*. 2016;56(1):170–178.
106. Di Buduo CA, Wray LS, Tozzi L, et al. Programmable 3D silk bone marrow niche for platelet generation ex vivo and modeling of megakaryopoiesis pathologies. *Blood*. 2015;125(14):2254–2264.
107. Strauss T, Sidlik-Muskatel R, Kenet G. Developmental hemostasis: Primary hemostasis and evaluation of platelet function in neonates. *Semin. Fetal Neonatal Med.* 2011;16(6):301–304.
108. Israels SJ, Rand ML, Michelson AD. Neonatal Platelet Function. *Semin Thromb Hemost*. 2003;29(4):363–372.
109. Rajasekhar D, Kestin AS, Bednarek FJ, et al. Neonatal platelets are less reactive than adult platelets to physiological agonists in whole blood. *Thromb. Haemost.* 1994;72(6):957–963.
110. Shattil SJ, Cunningham M, Hoxie JA. Detection of activated platelets in whole blood using activation-dependent monoclonal antibodies and flow cytometry. *Blood*. 1987;70(1):307–315.
111. Shattil SJ, Hoxie JA, Cunningham M, Brass LF. Changes in the platelet membrane glycoprotein IIb.IIIa complex during platelet activation. *J. Biol. Chem.* 1985;260(20):11107–11114.
112. Di Buduo C a., Wray LS, Tozzi L, et al. Programmable 3D silk bone marrow niche for platelet generation ex vivo and modeling of megakaryopoiesis pathologies. *Blood*. 2015;3:617–627.
113. Wang Y, Hayes V, Jarocha D, et al. Comparative analysis of human ex vivo-generated platelets vs megakaryocyte-generated platelets in mice: a cautionary tale. *Blood*. 2015;125(23):3627–3636.
114. Chen J, Tan K, Zhou H, et al. Modifying murine von Willebrand factor A1 domain for in vivo assessment of human platelet therapies. *Nat. Biotechnol.* 2007;26(1):114–119.
115. Savage B, Saldívar E, Ruggeri ZM. Initiation of platelet adhesion by arrest onto fibrinogen or translocation on von Willebrand factor. *Cell*. 1996;84(2):289–297.
116. Bertolini F, Battaglia M, Pedrazzoli P, et al. Megakaryocytic progenitors can be generated ex vivo and safely administered to autologous peripheral blood progenitor cell transplant recipients. *Blood*. 1997;89(8):2679–2688.
117. Xi J, Zhu H, Liu D, et al. Infusion of Megakaryocytic Progenitor Products Generated from Cord Blood Hematopoietic Stem/Progenitor Cells: Results of the

Phase 1 Study. *PLoS One*. 2013;8(2):.
118. Scheding S, Bergmannn M, Rathke G, et al. Additional transplantation of ex vivo generated megakaryocytic cells after high-dose chemotherapy. *hematologica*. 2004;89:630–631.
119. Mills JA, Paluru P, Weiss MJ, Gadue P, French DL. Hematopoietic differentiation of pluripotent stem cells in culture. *Methods Mol. Biol.* 2014;1185:181–194.
120. Ivanciu L, Krishnaswamy S, Camire RM. New insights into the spatiotemporal localization of prothrombinase in vivo. *Blood*. 2014;124(11):1705–1714.
121. Hockemeyer D, Soldner F, Beard C, et al. Efficient targeting of expressed and silent genes in human ESCs and iPSCs using zinc-finger nucleases. *Nat. Biotechnol.* 2009;27(9):851–7.
122. Sim X, Cardenas-Diaz FL, French DL, Gadue P. A doxycyline-inducible system for genetic correction of iPSC disease models. *Methods Mol. Biol.* 2016;1353:13–23.
123. Mali P, Yang L, Esvelt KM, et al. RNA-Guided Human Genome Engineering via Cas9. *Science (80-.).* 2013;339(6121):823–826.
124. Veazey KJ, Golding MC. Selection of stable reference genes for quantitative RT-PCR comparisons of mouse embryonic and extra-embryonic stem cells. *PLoS One*. 2011;6(11):.
125. Reems J, Pineault N, Sun S. In vitro megakaryocyte production and platelet biogenesis: state of the art. *Transfus. Med. Rev.* 2010;24(1):33–43.
126. Lee EJ, Godara P, Haylock D. Biomanufacture of human platelets for transfusion: Rationale and approaches. *Exp. Hematol.* 2014;42:332–346.
127. Avanzi MP, Mitchell WB. Ex Vivo production of platelets from stem cells. *Br. J. Haematol.* 2014;165:237–247.
128. Feng Q, Shabrani N, Thon JN, et al. Scalable Generation of Universal Platelets from Human Induced Pluripotent Stem Cells. *Stem Cell Reports*. 2014;3(5):817–831.
129. Lambert MP, Sullivan SK, Fuentes R, French DL, Poncz M. Challenges and promises for the development of donor-independent platelet transfusions. *Blood*. 2013;121(17):3319–3324.
130. Thon JN, Medvetz DA, Karlsson SM, Italiano JE. Road blocks in making platelets for transfusion. *J. Thromb. Haemost.* 2015;13(S1):S55–S62.
131. Wang B, Zheng J. Platelet generation in vivo and in vitro. *Springerplus*. 2016;5:787–797.
132. Sim X, Poncz M, Gadue P, French DL. Understanding platelet generation from megakaryocytes: Implications for in vitro-derived platelets. *Blood*. 2016;127(10):1227–1233.
133. Tomer A, Harker L, Burstein S. Flow cytometric analysis of normal human megakaryocytes. *Blood*. 1988;71(5):1244–1252.
134. Yamada E. The fine structure of the megakaryocyte in the mouse spleen. *Acta Anat.* 1957;29:267–290.
135. Ru YX, Dong SX, Liang HY, Zhao SX. Platelet production of megakaryocyte: A review with original observations on human in vivo cells and bone marrow. *Ultrastruct. Pathol.* 2016;40(4):163–170.
136. Takayama N, Nishimura S, Nakamura S, et al. Transient activation of c-MYC expression is critical for efficient platelet generation from human induced pluripotent stem cells. *J. Exp. Med.* 2010;207(13):2817–2830.
137. Blin A, Le Goff A, Magniez A, et al. Microfluidic model of the platelet-generating organ: beyond bone marrow biomimetics. *Sci. Rep.* 2016;6:21700–21712.
138. Fuentes R, Wang Y, Hirsch J, et al. Infusion of mature megakaryocytes into mice

yields functional platelets. *J. Clin. Invest.* 2010;120(11):3917–3922.
139. Bergmeier W, Burger PC, Piffath CL, et al. Metalloproteinase inhibitors improve the recovery and hemostatic function of in vitro-aged or -injured mouse platelets. *Blood*. 2003;102(12):4229–4235.
140. Bergmeier W, Piffath CL, Cheng G, et al. Tumor necrosis factor-α-converting enzyme (ADAM17) mediates GPIbα shedding from platelets in vitro and in vivo. *Circ. Res.* 2004;95:677–683.
141. Fox JE. Shedding of adhesion receptors from the surface of activated platelets. *Blood Coagul. Fibrinolysis*. 1994;5:291–304.
142. Michelson AD, Ellis PA, Barnard MR, et al. Downregulation of the platelet surface glycoprotein Ib-IX complex in whole blood stimulated by thrombin, adenosine diphosphate, or an in vivo wound. *Blood*. 1991;77(4):770–779.
143. Bergmeier W, Rackebrandt K, Schroder W, Zirngibl H, Nieswandt B. Structural and functional characterization of the mouse von Willebrand factor receptor GPIb-IX with novel monoclonal antibodies. *Blood*. 2000;95(3):886–893.
144. Hartley PS, Savill J, Brown SB. The death of human platelets during incubation in citrated plasma involves shedding of CD42b and aggregation of dead platelets. *Thromb. Haemost.* 2005;95:100–106.
145. Adachi M, Ryo R, Sato T, Yamaguchi N. Platelet factor 4 gene expression in a human megakaryocytic leukemia cell line (CMK) and its differentiated subclone (CMK11-5). *Exp. Hematol.* 1991;19:923–927.
146. Eto K, Murphy R, Kerrigan SW, et al. Megakaryocytes derived from embryonic stem cells implicate CalDAG-GEFI in integrin signaling. *Proc. Natl. Acad. Sci. U. S. A.* 2002;99(20):12819–12824.
147. Polgar J, Clemetson JM, Kehrel BE, et al. Platelet Activation and Signal Transduction by Convulxin, a C-type Lectin from Crotalus durissus terrificus (Tropical Rattlesnake) Venom via the p62/GPVI Collagen Receptor. *Biochemistry*. 1997;272(21):13576–13583.
148. Furman MI, Liu L, Benoit SE, et al. The cleaved peptide of the thrombin receptor is a strong platelet agonist. *Proc. Natl. Acad. Sci. U. S. A.* 1998;95(6):3082–3087.
149. Wilson DB, Salem HH, Mruk JS, Maruyama I, Majerus PW. Biosynthesis of coagulation factor V by a human hepatocellular carcinoma cell line. *J. Clin. Invest.* 1984;73:654–658.
150. Mazzorana M, Baffet G, Kneip B, Launois B, Guguen-Guillouzo C. Expression of coagulation factor V gene by normal adult human hepatocytes in primary culture. *Br. J. Haematol.* 1991;78:229–235.
151. Yang TL, Pipe SW, Yang A, Ginsburg D. Biosynthetic origin and functional significance of murine platelet factor V. *Blood*. 2003;102(8):2851–2855.
152. Camire RM, Pollak ES, Kaushansky K, Tracy PB. Secretable human platelet-derived factor V originates from the plasma pool. *Blood*. 1998;92(9):3035–3041.
153. Gould WR, Simioni P, Silveira JR, et al. Megakaryocytes endocytose and subsequently modify human factor V in vivo to form the entire pool of a unique platelet-derived cofactor. *J. Thromb. Haemost.* 2005;3:450–456.
154. Bouchard BA, Williams JL, Meisler NT, Long MW, Tracy PB. Endocytosis of plasma-derived factor V by megakaryocytes occurs via a clathrin-dependent, specific membrane binding event. *J. Thromb. Haemost.* 2005;3(3):541–551.
155. Gertz JM, Bouchard B a. Mechanisms Regulating Acquisition of Platelet-Derived Factor V/Va by Megakaryocytes. *J. Cell. Biochem.* 2015;2126(March):2121–2126.
156. Bouchard BA, Meisler NT, Nesheim ME, et al. A unique function for LRP-1: A component of a two-receptor system mediating specific endocytosis of plasma-derived factor V by megakaryocytes. *J. Thromb. Haemost.* 2008;6:638–644.

157. Lambert MP, Wang Y, Bdeir KH, et al. Platelet factor 4 regulates megakaryopoiesis through low-density lipoprotein receptor-related protein 1 (LRP1) on megakaryocytes. *Blood*. 2009;114(11):2290–2298.
158. Thon JN, Macleod H, Begonja AJ, et al. Microtubule and cortical forces determine platelet size during vascular platelet production. *Nat. Commun.* 2012;3(May):852–861.
159. Michelson AD, Adelman B, Barnard MR, Carroll E, Handin RI. Platelet storage results in a redistribution of glycoprotein Ib molecules. *J. Clin. Invest.* 1988;81:1734–1740.
160. Hirata S, Murata T, Suzuki D, et al. Selective Inhibition of ADAM17 effectively mediates glycoprotein Iba retention during ex vivo generation of human induced pluripotent stem cell-derived platelets. *Stem Cells Transl. Med.* 2016;5:1–11.
161. Caserta TM, Smith AN, Gultice AD, Reedy MA, Brown TL. Q-VD-OPh, a broad spectrum caspase inhibitor with potent antiapoptotic properties. *Apoptosis*. 2003;8:345–352.
162. Keoni CLI, Brown TL. Inhibition of apoptosis and efficacy of pan caspase inhibitor, Q-VD-OPh, in models of human disease. *J. Cell Death*. 2015;8:1–7.
163. Sommer A, Kordowski F, Büch J, et al. Phosphatidylserine exposure is required for ADAM17 sheddase function. *Nat. Commun.* 2016;7(May):11523.
164. Houwerzijl EJ, Blom NR, van der Want JJL, Vellenga E, de Wolf JTM. Megakaryocytic dysfunction in myelodysplastic syndromes and idiopathic thrombocytopenic purpura is in part due to different forms of cell death. *Leukemia*. 2006;20:1937–1942.
165. Sabri S, Foudi A, Boukour S, et al. Deficiency in the Wiskott-Aldrich protein induces premature proplatelet formation and platelet production in the bone marrow compartment. *Blood*. 2006;108(1):134–140.
166. Morison IM, Cramer Bordé EM, Cheesman EJ, et al. A mutation of human cytochrome c enhances the intrinsic apoptotic pathway but causes only thrombocytopenia. *Nat. Genet.* 2008;40(4):387–389.
167. Yang L, Wang L, Zhao CH, et al. Contributions of TRAIL-mediated megakaryocyte apoptosis to impaired megakaryocyte and platelet production in immune thrombocytopenia. *Blood*. 2010;116(20):4307–4316.
168. Ru YX, Zhao SX, Liu EB, et al. Ultrastructural characteristics of bone marrow in patients with hematological disease: a study of 13 cases. *Ultrastruct Pathol*. 2007;31(5):327–332.
169. Schmitt A, Jouault H, Guichard J, et al. Pathologic interaction between megakaryocytes and polymorphonuclear leukocytes in myelofibrosis. *Blood*. 2000;96(4):1342–1347.
170. Reilly JT. Idiopathic myelofibrosis: Pathogenesis to treatment. *Hematol. Oncol.* 2006;24(2):56–63.
171. Kraytman M. Platelet size in thrombocytopenias and thrombocytosis of various origin. *Blood*. 1973;41(4):587–598.
172. McDonald TP, Odell TT, Gosslee DG. Platelet size in relation to platelet age. *Proc. Soc. Exp. Biol. Med.* 1964;115:684–689.
173. Louache F, Debili N, Cramer E, Breton-Gorius J, Vainchenker W. Fibrinogen is not synthesized by human megakaryocytes. *Blood*. 1991;77(2):311–316.
174. Kile BT. The role of apoptosis in megakaryocytes and platelets. *Br. J. Haematol.* 2014;165:217–226.
175. De Botton S, Sabri S, Daugas E, et al. Platelet formation is the consequence of caspase activation within megakaryocytes. *Blood*. 2002;100(4):1310–1317.
176. Clarke MCH, Savill J, Jones DB, Noble BS, Brown SB. Compartmentalized

megakaryocyte death generates functional platelets committed to caspase-independent death. *J. Cell Biol.* 2003;160(4):577–587.
177. White MJ, Schoenwaelder SM, Josefsson EC, et al. Caspase-9 mediates the apoptotic death of megakaryocytes and platelets, but is dispensable for their generation and function. *Blood*. 2012;119(18):4283–4290.
178. Josefsson EC, Burnett DL, Lebois M, et al. Platelet production proceeds independently of the intrinsic and extrinsic apoptosis pathways. *Nat. Commun.* 2014;5:3455–3469.
179. Josefsson EC, James C, Henley KJ, et al. Megakaryocytes possess a functional intrinsic apoptosis pathway that must be restrained to survive and produce platelets. *J. Exp. Med.* 2011;208(10):2017–2031.
180. Zappelli C, Van Der Zwaan C, Thijssen-Timmer DC, Mertens K, Meijer AB. Novel role for galectin-8 protein as mediator of coagulation factor V endocytosis by megakaryocytes. *J. Biol. Chem.* 2012;287(11):8327–8335.
181. Roberts AW, Seymour JF, Brown JR, et al. Substantial susceptibility of chronic lymphocytic leukemia to BCL2 inhibition: Results of a phase I study of navitoclax in patients with relapsed or refractory disease. *J. Clin. Oncol.* 2012;30(5):488–496.
182. Wilson WH, Connor O a O, Czuczman MS, et al. Safety, Pharmacokinetics, Pharcodynamics, and Activity of Navitoclax, a Targeted High Affinity Inhibitor of BCL-2, in Lymphoid Malignancies. *Lancet Oncol.* 2010;11(12):1149–1159.
183. Gandhi L, Camidge DR, De Oliveira MR, et al. Phase I study of navitoclax (ABT-263), a novel bcl-2 family inhibitor, in patients with small-cell lung cancer and other solid tumors. *J. Clin. Oncol.* 2011;29(7):909–916.
184. Chipuk JE, Bouchier-Hayes L, Green DR. Mitochondrial outer membrane permeabilization during apoptosis: the innocent bystander scenario. *Cell Death Differ.* 2006;13(8):1396–1402.
185. Zamzami N, Marchetti P, Castedo M, et al. Inhibitors of permeability transition interfere with the disruption of the mitochondrial transmembrane potential during apoptosis. *FEBS Lett.* 1996;384(1):53–57.
186. Yoshida T, Tomioka I, Nagahara T, et al. Bax-inhibiting peptide derived from mouse and rat Ku70. *Biochem. Biophys. Res. Commun.* 2004;321(4):961–966.
187. Cassidy-Stone A, Chipuk JE, Ingerman E, et al. Chemical Inhibition of the Mitochondrial Division Dynamin Reveals Its Role in Bax/Bak-Dependent Mitochondrial Outer Membrane Permeabilization. *Dev. Cell*. 2008;14(2):193–204.
188. Johnston I, Hayes V, Poncz M. Threading an elephant through the eye of a needle: Where are platelets made? *Cell Res.* 2017;1–2.
189. Kennedy M, Awong G, Sturgeon CM, et al. T Lymphocyte Potential Marks the Emergence of Definitive Hematopoietic Progenitors in Human Pluripotent Stem Cell Differentiation Cultures. *Cell Rep.* 2012;2:1722–1735.
190. Ditadi A, Sturgeon CM, Tober J, et al. Human definitive haemogenic endothelium and arterial vascular endothelium represent distinct lineages. *Nat. Cell Biol.* 2015;17(5):580–591.
191. Sturgeon CM, Ditadi A, Awong G, Kennedy M, Keller G. Wnt signaling controls the specification of definitive and primitive hematopoiesis from human pluripotent stem cells. *Nat. Biotechnol.* 2014;32(6):554–61.